بسم الله الرحمن الرحيم

Sudan University of Science and Technology

College of Graduate Studies

Behavior of Reinforced Concrete Deep Beam with High Strength Reinforcement using SAP2000 Software

سلوك العارضات الخرسانية العميقة ذات حديد تسليح عالي المقاومة باستخدام برنامج SAP2000

A Thesis Submitted in Partial Fulfillment for MSc Degree in Civil Engineering (Structural Engineering)

By: Sarah Hashim Ebaid

BSc-Civil Engineering (Structure Engineering)

Sudan University of Science and Technology

Supervisor:

Dr. Abusamra Awad Attaelmanan

December 2019

الآيــة

قال تعالي:﴿وَلَا تَمْشِ فِي الْأَرْضِ مَرَحًا إِنَّكَ لَنْ تَخْرِقَ الْأَرْضَ وَلَنْ تَبْلُغَ الْجِبَالَ طُولًا (37) كُلُّ ذَلِكَ كَانَ سَيِّئُهُ عِنْدَ رَبِّكَ مَكْرُوهًا (38)

صدق الله العظيم

سورة الإسراء الآيات (37-38)

Dedication

First and foremost, praise and thanks goes to my parents, my brothers and my sisters for their unconditional love, moral support, and encouragement has been a major stabilizing force till this moment.

Acknowledgements

I wish to express my sincere gratitude and appreciation to my supervisor**: Dr. Abusamra Awad**, for his valuable guidance, inspiration, suggestions and continuous support throughout of this study.

I am deeply indebted to **Eng. Akrm Mohammad Khair**, for the motivation, guidance, throughout the research work. I appreciate his broad range of expertise and attention to detail, as well as the constant encouragement he has given me.

Abstract

The use of Finite Element Methods in the analysis of deep beams has become a very useful tool in modern times due to the emergence of powerful computers. The use of Finite Element Analysis is extremely fast and economical as compared to laboratory testing.This thesis consists of two major parts. the first part is about design deep beams by a simply supported beam **MS1-2** having shear span to depth ratio of less than 2 has been first designed using truss modeling in **SAP2000** Software, using modeling thick shell element technique.

The results of design obtained from **FEM** modeling has been compared with design obtain in the available literature. The second part is about study the behavior of deep beams with high strength reinforcement with various shear span to depth (**a/d**) ratios and deferent reinforcement ratio $\boldsymbol{\rho}$ to study the strength parameters such as, first crack load, the ultimate failure load, load of yielding in main tension reinforcement, strains in main tension reinforcement, deflection at ultimate load, and mode of failure. The design results obtained from **SAP2000** shell thick model was show a good agreement compared with results obtained in the available literature. Comparison showed of the design results using **SAP2000** shell (thick) for design deep beam match with the available literature beam (**MS1-2**).The results obtained from **SAP2000** modeling nonlinear shell layered technique have been compared with experimental studies in the available literature. And Comparison of the results showed that the difference between finite element **SAP2000** results with experimental results are very acceptable in yielding of rebar of reinforcement , at failure load deference did not exceed **30%** in deflection at mid span and not exceed **12.5%** in strain of steel layered in all beams. The flexural crack pattern slightly deferent while the mode of failure of all the test beams was almost similar despite the Variations in web reinforcement arrangement. At the last best results obtained when the moment of inertia is reduced to **35%** and based on this comparison, it is found that **SAP2000** the modeling nonlinear shell layered technique results holds good with the experimental results and that gives satisfactory results with engineering accuracy.

مستخلص

إستخدام طريقة العناصر المحددة في تحليل العارضات العميقة أصبح مفيدا جدا في العصر الحديث، طريقة العناصر المحددة سريع وإقتصادي مقارنة مع التجارب المعملية .الهدف من هذا البحث هو دراسة سلوك العارضات العميقة للإنحناء ،قوة القص ،الإنحراف وطريقة الإنهيار للعارضات العميقة المسلحة التي تم إختبارها في المعمل ومقارنة نتائج طريقة العناصر المحددة مع نتائج التتجارب المعملية.هذا البحث يتكون من قسمين رئيسين .القسم الاول تصميم العارضات العميقة بسيطة الاسناد بها نسبة زراع قص الى عمق (**a/d**)اقل من 2 يدويا بطريقة (**STM**) ،اولا باستخدام نموزج الجملون الموجود في برنامج **SAP2000** لعمل نموذج للعارضة (**MS1-2**) ثانيا بنمزجة العارضة بتقنية القشريات ومن ثم تمت مقارنة نتائج التصميم للطريقتين مع التصيميم في الدراسة السابقة. القسم الثاني هو دراسة سلوك الابيام العميقة ذات حديد تسليح عالي المقاومة،وذلك باستخدام قيم مختلفة لكل من زراع قص الى عمق (**a/d**) ونسبة حديد التسليح ρ، لدراسة مقاومة الحمل الذي يحدث اول تشققات،الحمل الاقصى للانهيار،والحمل الذي يصل فيه حديد التسليح الرئيسي للخضوع،الانفعال في حديد التسليح الرئيسي،الانحراف للحمل الاقصى وشكل الانهيار.تم تحقيق هذا الهدف باختيار نماذج من التجارب المعملية اختبرت في دراسة سابقة لقيم مختلفة من طول القص الى العمق (**a/d**) و قيم مختلفة لنسبة حديد اتسليحρ .برنامج**SAP2000** استخدم لتحليل النتائج.من خلال مقارنة نتائج التصميم الي تم الحصول عليها من برنامج **SAP2000** اتضح تطابق كبير معا النتائج الموجودة في الدراسات السابقة. عند نمزجة العارضات باستخدام تقنية القشريات الطبقية الغير خطية تمت مقارنة النتائج معا التجارب المعملية في الدراسة السابقة أظهرت المقارنة بين النتائج أن الفرق عند استخدام **SAP2000**مقبولة لحد كبير، حيث لم يتعد الفرق **30%** في نتائج الانحراف في منتصف العارضة و **12.5%**في نتائج إنفعال المحسوب في حديد التسليح.ومن النتائج التحليل نجد اختلاف في اجهاد التشققات الناتجة من الانعطاف وبالرغم من ذلك نجد تطابق كامل في شكل الانهيار لجميع نمازج العارضات مقارنة بنتائج الاختبار المعملية في الدراسات السابقة .في نهاية هذه الدراسة افضل نتائج تم الحصول عند تخفيض عزم القصور الذاتي للقشريات الطبقية بنسبة **35%** ، ومن خلال هذه المقارنة اتضح استخدام تقنية القشريات الطبقية الموجودة في برنامج **SAP2000** نتحصل على نتائج جيدة وفي حدود المقبول من حيث المطلبات الهندسية مقارنة بالنتائج المعملية.

Table of Content

List oF Figurers

List of Table

List of Symbols

a	Shear span measured from center of support to center of loading point.
a_{max}	the maximum allowable depth of the rectangular compression block.
A_h	Area of horizontal web reinforcement with a spacing S_h.
A_{nz}	Smaller area between the areas of face of the nodal zone perpendicular to the loading acting in that face and the area of section through the nodal zone perpendicular to the resultant force of the section.
A_s	Area of main longitudinal reinforcement.
A_{si}	Total area of surface reinforcement at spacing s_i in layer for reinforcement crossing a strut an angle α_i to the axis of the strut.
$A_{s\,min}$	Minimum area of steel reinforcement.
A_v	Area of vertical web reinforcement within a spacing S_v
b	Width of beam.
C_{max}	The maximum depth of compressive zone.
d	Effective depth of deep beam.
f_C'	Concrete compressive strength.
f_{ce}	Effective compressive strength of concrete in a strut.
f_{cen}	Effective compressive strength of concrete in nodal zone.
f_{nn}	Compressive strength of concrete in nodal zone.
f_y	Yield strength of reinforcement steel.
FEA	Finite Element Analysis
FEM	Finite Element Method
H	Over all depth of deep beam.
L	Span of reinforced concrete deep beam.
L_n	Clear span of reinforced concrete deep beam.
M_u	Design ultimate moment; moment capacity
S_h	Spacing of horizontal web reinforcement
STM	Strut and Tie Method.
S_v	Spacing of vertical web reinforcement

V	Shear force
V_c	Shear strength provided by concrete.
V_s	Shear strength provided by steel.
V_n	Nominal shear strength.
V_u	Ultimate shear strength.
ρ	Reinforcement ratio.
ρ_h	Percentage of horizontal reinforcement.
ρ_v	Percentage of vertical reinforcement.
Φ	Is the capacity reduction factor for shear taken as0.75.
β	Coating factor.
βn	Strength reduction factor for nodes.
β_s	Strength reduction factor for struts.
β_1	Ratio of depth of rectangular compression block to depth to the natural axis.

Chapter One

Introduction

1.1 Introduction

Deep beams are structural elements loaded as beams in which a significant amount of the load is transferred to the supports by compression thrust joining the load and the reaction. As result, the strain distribution in no longer considered linear and the shear deformations become significant when compared to pure flexure.

The ACI318-11code, defines a deep beam as a structural member whose span depth ratio $L/H \leq 5$ shown in figure 1.1.but the Euro- International Concrete committee, decided that a beam could be considered deep if $L/H < 2$ or 2.5 for simply supported and continuous beams respectively.

To design a deep beam, Requirements of the Building Code for Structural Concrete of American Concrete Institute (ACI 318-11) provides two methods. These methods include Strut and Tie Method (STM) and/or Deep Beam Method (DBM). The DBM method consists of an appropriate and rational way to design the cracked reinforced concrete beam based on various testing data by many researchers. The STM is a modified version of the truss analogy which includes the concrete contribution through the concept of equivalent stirrup reinforcement. The STM is included in the ACI code, ACI 318-11, in its Appendix A. Actual stresses of a deep beam are non-linear, therefore more widely used design approach for deep beams is through a nonlinear distribution of the strain by DBM and is covered in ACI-318, Sections 10.2.2, 10.2.6, 10.7 and 11.7. Typically, a reinforced concrete beam is analyzed by a linear-elastic method and designed for the redistributed stresses after cracking. Analysis of deep beams by linear elastic method revealed that the stresses determined were less than the actual stresses near the center of the span (ACI Task

Committee 426, 1973). For the analysis of deep beams, various analytical tools are available. Among all these available analytical tools, finite element analysis (FEA) presents a better and convenient option. The FEM is a numerical procedure for the analysis of structures and continua.

The classical analytical methods cannot be used for the satisfactory solution as the problem addressed is too complicated normally. The problem may be required to perform many analysis e.g. stress analysis, heat conduction, or many other areas. Digital computers are used to generate and solve many simultaneous algebraic equations which are produced by finite element procedure. Results are not too much accurate. However, the approximately exact solution may be obtained by processing these equations. Results are accurate enough for engineering purposes and obtainable at reasonable cost. To fully understand the behavior of RC deep beams, FEM is a powerful and general analytical tool for linear and non-linear behavior of deep beam structural elements and finite element method can provide realistic and satisfactory solutions.

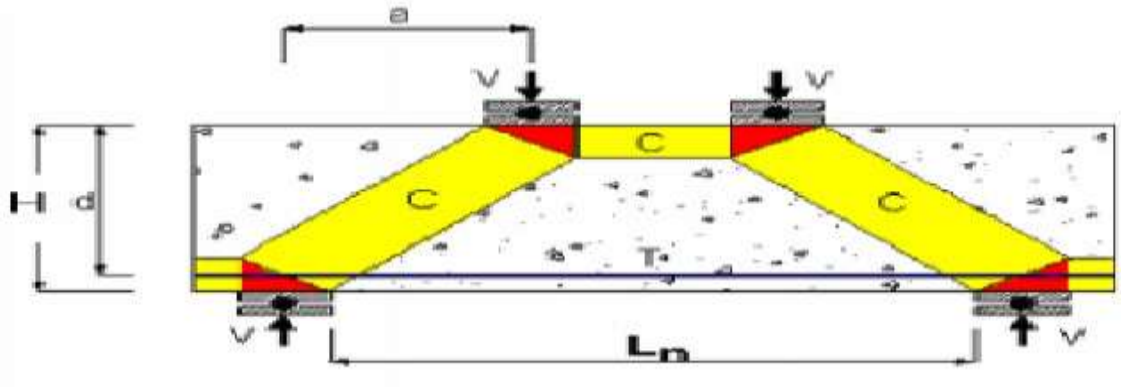

Figure1. 1: Reinforced concrete deep beam

beam

.

1.2. Problem Statement and Significance

For the prediction of deep beam behavior, either elastic theory or semi empirical equation is commonly used now-a-days. As these theories are based on linear analysis, thus they may not be acceptable (Yoo, et. al. 2007, Kong and Chemrouk, 2002). Typically, a reinforced concrete beam is analyzed and designed by linear-elastic method. A stiffness modification factor is sometimes used for the consideration of cracking effect. However, the actual stresses distribution of a deep beam is non-linear (Hassoun and Al-Manaseer, 2008). The stiffness modification factor of 0.35 given in ACI code may not be correct for deep beams.

Currently, ACI-318 does not provide equations for the design of non-linear stress distribution. The present research program analyzes the behavior of deep beams using different modeling techniques i.e., thick shell/area element, nonlinear shell layered, and STM. A small prototype deep beam (see chapter-03) has been manually designed using STM and then modeled using the thick shell/area technique. And use nonlinear shell layered technique to study behavior of deep beam. The numerical modeling has been compared to other provisions/experimental studies and a reference model has been selected.

1.3. Research Objectives

- The main objective of this study is to discuss the behavior and accuracy of SAP2000 nonlinear shell layered technique in simulation of concrete deep beam with high strength of reinforcement.
- find the best techniques in SAP2000 Software to analysis and design concrete deep beams

- Discuss the deference of results obtained from SAP2000 models with experimental results.

1.4. Research Methodology

The following methodology is adopted in this study:

- The beam was analysis by using Truss modeling (STM) and From Shell (thick) analysis the design membrane force using for (reinforcement layer) by ACI 318-11 code and compared design with the design results available in literature. Best design is recommended for the designing of deep beam.
- Study behavior of deep beam such as the cracks pattern, stress, yielding in longitudinal reinforcement, horizontal shear reinforcement and vertical shear reinforcement by nonlinear shell layered technique in SAP2000 and results were compared with the results available in literature.

1.5. Research Outline

This thesis has five chapters as shown below.

Chapter one: includes the introduction of research and

Chapter two: is literature Review and previous studies.

Chapter three: includes the research methodology.

Chapter four: results and discussion from SAP2000 software and Experimental.

Chapter five: summarizes the research conclusions and recommendations.

Chapter Two

Literature Review

2.1 Introduction

In this chapter, a literature review is presented of previous research on the behavior of reinforced concrete members incorporating high strength steel reinforcement. Also, a plasticity truss-model technique suitable for the design of deep beams is described. This technique, called Strut and Tie Modeling, was adopted by codes of practice for the design of non-slender reinforced concrete members such as deep beams. Design provisions for code (ACI 318-05) considered in this project are discussed.

2.2 General

The use of high strength steel reinforcement (ASTM A1035) in concrete structures is gaining popularity due to its higher effective yield strength, improved corrosion resistance in comparison with normal strength reinforcing steel and better behavior under low temperatures [Darwin et al, 2002 and El Hacha, 2002]. Normal strength reinforcing steel becomes brittle around -17° to -28° C, while ASTM A1035 reinforcing steel maintains excellent mechanical behavior at temperatures below -128° C [MMFX Technologies Corporation, 2008].

The mechanical properties of high strength reinforcing steel can be useful to reduce the quantity of reinforcement required, thereby lessening reinforcement congestion and improving constructability. The improved corrosion resistance [Darwin et al, 2002] makes ASTM A1035 ideal for use as reinforcement in foundations, bridges, buildings, offshore structures, etc.

ASTM A1035 high strength steel has been used as reinforcement for concrete

bridge decks and foundation walls for two primary reasons: the viability of concrete member design using the highest yield strength allowed by current design codes [Seliem et al, 2008] and the improved corrosion resistance compared to traditional Grade 400R reinforcement. However, the use of the full strength of the high strength reinforcing steel bars is not allowed in practical designs because of limitations on permitted design stress in current design code provisions. These provisions, some of which are semi-empirical, based on research completed on reinforced concrete members containing normal strength reinforcement. The stress-strain response of ASTM A1035 and conventional reinforcing steel are similar for values only up to the yielding point of conventional steel. After that point, the strain-stress responses of both types of reinforcing steel are different.

The main differences include the nonlinear stress-strain response for ASTM A1035 steel after an applied stress of approximately 650 MPa, and the lack of a defined yield point and corresponding yield plateau for ASTM A1035. Yielding strains in ASTM A1035using 0.2%offset method are about three times the yielding strains of conventional reinforcing steel.

2.3 Concrete members with high strength reinforcing steel

Research on the performance of concrete members reinforced with high strength reinforcing steel has been mainly focused on the flexural behavior of slender beams.

Malhas (2002) tested 22 slender beams (a/d ~ 3.3) under four point bending. All specimens had cross-section 305 mm wide x 457 mm high. Two types of reinforcing steel were used: high strength ASTM A1035 reinforcing steel and normal strength reinforcing steel. Specimens were longitudinally and vertically reinforced either with ASTM A1035 or normal strength steel. These beams were designed using $f_{c\backslash}$ of 40 MPa and 60 MPa.

The reinforcement ratios were between 0.21% and 1.0%. Malhas observed that all

specimens exhibited ductile behavior prior to flexural failure. Malhas concluded that ultimate strengths of the beams were accurately predicted using the ACI 318 code theories and that detailing of development length and serviceability deflections appeared adequate using this code. Malhas also observed that after flexural cracking, the stiffness of the beams reinforced with high strength steel reinforcement was significantly reduced compared with the beams reinforced with normal strength steel. Other than the reduction in flexural stiffness, Malhas concluded that the behavior of slender beams using high strength steel were comparable with those beams reinforced with normal strength steel. Therefore, he stated that the direct replacement of regular steel with high strength steel was reasonable for slender beams.

Vijay et al (2002) carried out a project to study the bending behavior of slender beams reinforced with high strength ASTM A1035 steel. The results obtained during the tests were compared with the predictions using ACI 318 code provisions. Four beams were tested under four-point bending with a/d of approximately 3.5. Cross section dimensions of 305 mm wide x 457 mm high were similar for all the specimens. Concrete strength varied from 55 MPa to 77 MPa and reinforcement ratios used were between 0.40% and 0.80%. The researchers concluded that theories used in ACI 318 can also be used to predict the flexural capacity of slender beams with high strength reinforcement.

Ansley et al (2002) compared the behavior of slender beams reinforced with high strength ASTM A1035 reinforcing steel and similar slender beams reinforced with normal strength reinforcing steel. All specimens had cross-section 305 mm wide x 457 mm high. Two types of reinforcing steel were used, high strength ASTM A1035 reinforcing steel and normal strength reinforcing steel. To compare the flexural behavior of slender beams reinforced with different types of steel (ASTM A1035 and conventional Grade 60), two beams with the same dimensions and

different types of reinforcement were tested under four-point bending with a/d of 4.0. They also compared the contribution to shear strength of stirrups made with ASTM A1035 and conventional Grade 60 reinforcing steel.

For this purpose, two shear-critical beams, one with ASTM A1035 steel stirrups and another with normal strength steel stirrups, were tested under three-point bending with a/d of 1.4. For the flexure-critical tests, the authors found that the behavior of the beams up to the yield point of the normal reinforcing steel was similar, regardless of the reinforcement strength. After that point, the load deflection curve for the beam reinforced with high strength steel maintained the same path. However, for the beam with normal steel, the deflection rates increased, governed by yielding of the main tension reinforcement. At failure, the beam reinforced with high strength steel resisted 76% more applied load and it had 40% more ductility, considered by Ansley as the area under the load-deflection response, than the beam reinforced with normal strength steel. For the beams designed to fail by shear, it was concluded that the high strength steel stirrups played a minor part in the shear capacity of the section, with an increase in capacity of only 9%. However, only one specimen with high strength steel stirrups was tested and additional tests are required to generalize the contribution to shear strength of stirrups made with high strength steel.

The behavior of non-slender beams or deep beams cannot be accurately predicted using the traditional sectional methods of design because the Bernoulli bending theory does not apply. Since the axial strain distribution is not linear over the member height in deep beams, alternative design methods are necessary.

2.4 Deep beams

On slender beams, or deep beams, are frequently found in reinforced concrete structures. Examples of this type of beam include transfer girders, bridge piers and foundation walls where large concentrated loads are located close to the supports and where the shear-span-to-depth ratio (a/d) is less than 2.5. These structural members need special attention in their design due to the development of non-linear strain gradients under loading.

Deep beams are structural members loaded in a way that a significant part of the load transfer to the supports is through direct compression struts or arch action.
Generally, a beam is classified as a deep beam according to the overall span to overall depth ratio (L/h) or the shear span to depth ratio (a/d). Each of the design codes used in this project establishes different limits for these ratios to classify a beam as a deep beam. CSA A23.3-04 considers deep beams as flexural members with $L/h<2$. For ACI 318-05 and Euro code 2, deep beam design methods apply for $L/h<4$ or for beam regions with $a/d<2$.
Traditional sectional design methods for slender beams, where Bernoulli theory applies, do not accurately predict the behavior of deep beams. It has long been recognized that the strength of beams increases for smaller shear-span-to-depth ratios (a/d) [Kani et al., 1979; Varghese and Krishnamoorthy, 1966; Watstein and Mathey, 1958] and that the sectional approaches do not accurately predict the shear capacity of members with $a/d<2.5$ [Collins and Mitchell, 1991; Rogowsky and MacGregor, 1986].

Since the 1960's, there has been strong interest in developing simple but accurate techniques to design and analyze non slender members, including deep beams. It was necessary then, to find a technique that considered the gain in capacity of the beams for smaller a/d ratios. The Strut and Tie Method (STM) gave the designers a

very important tool to predict the capacity of deep beams as it considers the capacity as a function of a/d. This method analyzes concrete members with a plastic truss analogy that transfers the forces from the loading point to the supports using concrete struts and reinforcement ties [Schlaich et al., 1987; Marti, 1985].

Other methods for the design of deep beams have been proposed [Zsutty, 1968; Bazant and Kim, 1984; Nielsen, 1998]. The most recent method of design proposed was the Unified Shear Strength Model [Choi et al, 2007], which considers that the overall shear strength of a beam is given by the combined failure mechanism of tensile cracking and crushing of the top compression zone. These methods can be used for design of slender and/or non-slender beams with and without web reinforcement. However, none of these methods have been adopted by current design codes, and are not considered further in this study.

2.5Methods of Analysis

2.5.1. Finite Element Modeling (FEM) of Deep Beam

For the basic formulation of flexural beam models, two theories are used. The Euler-Bernoulli theory, which is a classical theory, is used for thin beams. The basic assumptions of this theory are that, after loading (a) the X-sections of the beam remain plane and (b) normal to the axis of bending. The Timoshenko's theory is used for deep beams. This theory takes into account the effect of transverse shearing deformations. According to this theory, the assumption (a) for Euler-Bernoulli theory may be valid but assumption (b) is not valid. In case of deep beams, one reason for the transferring of significant amount of load to the supports by compression strut, which joins the load and the reaction, is the large overall depth to span ratio. Due to this transfer of load, the strain distribution is no longer

assumed linear. Also, as compared to pure flexural, the shear deformations are significant.

The first order linear load deflection relationship is normally used for the analysis of reinforced concrete structures or deep beams and the strains developed in the structures are assumed small. This means that the geometric non-linearity is not taken into account. So the real behavior and the computed behavior of the member differ from each other normally, which ultimately lead to approximate solutions. The exact figure for the difference in results, when geometric nonlinearity is taken into account, is not known. It is obvious that plain concrete has a little resistance to crack propagation due to low tensile strength and limited amount of ductility. In case of compression, about one-third of the ultimate strength is occupied by these micro-cracks propagation. In case of tension (approximately to one-tenth of the compressive strength) brittle failure is occurred due to these cracks.

Existing methods used for the prediction of deep beam behavior is either based on elastic theory or semi–empirical formulation, none of them is entirely satisfactory (Yoo, et. al. 2004, Kong and Chemrouk, 2002).

- In recent years, various proposals have been floated for the design of reinforcement for in-plane forces based on the lower bound limit state approach where a stress field in equilibrium at the ultimate load is used in conjunction with an appropriate yield criterion. Such a stress field can be obtained by any suitable procedure such as a linear elastic finite element analysis. Reinforcement is then provided so that the combined resistance of the steel and concrete at every point is equal to or greater than the applied stress.

In theory, by satisfying equilibrium and yield exactly at every point simultaneously, the entire structure will become a mechanism at ultimate load. Practical considerations, such as reinforcement being provided as discrete bars, make it

impossible to achieve this idealized behavior. Also, the theory gives no guarantee that serviceability behavior will be satisfactory. However, if verified as an acceptable design process, the following advantages ensure:

- Analysis and design becomes one continuous process which is suited to automatic computation.
- steel is used economically as the design equations are based on minimizing steel requirements, although this will be affected by the convenience of fabrication;
- Excessive ductility demands are minimized by aiming for most parts of the structure to yield simultaneously at a particular ultimate load. The difference between the load at which yielding starts and the ultimate load is kept at a reasonable level which should prevent excessive cracking at working load.

Verification for practical reinforcement details can be provided by non-linear finite element modeling of the resulting designs, backed up by large experimental tests.

For the analysis of deep beams, various analytical tools are available. Among all these available analytical tools, finite element analysis (FEA) presents a better and convenient option. The FEM is a numerical procedure for the analysis of structures and continua. The classical analytical methods cannot be used for the satisfactory solution as the problem addressed is too complicated normally. The problem may be required to perform many analysis e.g. stress analysis, heat conduction, or many other areas. Digital computers are used to generate and solve many simultaneous algebraic equations which are produced by finite element procedure. Results are not too much accurate. However, the approximately exact solution may be obtained by processing these equations. Results are accurate enough for engineering purposes and obtainable at reasonable cost. The FEA usually involves the following steps;

- Division of the structure or continuum into finite elements. Mesh generation's programs, which are known as preprocessors, help the user in doing this work.
- Formulation of the properties of each element.
- Assembling of elements to obtain the FEM of the structure.
- Application of the known loads, nodal forces and/or moment.
- In case of stress analysis, specification of the supporting mechanism of the structure. This step involves setting many nodal displacements into known values.
- Solution of the simultaneous linear algebraic equations for the determination of nodal degree of freedom (DoF).
- In case of stress analysis, calculation of the element strains from the nodal DoF and the element displacement field interpolation, and finally calculation of stress from strains.

For linear and non-linear behavior of deep beam structural elements, finite element method can provide realistic and satisfactory solutions (Quanfeny and Hoogenboom, 2004, Samir and Chris, 2005). Computer based programs are used to reduce the effort and fatigue involved in manual analysis. The following factors influence the effectiveness of a program: (i) the use of efficient finite elements, (ii) efficient programming methods and effective use of the available computer hardware and software, and (iii) a very important aspect is the use of appropriate numerical techniques (Klus, 1990, Enem, et al., 2012). Many modeling techniques i.e. frame/line element, area/shell element, solid/3D element, STM and non-linear shell layered element, are available in commercially available software's e.g. SAP2000, ANSYS etc.

2.5.2. Nonlinear finite element

Non-linear finite element (FE) analysis of reinforced concrete (R.C) members like beams, slabs etc. using the majority of available commercial finite element software poses many numerical difficulties. Major difficulty is faced because of strain-softening behavior of concrete once it is yielded. This commercial finite element software of FE analysis remains totally inadequate in handling strain-softening behavior of concrete.

This is because this software offers only the traditional non-linear solution techniques like Newton-Raphson (N-R), modified Newton-Raphson (mN-R) methods etc. which cannot handle the non-linear post-yielding analyses of members made of materials like concrete, soil, rock etc. which exhibit strain softening behaviors after their yielding.

2.5.3. Strut and Tie Method

Design of concrete members where Bernoulli bending theory applies can be accurately predicted using the traditional sectional methods of design. However, for concrete members with disturbed regions, where the assumption of 'plane sections remain plane' does not apply, the Strut and Tie Method (STM) is probably the most practical and accurate hand calculation technique for design. The STM analyzes concrete members with a plastic truss analogy to internally transfer the applied forces from the loading points to the supports using concrete struts acting in compression and steel reinforcing ties acting in tension [e.g., Schlaich et al., 1987; Marti, 1985]. The struts and ties are interconnected at nodes. The forces in the elements must always satisfy statically equilibrium with the applied loads. Various stress limits are defined for the struts, ties and nodes.

STM are recommended to be used in the design of members with regions with non-linear strain distributions due to geometrical discontinuities, like dapped-end

beams, corbels, pile caps or corners of a frame. They are also appropriate at locations of statically discontinuities like deep beams, regions of members near to supports or at concentrated loads (Schlaich et al, 1987).

Schlaich et al (1987), Marti (1985), Rogowsky and MacGregor (1986) and others have described how the STM can be developed by following an assumed flow path of forces in a region of a structural member. Adoption of STM techniques into design codes has occurred over the last few decades. CSA A23.3-84 was the first North American design code to adopt the STM as a standard design technique of concrete members with disturbed regions, with provisions based on the Compression Field Theory (Collins, 1978). More recently, ACI 318-02 incorporated the STM in its Appendix A. Considerable research has been completed to study the viability of the STM for the design of deep beams using STM provisions given in the codes. Representative research done to study the viability of STM as a design technique for deep beams is described below.

Tan and Lu (1999) analyzed twelve deep beams loaded in four point bending using STM techniques. All specimens had the same reinforcement ratio of 2.6% with three different a/d ratios: 0.56, 0.84 and 1.13. The concrete strength varied from 41 MPa to 54 MPa. Three of the twelve beams were built without web reinforcement. The design code provisions used to predict the load capacity of the specimens were from CSA A23.3-94, in which the Strut and Tie Method provisions were similar to the current CSA A23.3-04 design code. The researchers concluded that the STM provisions provided uniform safety margins of capacity for deep beams with web reinforcement, since the quality of predictions did not deteriorate with the change in a/d. The average test/predicted capacity of specimens with web reinforcement was 1.10. For beams without web reinforcement, the predictions became more conservative for larger a/d ratios. The averages test/predicted capacity of specimens without web reinforcement was 1.27.

Aguilar et al (2002) studied the accuracy of the Strut and Tie Method given in Appendix A of the ACI 318-02 code in the prediction of four deep beams loaded in four-point bending. Appendix A of ACI 318-02 is similar to the current ACI 318-05 code provisions. The specimens tested had the same reinforcement ratio of 1.2% and same a/d of 1.13. Three beams had more than the minimum web reinforcement and one specimen had no horizontal web reinforcement and less than the minimum vertical web reinforcement in the shear span zone specified in Appendix A of ACI 318-02 Code. The capacity of all specimens, despite different failure modes, was within 6% of each other. The researchers found that by using the STM for the analysis, good predictions were obtained with an average test/predicted capacity ratio of 1.26.

For non-slender beams with normal strength concrete, normal strength reinforcement and minimum web reinforcement ratios, the reduction factors for strut strength established in the ACI 318-05 and CSA A23.3-04 codes for the STM technique have been shown to give safe predictions of capacity [e.g. Collins and Mitchell, 1991; Tan and Lu, 1999; Aguilar et al., 2002; Quintero et al., 2006]. However, it is important to consider the adequacy of those reductions factors in the design of deep beams reinforced with high strength steel reinforcement using Strut and Tie Method. Strain conditions of the reinforcement and differences in dowel action are the principal parameters that differentiate the behavior of the strut between beams reinforced with normal steel and those reinforced with high strength steel. In ACI 318-05, the strut strength reduction factors account for parameters that affect the strut strength including concrete strength, transversal reinforcement arrangements (when applicable), strain conditions of reinforcement, dowel action and uncertainties in the truss model [Quintero et al, 2006 and Aguilar et al, 2002]. However, these reduction factors have an empirical origin based on research completed for concrete members reinforced with normal strength steel. In

CSA A23.3-04, the strut strength reduction factor takes into consideration the strain conditions of reinforcement crossing the struts, but they omit direct consideration of the effect of dowel action.

2.6. Factors Affecting the Shear Strength of Deep Beams

The important factors that affected the shear capacity of the deep beams were shear span to depth ratio, compressive strength of concrete, longitudinal reinforcement, horizontal shear reinforcement and vertical shear reinforcement .the contribution of each factor on the shear capacity of deep beams is discussed below.

2.6.1Shear Span to Depth Ratio (a/d)

The shear strength of a deep beam largely depends on its span to depth ratio. This has been established after Kani's investigations in the 1960s. Later other researchers (Rogowsky 1986 and Collins 1991) also investigated the size effect on deep beams and made the same conclusion. All experimental investigations on deep beams showed that the shear span to depth ratio is the main parameter that affects their shear strength as it increases with the decrease of a/d ratio (Manuel 1971, Smith 1982, Mau 1989, Tan 1995, Ashour 2000, Londhe 2010). This is because as the (a/d)ratio decreases, the sheer force transferred by the concrete strut directly to the supports. This mechanism is called the strut and tie action in deep beam.

2.6.2 Beam Span to Depth Ratio (L_n/d)

Manuel et al. (1971) performed 12 experiments on deep beams with different span to depth ratio and commented that, similar to (a/d)ratio, (L_n/d) ratio has a significant influence on the shear strength of deep beam where the shear strength is inversely proportional to (L_n/d) ratio .This is because as the (L_n/d) ratio increased, a longer arch is required to transfer the load to the support and, at the same time,

the mid span deflection increases which results in wider flexural crack and therefore, the shear strength decreases (Tan 1995).

2.6.3 Compressive Strength of the Concrete fc'

The shear strength is a function of the compressive strength, fc'. El-Sayed et al. (2006) showed that the shear strength increased by 10.7% when $f_{c/}$ increased by 44.5% (fc' from 43.6 MPa to 63 MPa). This increase is not proportional, however, because in the case of high strength concrete (> 60 MPa), the fractured aggregates at ultimate load will generate less friction compared to normal strength concrete .Similarly, Smith's (1982) investigation on deep beam showed that $f_{c\backslash}$ has a great influence on the shear capacity. Their results showed that the capacity is higher in the case of a deep beam with high fc' and low web reinforcement compared to a beam with low fc' and high web reinforcement. However, their tests were limited to only normal strength concrete ($fc' = 16$ to 23 MPa). On the other hand, Londhe (2010) showed that the compressive strength of concrete ($fc' = 24$ to 37 MPa) has small effect on the shear increase of deep beams.

2.6.4Longitudinal Reinforcement

Mau and Hsu (1989) conducted 64 experiments on deep beams and found that with the increase of longitudinal reinforcement, the shear strength of deep beam increased significantly. Similar studies by Ashour (2000) and Londhe (2010) found that the longitudinal reinforcement has linear correlation with the shear strength up to a certain limit for deep beams without shear reinforcement and beyond that it has no effect. Longitudinal reinforcement increases the shear strength of deep beams by reducing the crack width, by improving the interface shear transfer mechanism and by increasing the dowel action (Londhe 2010).

2.6.5Horizontal Shear Reinforcement

Although the reason to provide the horizontal shear reinforcement was to improve the shear capacity, some studies showed that it has no effect on the shear strength (Kong 1970). Other researchers found that there will be a little increase in shear strength with the increase in horizontal shear reinforcement (Smith 1982). This is specially the case of low vertical shear reinforcement, where adding horizontal shear reinforcement ratio in deep beams will not have further contribution on its shear strength (Smith 1982). On the other hand, Ashour (2000) reported that horizontal shear reinforcement is more effective compared to vertical shear reinforcement in case of $(^{a}/_{d})$ <0.75.

2.6.6Vertical Shear Reinforcement

Vertical web reinforcement is one of the major parameters that affect the shear strength of deep beams. The primary purpose of vertical web reinforcement is to provide confinement to the concrete which helps to improve the shear capacity of deep beams. In addition to this, it is more effective in improving the shear strength compared to horizontal shear reinforcement and in case of a shear failure it makes the beam fail in a more ductile manner. All studies showed that the shear strength of a deep beam increases linearly with the increase of the vertical shear reinforcement (Clark 1951, Kani 1967, Kong 1970, Smith 1982, Oh 2001, Quintero-Febre 2006, Tan 1995). However, Smith (1982) found that the contribution of the vertical shear reinforcement diminishes as the $(^{a}/_{d})$ decreases $(^{a}/_{d}<1)$. Similar study by Ashour (2000) confirmed that the higher the (a/d) ratio $(^{a}/_{d}>0.75)$, the higher the contribution of the vertical web reinforcement. On the contrary, Londhe (2010) reported that the shear strength increase was observed up to a vertical shear reinforcement ratio of 1.25%.

2.7 The nature of failure of deep beams

The failure of deep beams subjected to either central point load or two symmetrical point loads is related to the failure of the tied arch which is formed in the beam after diagonal cracking. According to de Paiva and Sies , the primary modes of failure of the tied arch are flexure failure and shear failure. A flexural failure occurs either when the concrete rib of the tied-arch fails by crushing at the crown or the tension tie ruptures. The failure is termed flexure failure because the full flexural capacity and ductility are realized. A shear failure contains two types:-

- Diagonal compression failure: in this type of failure an inclined crack first develops nearly along a line joining the load point and the support point. After further increase in load, a second inclined crack parallel to the previous crack appears. The final failure is due to the destruction of the portion of concrete between these two cracks which acts as a strut between the load and support point.
- The second type of shear failure is a diagonal tension failure: in this mode failure occurs by a clean and sudden fracture nearly along a line joining either support with the nearest loading point. The failure is similar to splitting of a cylinder under diagonal compression. This mode sometimes called shear proper failure.

Bresler and Macgrego have included anchorage failure and bearing failure as deep beam failure modes along with the flexure and shear failure mentioned above. These two additional modes of failure are generally undesirable and are not limited to deep beams although the geometry and behavior of deep beams have increased the likelihood of their occurrence. Anchorage failure results fromthe very high tension stresses in the main longitudinal reinforcement in the region near the supports. Special anchorage provisions, such as hooking the bars, can be used to

prevent this mode of failure. Baring failures on the other hand result from the high vertical stresses at the support and load points. Adequate design and detailing of the bearing and load blocks will prevent this mode of failure.

2.9 Strut and Tie Model

Design of concrete members where Bernoulli bending theory applies can be accurately predicted using the traditional sectional methods of design. However, for a concrete member with disturbed regions, where the assumption of plan sections remains plan does not apply, the strut and tie method (STM) is probably the most practical and accurate hand calculation technique for design. The STM analyzes concrete members with plastic truss analogy to internally transfer the applied forces from the loading points to the supports using concrete struts acting in compression and steel reinforcing ties acting in tension. The strut and ties are interconnected at nodes. The forces in the elements must always satisfy statically equilibrium with the applied loads. Various stress limits are defined for the struts, ties and nodes.

2.9.1 Element of Strut and Tie Model

A strut and Tie model is a truss model representation of reinforced concrete member (or region) consisting of concrete struts acting in compression and steel reinforcing ties acting in tension. The strut and ties are interconnected at nodes .the forces in the element must always satisfy statically equilibrium with the applied loads.

- **Strut**

Struts are the components within the STM that carry compressive stresses. Their geometries vary widely and depend upon the force path from which they arise. The most common types of struts are shown in Figure 2. 1.

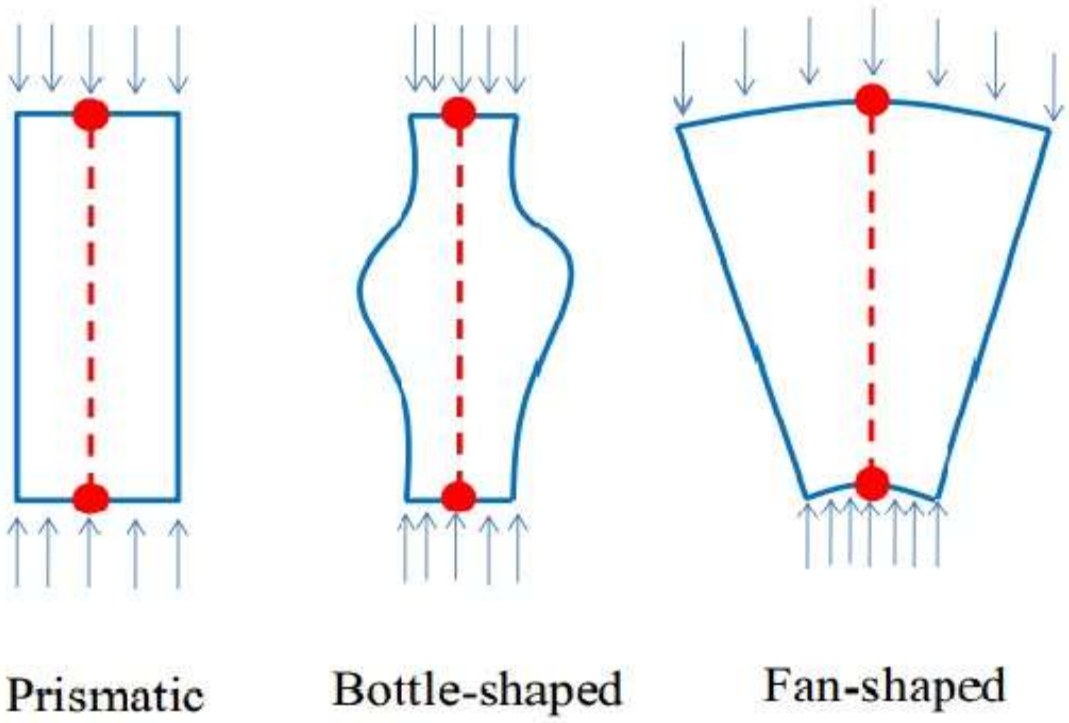

Figure2. 1: Types of struts

A prismatic strut is the most basic type, has a uniform cross-section and is typically used to model the compressive stress block of a beam element.

A strut that forms when the geometrical condition at its end is well defined, but the rest of it is not confined to a specific portion of the structural element are known as a bottle-shaped strut. As, to avoid premature failure, appropriate crack control reinforcement should always be placed across bottle-shaped struts, most design specifications require minimum amounts of crack control reinforcement in regions designed using STMs.

A compression fan is another type of strut formed when stresses flow from a large to a much smaller area. It is assumed to have negligible curvature and, therefore, to not develop transverse tensile stresses. A strut that carries a uniformly distributed load to a support reaction in a deep beam is the simplest example of a compression fan.

- **Ties**

Ties are the components that carry tension and are generally confined to reinforcing or pre-stressing steel. Therefore, the geometry of a tie is much simpler than that of a strut and is confined to elements that can carry high tensile forces with the allowable force generally given as a fraction of the yield force.

- **Node**

Nodes are analogous to joints in a truss and transfer forces between struts and ties, and as a result, are subjected to multi-directional states of stress. The limiting compressive strength of a node is typically obtained from the product of the concrete strength and a reduction factor which is determined based on the node type. Nodes are sorted by the types of forces being connected: C-C-C for three compressive forces; C-C-T for two compressive forces and one tensile force; C-T-T for one compressive force and two tensile forces; and T-T-T for three tensile forces. Figure 2.2 shows the basic types of nodes in a 2-D member, with C denoting compression and T tension.

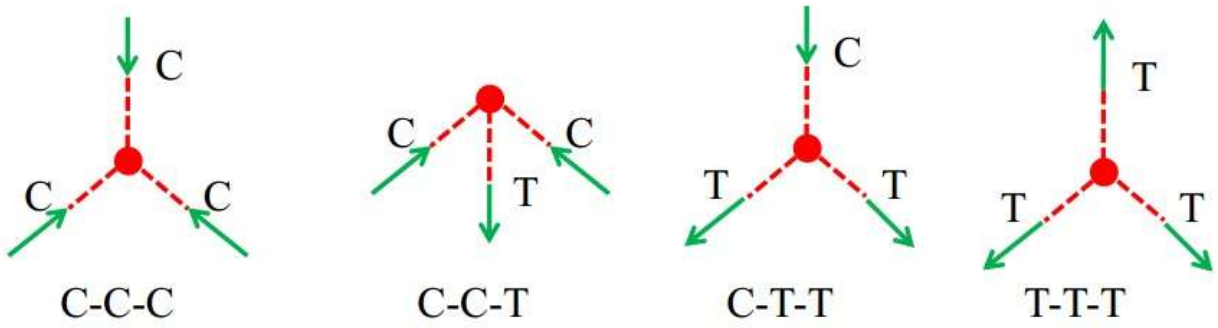

Figure2. 2: Basic types of nodes.

2.10 Modes of failure

The STM is a method for evaluating the ultimate limit state of a member .therefore, during the analysis or design of concrete elements, different modes failure can be assumed. The predicated ultimate capacity of a concrete member designed by STM will be governed by crushing of the strut, yielding of the tension ties, and failure of the nodes by reaching stresses larger than the allowable nodal stresses, or by anchorage failure of the reinforcement.

2.11 Configurations for strut and tie model

For a given planer deep beam with concentrated load, different admissible configurations of strut and tie models can be developed. These configurations shown in Figure 2.3 and described in the following sections, are classified direct strut and tie model (STM.D), indirect strut and tie model (STM.I) and the combined strut and tie model (STM.C).

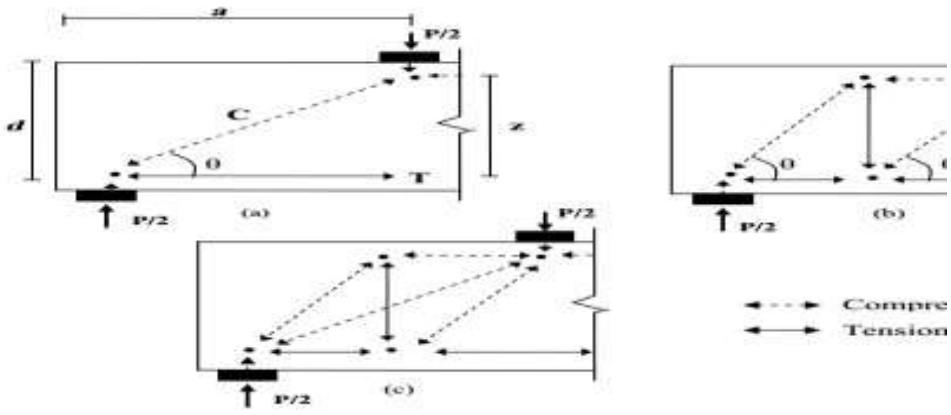

Figure2. 3: (a) direct strut and tie model. (b)Indirect strut and tie model. model. (b)Indirect strut and tie model. (c)Combined strut and tie model

(c)Combined strut and tie model

2.11.1 Direct Strut and Tie Model

In the design of simply supported beams subject at two concentrated loads, several ways to present the stress flows can be done. The simplest configuration to represent the flow of the forces using strut and tie model consists of three compression strut and tension tie (see Figure 2.3a and 2.4).one horizontal compression strut it located between the loading points and the other two struts are diagonally oriented from the loading points to the supports. The tension tie goes from support to support. The location of the tension tie is at the centroid of the line of the action of the reinforcement, this model is called direct strut and tie model (STM.D).

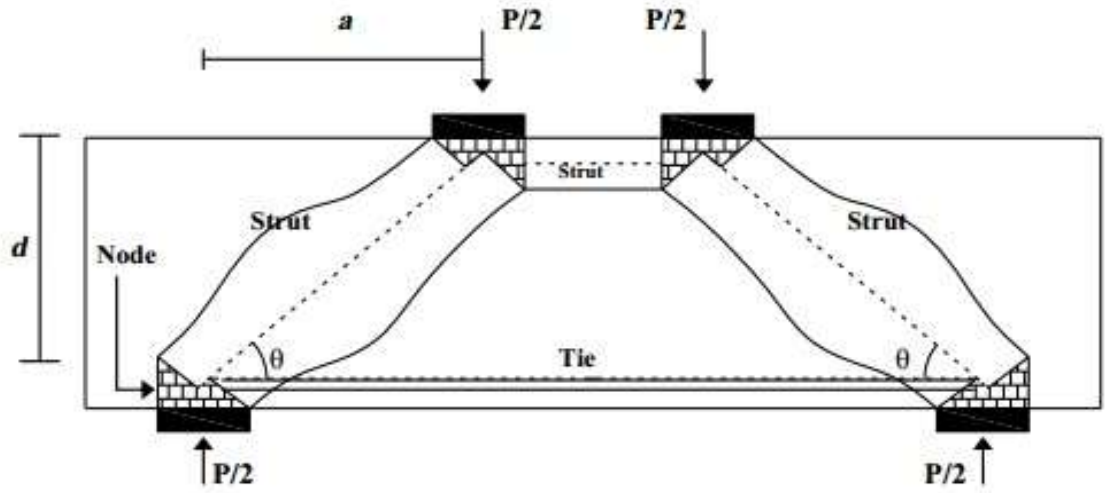

Figure2. 4: Direct struts and tie model

2.11.2 Indirect Strut and Tie Model

In this mode, the forces are transmitted from the loading point to the support through series of parallel diagonal compression struts and associated ties. Two assumptions must be satisfied. No strut is developed directly from the loading point

to the support and vertical component of the strut forces to the top of member. This model is called indirect strut and tie model (STM.I) see Figure 2.3.b.

2.11.3 Combined Strut and Tie Model

In this strut and tie model, the primary shear strength comes from truss developed from the contribution of the vertical web reinforcement similar to STM.I. After yielding of the vertical web reinforcement, additional load is also taken by the direct diagonal strut going from the loading to the support .this called combined strut and tie model (STM.C) see Figure 2.3c.

2.12Limit of angle between inclined strut and tie

ACI code defines the lower limit of the angle between the inclined strut and the tie as 25^{o} based on the principal of Saint-Venant. This lower limit guarantees that B-region does not exist in the beam and trapezoidal Strut-Tie model may be applied. The angle converges consequently to about 72^{o}.The result indicates that in the case of the beam with h/l greater than about 1.2 , the upper part of the beam should be modeled as B-region.

2.13Design Procedure for STM

The design of a STM entails laying out a truss that fits within a deep beam with an appropriate cover while being able to transfer the forces without failing, in accordance with the following process

1. Fix the boundaries of the D-region and calculate the boundary forces (the ultimate design forces) from the imposed local and sectional forces.

2. Propose a STM and solve for the truss member forces.

3. Calculate the reinforcement for the tie and select a suitable bar size.

4. Evaluate the dimensions of the nodes such that their capacities are sufficient to carry the truss member forces.

5. Evaluate the dimensions of the struts such that their capacities are sufficient to carry the truss member forces.

6. Provide details of the reinforcement required for the structure.

The STM design provisions consist of rules defining the dimensions and ultimate stress limits of the struts and nodes as well as the requirements for the distribution and anchorage of reinforcements. The major codes are discussed individually in the following sections.

2.14 Code provisions for strut and tie method

According to ACI, the strength of strut depends on the geometry of the strut .the effective compressive strength of the concrete in a strut is calculated with equation:

$f_{ce} = 0.8\beta_s f_c$……..……...**2.1**

β_s=1.0 for struts with uniform cross section area over it length

=0.75 for bottle shape struts with distributed reinforcement crossing.

=0.6 for bottle shape struts without distributed reinforcement crossing.

=0.4 is used for struts in tension members.

The compressive strength of nodal zones is calculated with equation:

$f_{nn} = f_{cen} A_{nz}$…..……..……**2.2**

A_{nz}=smaller of(1)area between the area of the face of the nodal zone perpendicular to the load acting on that face, and (2) the area of a section through the nodal zone perpendicular to resultant force on the section.

f_{cen} =effective compressive strength of the concrete in the nodal zone .it is calculated with equation:

$f_{cen} = 0.85\beta_s f_c$…..……**2.3**

β_s=1.0 for nodal zones bounded by struts or bearing areas or both (CCC node).

=0.8 for nodal zones anchoring one tie (CCT).

=0.6 for nodal zones anchoring more than one tie (CTT node).

The amount of transverse reinforcement required to resist transverse tensile cracks can be calculated by:

$\frac{A_{si}}{b_{si}} \sin \alpha_i \geq 0.003$…..……..…**2.4**

Where

A_{si}=The total area of surface reinforcement.

s_i = the spacing of surface reinforcement.

b=the effective width of the beam.

2.15Previous study

2.15.1 Previous experimental work

Juan de diosGaray-Moran and Adam S. Lubel (January, 2008) study the behavior of deep beams under four-point bending containing high strength longitudinal reinforcing steel (ASTM A1035). Specimens were constructed at full scale, according to the general requirements of CSA A23.3-04, ACI 318-05 and Euro code 2 design provisions.

Different parameters were examined for their influence on specimen behavior.

These parameters were the shear span to depth ratio (a/d), the longitudinal main reinforcement ratio (ρ), and the presence or omission of vertical web reinforcement. The strength of main longitudinal reinforcement was studied through comparison

against specimens with Grade 400R normal strength reinforcement.

A total of ten specimens were constructed. Six beams were reinforced longitudinally with high strength steel and contained normal strength vertical web reinforcement. Two specimens were longitudinally and vertically reinforced with normal strength steel reinforcement. Finally, two specimens were built with only main longitudinal high strength steel and no web reinforcement. Concrete with compressive strength ranging from 23 MPa to 48 MPa was used in the specimens.

2.15.2Previous study of analytical work

Chow, Conway and Winte used the method of finite different to formulate equations to calculate shear and normal stresses for single span deep beams. Although the method was directly applicable to structure mode of homogeneous materials. In their discussions of the application of this work to reinforced concrete structures stated:

"The stress distribution in such reinforced concrete members must be expected to differ from that given on two counts, the non-homogeneity of the material; and the cracking of the tension zone. For this reason, no unique and strictly justified design procedure can be proposed. Chow et al. proposed that the total steel area provided is given by:

$$A_s = \frac{1.5T}{F_s} \quad \textbf{2.5}$$

The stress distribution in deep members of homogenous materials has been studied and well established by many authors, using analytical models. Most of these models are based on the classical theory. A common method for solving two-dimensional problems involves the determination of the Airy stress function, F, to satisfy the boundary conditions and comply with the bi harmonic equation:

$$\frac{a_4 F}{a x_4} + \frac{2a_4 F}{2a x_2 a y_2} + \frac{a_4 F}{a y_4} = 0 \quad \textbf{2.6}$$

Once the Airy stress function has been found, the stresses arising from the subsequent derivatives of the function are as follows:

$$\sigma_x = \frac{a_2 F}{ay^2} \quad \text{.....} \quad \textbf{2.7}$$

$$\sigma_y = \frac{a_2 F}{ax^2} \quad \text{.....} \quad \textbf{2.8}$$

$$\tau_{xy} = \frac{a_2 F}{axay} \quad \text{.....} \quad \textbf{2.9}$$

Also Coul (February 1966) studied deep beams using a numerical method for the analysis of plane stresses of deep beams or any structure in which the stress system can be considered planar. In this method the stresses are given by a Fourier series as a function of one direction; the coefficients of the series depend upon the other direction. By utilizing the principle of least work the coefficients can be determined. This procedure differs from the methods using Airy stress functions in that the stresses are obtained directly from the solution of Fourier series, without the differentiation involved in the other methods. The series were chosen to satisfy the boundary conditions in every direction .The finite difference method, a simplified procedure for the numerical solution of deep flexural members.

Chapter Three

Prototype Beams

3.1 Introduction

The main objective of this study is to present the suitable modeling techniques. In order to meet the objective, a small deep beam having shear span to depth ratio less than 2.5,The beam was designed by using modeling in SAP2000 Truss modeling (STM) and From Shell (thick) analysis the design membrane force using for (reinforcement layer)modeling in (SAP2000) by ACI 318-11 code . best modeling technique is recommended for the modeling and designing of deep beam. This chapter focuses on the description of beams and design of deep beam by two techniques.

3.2Data Collection and Details of Specimens

Data has been collected from previous study Juan de dios Garay-Moran and Adam S. Lubel (January, 2008)who performed experimental works.tested reinforced concrete deep beams to failure under two symmetrical loads.All specimens had a rectangular cross section of 300 x 607 mm, the variable were the depth-to-span ratio,the first cracking load, failure load, a/d ratio, the mode of failure and the type of loading two symmetrical point loads. In this Information of tested reinforced concrete deep beams was collected from above research and selected beam from above research is (MS1-2) to design by two technique strut and tie method STM (truss modeling) and shell thick technique .and select beams MS1-3, MS2-3, MS3-2, MW1-2 and MW3-2 to study the behavior of deep beam by nonlinear shell layered technique in software program SAP2000.

3.2.1Details of Specimen MS1-2

Beam MS1-2 had longitudinal main tensile reinforcement consisted of 6-#6 bars with an effective yield strength f_y of 870 MPa. This arrangement of main longitudinal steel gave a reinforcement ratio ρ of 1.13%. Vertical web reinforcement consisted of 10M Grade 400R bars with f_y of 405 MPa and average longitudinal spacing of 200 mm. Longitudinal web reinforcement consisted of 2-#4 bars at the top and 2-#4 bars near mid-height. The beam span was 1700 mm and the shear span, a, was 600 mm, giving a shear span to depth ratio of 1.19. Reinforcement details of beam MS1-2 are shown in Figure 3.1. The dimensions shown in this figure are in mm.

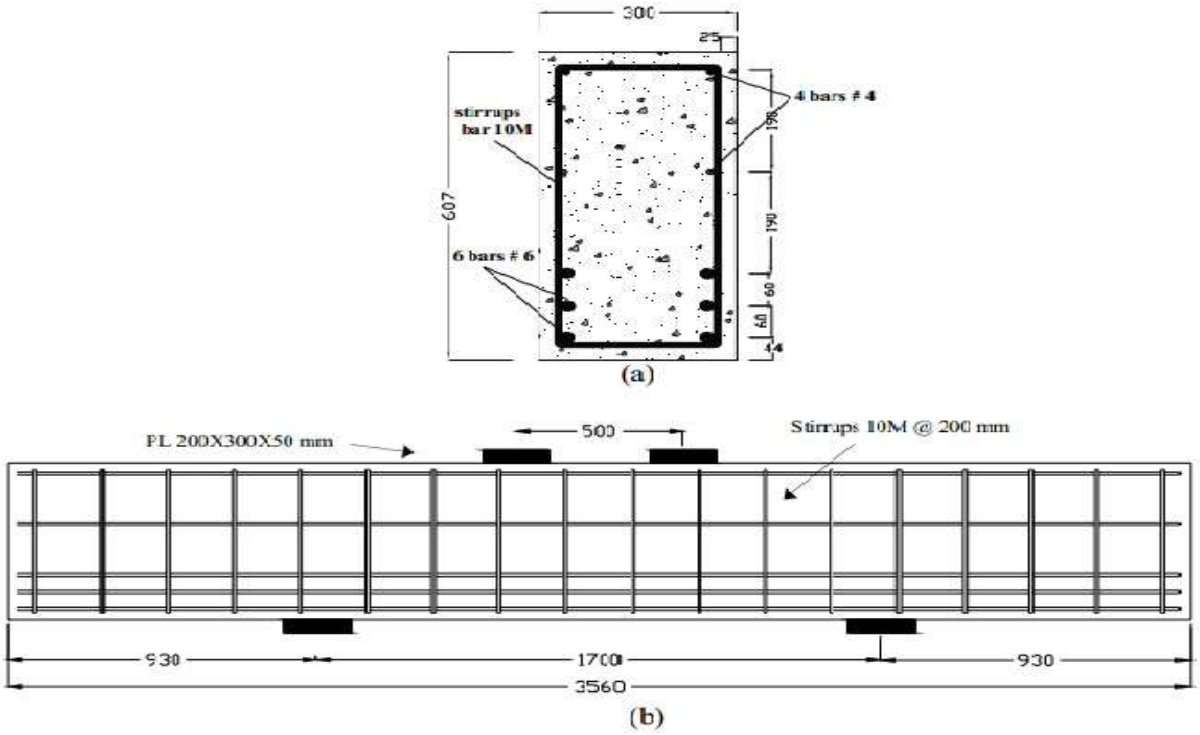

Figure3. 1: Beam MS1-2(a) Cross Section (b) Elevation

Section (b) Elevation

3.2.2Details of Specimen MS1-3

Beam MS1-3 had longitudinal main tensile reinforcement consisted of 9-#7 bars with an effective yield strength f_y of 870 MPa. This arrangement of main longitudinal steel gave a reinforcement ratio ρ of 2.29 %. Vertical web reinforcement consisted of 10M Grade 400R bars with f_y of 405 MPa and average longitudinal spacing of 200 mm. Longitudinal web reinforcement consisted of 2-#4 bars at the top and 2-#3 bars near mid-height. The beam span was 1700 mm and the shear span, a, was 600 mm, giving a shear span to depth ratio of 1.19.Reinforcement details of beam MS1-2 are shown in Figure 3.2.

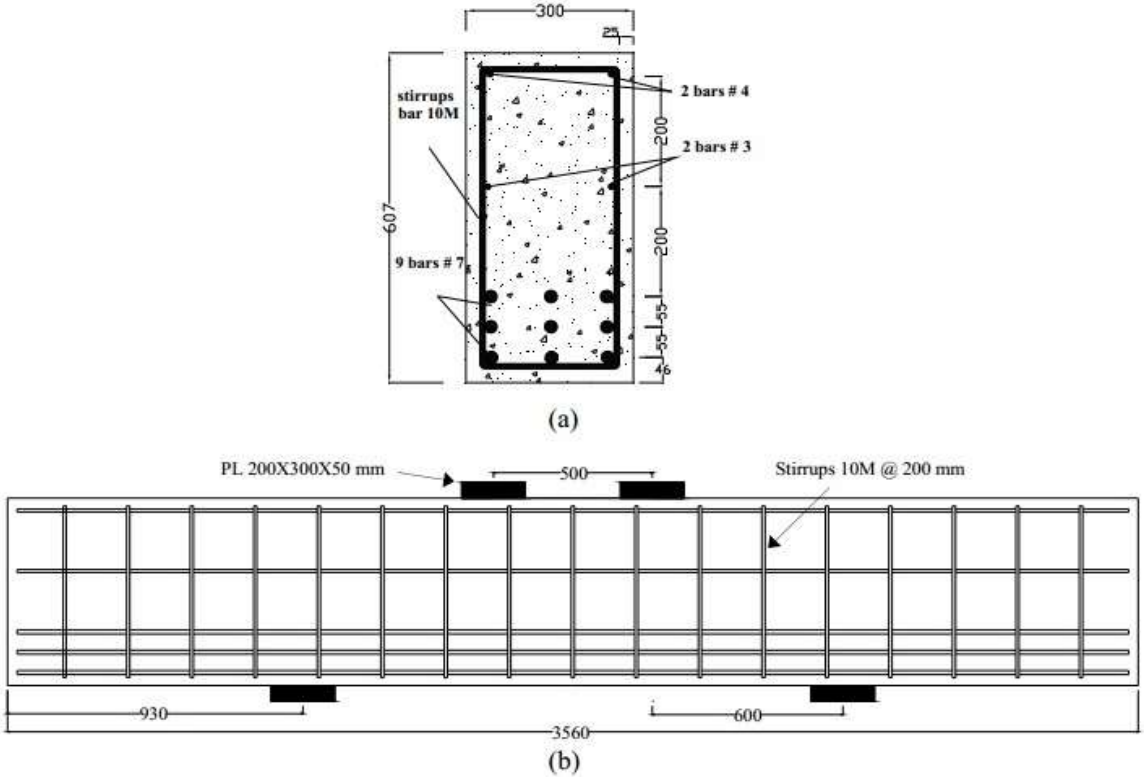

Figure3. 2: Beam MS1-3(a) Cross Section (b) Elevation

Section (b) Elevation

3.2.3Details of Specimen MS2-3

Beam MS2-3 had the longitudinal main tensile reinforcement consisted of 9-#7,the effective yield strength f_y of 870 MPa. This arrangement of main longitudinal steel gave a reinforcement ratio ρ of 2.29 %. Vertical web reinforcement consisted of 10M Grade 400R bars with f_y of 405 MPa and average longitudinal spacing of 200 mm. Longitudinal web reinforcement consisted of 2-#4 bars at the top and 2-#4 bars near mid-height. The beam span was 2300 mm and the shear span, a, was 900 mm, giving a shear span to depth ratio of 1.78. Dimension and reinforcement details of beam MS2-3 are shown in Figure 3.3.

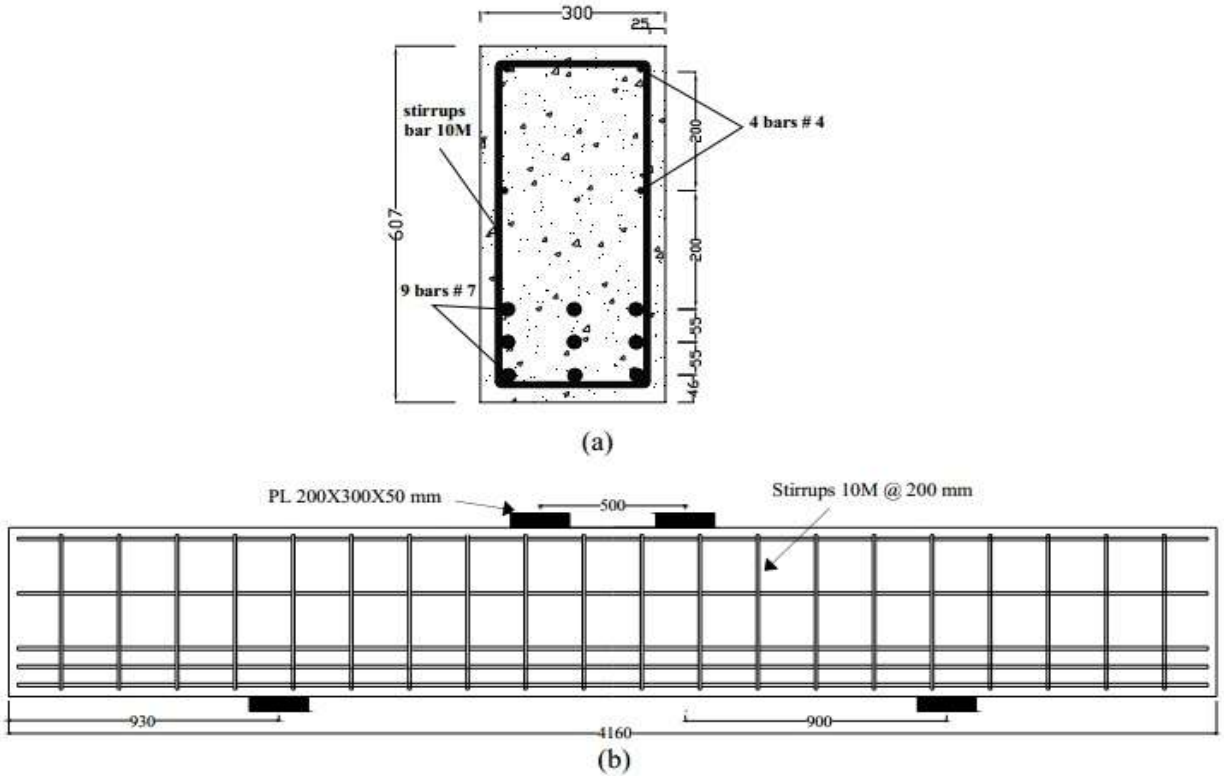

Figure3. 3: Beam MS2-3(a) Cross Section (b) Elevation

Section (b) Elevation

3.2.5Details of Specimen MS3-2

Beam MS3-2 had the longitudinal main tensile reinforcement consisted of 6-#6 bars with an effective yield strength f_y of 870 MPa. This arrangement of main longitudinal steel gave a reinforcement ratio ρ of 1.13%. Vertical web reinforcement consisted of 10M Grade 400R bars with f_y of 405 MPa and average longitudinal spacing of 150 mm. Longitudinal web reinforcement consisted of 2-#4 bars at the top and 2-#4 bars near mid-height. The beam span was 2900 mm and the shear span, a, was 1200 mm. For this specimen, the shear span to depth ratio was 2.38. Dimension and reinforcement details of beam MS3-2 are shown in Figure 3.4.

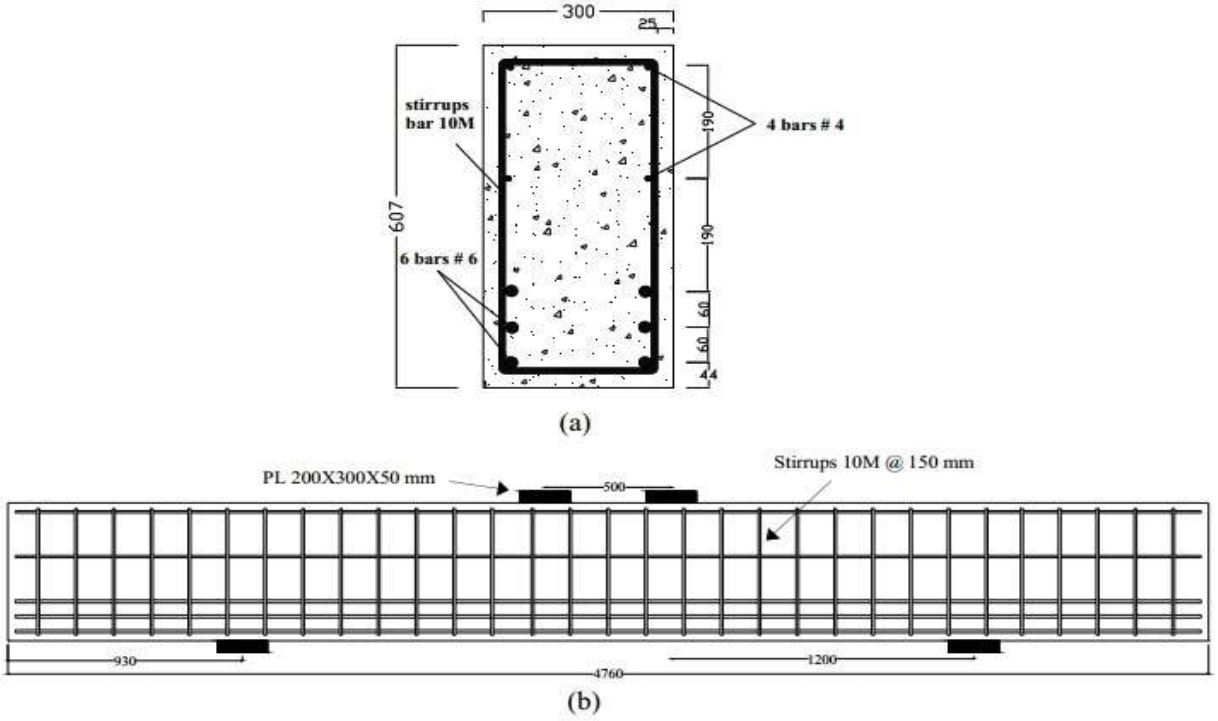

Figure3. 4: Beam MS3-2(a) Cross Section (b) Elevation

Section (b) Elevation

3.2.6Details of Specimen MW1-2

Beam MW1-2 had The longitudinal main tensile reinforcement consisted of 6#6 ASTM A1035 bars with an effective yield strength f_y of 870 MPa. This arrangement of main longitudinal steel gave a reinforcement ratio ρ of 1.13%. No vertical web reinforcement was provided within the beam span. Three 10M stirrups at 200 mm spacing were provided at beam ends beyond the supports. 2-#4 bars were placed at the top of the beam to hold the stirrups at the end of the beam and to maintain the same longitudinal reinforcement configuration with respect to the beams with vertical web reinforcement. The beam span was 1700 mm and the shear span, a, was 600 mm, giving a shear span to depth ratio of 1.19. Dimension and reinforcement details of beam MW1-2 are shown in Figure 3.5.

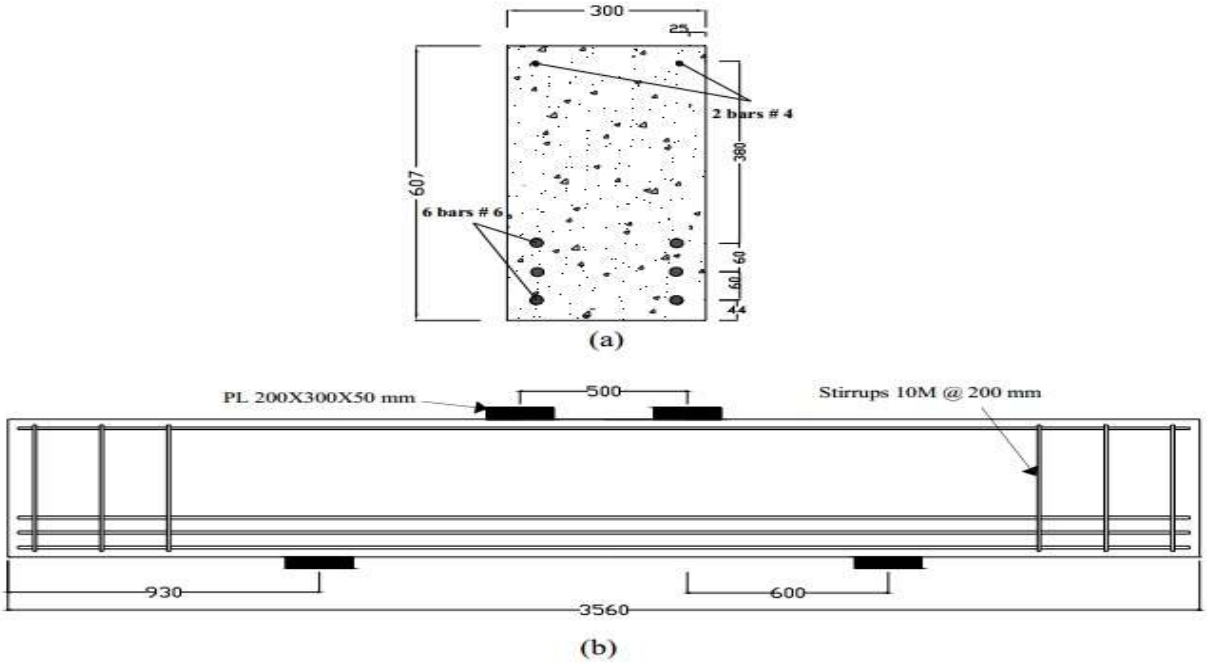

Figure3. 5: Beam MW1-2(a) Cross Section (b) Elevation

Section (b) Elevation

3.2.7 Details of Specimen MW3-2

Beam MW3-2 had the longitudinal main tensile reinforcement consisted of 6–#6 bars with a yield strength f_y of 870 MPa. This arrangement of main longitudinal steel gives a reinforcement ratio ρ of 1.13%. No vertical web reinforcement was provided within the beam span. Three 10M stirrups at 200 mm spacing were provided at beam ends beyond the supports. 2-#4 bars were placed at the top of the beam to hold the stirrups at the end of the beam and to maintain the same longitudinal reinforcement configuration with respect to the beams with vertical web reinforcement. The beam span was 2900 mm and the shear span, a, was 1200 mm, giving a shear span to depth ratio of 238. Dimensions and reinforcement details are shown in Figure 3.6.

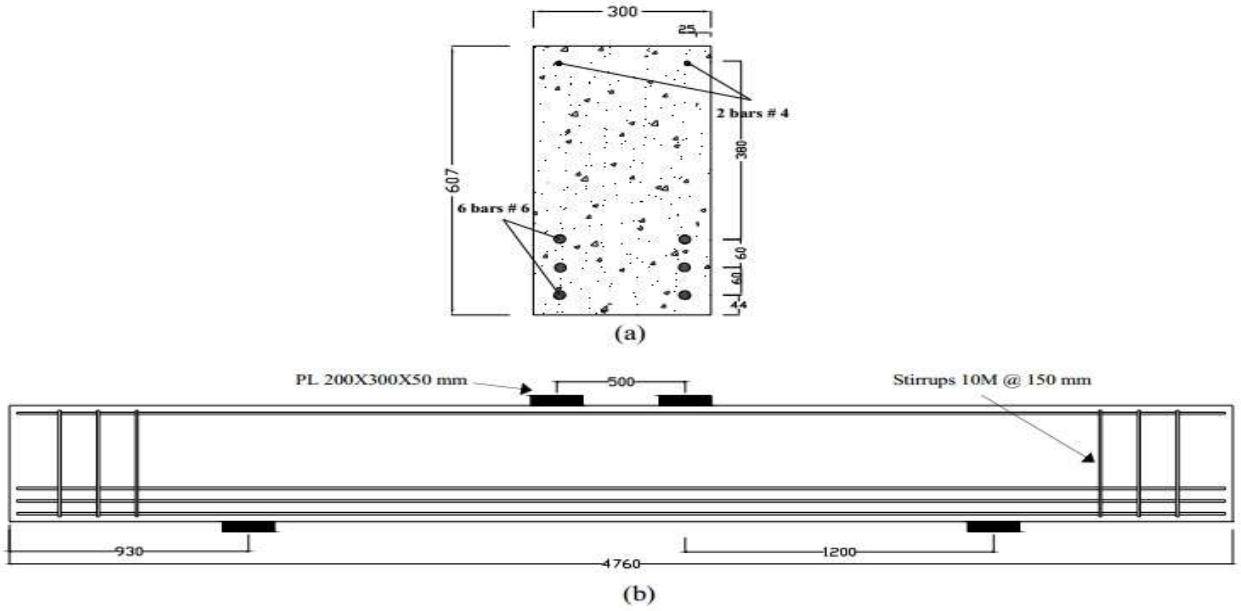

Figure3. 6: Beam MW3-2(a) Cross Section (b) Elevation

Section (b) Elevation

3.3 Different Modeling Techniques

3.3.1Shell/Area Element (Thick Shell Element)

The thick shell elements have both in-plane stiffness and out-of plane stiffness. In case of non-planer element, in-plane and out-of-plane behaviors become coupled. For the modeling of each homogenous shell element in the structure, pure membrane, pure plate, or full shell behavior may be used. For non-planer element, the full shell behavior is generally recommended, unless the entire structure is planer and is adequately restrained. The material for thick shell/area element is modeled as linear and homogenous.

The beam MS1-2 is modeled in SAP2000 using shell/thick technique which is assigned end releases, the distance of supports is 930mm from the edges, The effective depth of the beam is 503mm; the loading is symmetrical in two point loads, 456kN applied at the distance 600mm from the support joint (shear span), the beam span is 1700mm;the distance between loads is 500mm.and defines material of concrete and reinforcement available in literature. (f_y=870MPa and $f_{c/}$=44MPa).

3.3.2Truss modeling in SAP2000

The beam MS1-2 is modeled in SAP2000 using 2D truss element which is assigned end releases. The truss height is the effective depth of the beam is 503mm; the loading is symmetrical in two point loads, 456kN applied at the distance 600mm from the support joint (shear span). The length of the tie in bottom is the beam span is 1700mm;the span of the tie in top is the distance between loads is 500mm.and defines material of concrete and reinforcement available in literature.(f_y=870MPa and $f_c{}^{\backslash}$ = 44MPa).

3.3.3Nonlinear shell layered Element

In layered shell, material nonlinearity can be considered. To define number of layers in the thickness direction, each with an independent location, thickness, behavior, and material, the layered shell is used. Although layered shell can be controlled on a layer-by-layer basis, this usually represents full shell behavior. Actual stress-strain relationship of the materials used in different layers can be incorporated; therefore, this model may be the most suitable technique for assessing the true behavior of the deep beams as the material non-linearity and strain distribution across thickness can be incorporated using rebar and concrete layers.

For all beams in this study (MS1-3,MS2-3,MS3-2,MW1-2 and MW3-2) the thickness of the shell is 300mm, depth of shell is 607mm and divided shell to many layers, some of layers for main tension reinforcement, for horizontal reinforcement, for top reinforcement and some of layers for concrete .and defines material of concrete and reinforcement available in literature.

3.4 Design calculations of Deep Beam (MS1-2)

3.4.1 SAP2000 Truss (STM)

1. Flexural design

- **Main Reinforcement (Tension):**

From result of truss analysis in SAP2000 software (F_{Tie} =543.94 kN)

$$A_S = \frac{F_{Tie}}{0.7 f_y} = \frac{543.94 * 10^3}{0.7 * 870} = 893.16 \text{ mm}^2 \ (2.98 \text{ mm}^2/\text{ mm})$$

Use steel bar # 6

4#6 Bars (As provided= 1141mm^2)

- **Minimum Reinforcement (As_{min})**

$As_{min} = \frac{1.4}{f_y} * b * d = \frac{1.4}{870} * 300 * 503 = 242.8\ mm^2$

$As_{min} = \frac{0.25 * \sqrt{f_{\grave{c}}}}{f_y} * b * d = \frac{0.25 * \sqrt{44}}{870} * 300 * 503 = 287.63\ mm^2$

Take max $As_{min} = 287.63\ mm^2$

Check Main Reinforcement

$As > As_{min}$(O.K)

- **For top reinforcement**:

Use steel bar # 4 and minimum area of steel

3#4 Bars (As provided= $381mm^2$)

Shear Design

- **Percentage of Reinforcement to Control Cracking (Strut Forces)**

A summing Steel bar **ASTM** 10M for vertical web reinforcement and steel bar **# 4** for horizontal web reinforcement

- **Percentage of Vertical reinforcement**

UseNo.10M ties with two legs at spacing of 120 mm

$A_{bar} = 100.29\ mm^2$

$\rho_v = \frac{Av}{S*b} = \frac{2*100.29}{120*300} = 0.005572 > 0.0015$ (O. K)

- **Percentage of Horizontal reinforcement**

Use 2 #4 @ Space200 mm

A_{bar} (h) $= 126.7mm^2$

$\rho_h = \frac{2*126.7}{200*300}$ =0.004223>0.0025 (O. K)

- **Percentage of Web reinforcement (Check)**

$\Sigma (\rho_i) (\text{Sin } \gamma_i) = \rho_v \text{ Sin } (90-\theta) + \rho_h \text{ Sin } (\theta)$

= 0.005572 *Sin (90-39.97) +0.004223*Sin (39.97)

$\Sigma (\rho_i) (\text{Sin } \gamma_i)$ =0.00698>0.003 (O. K)

- **Check the Strength for Strut and Tie Model**

The effective compressive strength for a node is defined as:

$F_{cu} = 0.85\beta_n f_c^{/}$

Node 1 is a compression-compression-tension (CCT) node, so β_n= 0.8. Thus, the effective compressive strength for Node 1 at nominal conditions is

$f_{cu} = 0.85 * 0.8 * 44 = 29.92\text{Mpa}$

Use this nominal strength and ϕ=0.75to check stress at the base of the node

$f_{base} = \frac{R_1}{b_w * l_b} = \frac{456 * 1000}{300 * 300} = 5.07\text{Mpa}$

$f_{base} \leq \emptyset f_{cu}$

$\emptyset f_{cu} = 0.75 * 29.92 = 22.44\text{Mpa}$

$5.07 \leq 22.44$ OK

Also, find the width of Tie, which defines the height of Node 1

$W_{Tie} = \frac{F_{Tie}}{\emptyset b_w f_{cu}} = \frac{543.94 * 1000}{0.75 * 300 * 29.92} = 80.8\text{mm}$

- **The effective compressive strength for Strut $f_{cu\ (strut)}$**

Use β_s=0.75

$f_{cu}(Strut) = 0.85\beta_s f_c{}' = 0.85 * 0.75 * 44 = 28.05\text{Mpa}$

- **Determine the width of Strut**

$w_{strut} = w_{Tie}\cos\alpha + b_w \sin\alpha$

$=80.8\cos 39.92 + 300\sin 39.92$

=80.8*0.767+300*0.642=254.48mm

- **Check the strut capacity**

$\emptyset f_{ns}(strut) = \emptyset f_{cu} w_s(Strut) b_w$

=0.75*28.05*254.48*300=1606086.9N=1606.09kN

$1606.09 > 709.58$ OK

- **Step2 Check maximum shear force permitted in a deep beam**

$V_u \leq \emptyset V_{n(\max)}$

$0.75 * 10\sqrt{f_c{}'} b_w d = 0.75 * 10\sqrt{44} * 300 * 503 = 7507.18\text{KN}$

$456 \leq 7507.18$ OK

- **Step3 Make checks at node 2**

Check the stress on the top face of Node 2 (CCC node) using $\beta_n = 1.0$

$f_{cu} = 0.85\beta_n f_c{}' = 0.85 * 1 * 44 = 37.4\text{Mpa}$

$\emptyset f_{cu} = 0.75 * 37.4 = 28.05\text{Mpa}$

$f_{(top)} = \frac{456 * 1000}{300 * 300} = 5.0667\text{Mpa}$

$f_{(top)} \leq \emptyset f_{cu}$

$5.066 \leq 28.05$ OK

Check stress on vertical face of left part of Node 2

$\emptyset f_{ns}(\text{strut}) = \emptyset f_{cu}(\text{strut}) w_s(\text{strut}) b_w$

=0.75*28.05*254.48*300=1606086N=1606.09kN

$1606.09 > 709.85$ OK

3.4.2Shell Element Design

i Direct design:

From Shell (thick) analysis the design membrane force using for (reinforcement layer) area of steel for maximum tension stress in the bottom of beam as follow below:

Maximum force in X-direction (Average force in area element at bottom fiber of beam)

N_{11} = 2339.5 N/mm (701.85kN) tension force

$\mathbf{A_S} = \frac{\mathbf{N_{11}}}{\mathbf{0.7} f_y} = \frac{\mathbf{701.85 * 10^3}}{\mathbf{0.7 * 870}}$=1152.46 mm^2 (3.84 mm^2/ mm)

Use steel bar # 6

6#6 Bars (As provided= 1707mm^2)

- **Minimum Reinforcement (As_{min})**

$As_{min} = \frac{1.4}{f_y} * b * d$

$= \frac{1.4}{870} * 300 * 503 = 242.8\ mm^2$

$As_{min} = \frac{0.25 * \sqrt{f_{\grave{c}}}}{f_y} * b * d$

$= \frac{0.25 * \sqrt{44}}{870} * 300 * 503 = 287.63\ mm^2$

Take max As_{min} =287.63 mm^2

Check Main Reinforcement

As >As_{min} (O.K)

- **For top reinforcement**:

Use steel bar # 4

2#4 Bars (As provided= 254 mm^2)

- **Shear Design**

The web reinforcement design required for diagonal shear in shell elements .And the maximum shear force (force in area element at diagonal of maximum shear rang)

$V_u(N_{12})$ = 1189.47 N/mm (356.84kN)

$V_C = 0.83\sqrt{fc}\, b.d$

$= 0.83\sqrt{44} * 503 * 300$=830794.61 N**(830.79kN)**

$\Phi V_n = \Phi V_C$ =0.75*830.79 =623.096 kN

$V_u < \Phi V_n$ (O.K)

But h >450mm , $N_{12} > 0.5\varphi V_C$ then

- **Vertical Percentage of reinforcement**

Minimum shear reinforcement requirements

Space(S) =200 mm

$A_{v,min} = \rho * b * S$

$A_{v,min}$=300*200*0.0025 =112.5 mm^2

Use steel bar # 3; A_{bar} =77.37mm^2

Use No #3 ties with two legs at spacing of 200 mm

- **Horizontal Percentage of reinforcement**

Minimum shear reinforcement requirements

Space(S) =200 mm

$A_{h,min}$ =$\rho * b * S$

$A_{h,min}$= 0.0025 *300*200=112.5 mm^2

Use steel bar # 4; A_{bar}=126.7mm^2

Use 2 #4 @ Space200 mm

ii Section Cut Technique

We get the design moment by draw section cut at mid of shell element

The design moment (M_u) =M_{22}=273.6 kN.m

The design Shear force (V_U) =Pu =456 kN

- **The depth of the compression block (a):**

a =d-$\sqrt{d^2 - \frac{2*\mathrm{Mu}}{\emptyset*\mathrm{b}*0.85*\mathrm{fc}'}}$ =503-$\sqrt{503^2 - \frac{2*273.6*10^6}{0.9*300*0.85*44}}$

a= 57.11mm

$\varepsilon s,_{min}$ = 0.005$\varepsilon c,_{max}$= 0.003

- **The maximum depth of the compression zone (C_{max})**

C_{max} =$\frac{\varepsilon c,_{max}}{\varepsilon s,_{min}+\varepsilon c,_{max}}$ *d

= $\frac{0.003}{0.003+0.005}$ *503 =188.62 mm

- **The maximum allowable depth of the rectangular compression block (a_{max})**

β_1 =0.85-0.05*$\frac{fc'-28}{7}$

= 0.85-0.05*$\frac{44-28}{7}$ =0.74

$a_{max}= \beta_1 C_{max}$

=0.74*188.62 =139.58 mm

$a < a_{max}$

The area of tensile steel reinforcement (As)

$$As = \frac{Mu}{\emptyset * fy * [d - \frac{a}{2}]} = \frac{273.6 * 10^6}{0.9 * 870 * [503 - \frac{57.11}{2}]} = 736.49 \text{ mm}^2$$

Use steel bar # 6

3#6 Bars (As provided= 856 mm^2)

- **Shear Design**

The design Shear force (V_U) =P_u =456 kN

$V_C = 0.83\sqrt{fc}\, b.d$

$= 0.83\sqrt{44} * 503 * 300$=830794.61 N **(830.79 kN)**

$\Phi V_n = \Phi V_C$ =0.75*830.79 =623.096 kN

$V_u < \Phi V_n$ (O.K)

But h >450mm , N12 >0.5φ V_C then

- **Percentage of vertical reinforcement**

Minimum shear reinforcement requirements

Space(S) =200 mm

$A_{v,min} = \rho * b * S$

$A_{v,min}$= 300*200*0.0025 =112.5 mm^2

Use steel bar # 3; A_{bar} =77.37mm^2

Use No #3 ties with two legs at spacing of 200 mm

- **Percentage of horizontal reinforcement**

Minimum shear reinforcement requirements

Space(S) =200 mm

$A_{h,min}$ =$\rho * b * S$

$A_{h,min}$= 300*200*0.0025 =112.5 mm^2

Use steel bar # 4; A_{bar}=126.7mm^2

Use 2 #4 @ Space200 mm

iii Section Cut Technique

We get the design moment by draw section cut at mid of plane stress

The design moment (M_u) =M22=273.6 kN.m

The design Shear force (V_U) =Pu =456 kN

- **The depth of the compression block (a):**

a =d-$\sqrt{d^2 - \frac{2*\mathrm{Mu}}{\emptyset*\mathrm{b}*0.85*\mathrm{fc}'}}$ =503-$\sqrt{503^2 - \frac{2*273.6*10^6}{0.9*300*0.85*44}}$

a= 57.11mm

$\varepsilon s,_{\min}$ = 0.005$\varepsilon c,_{\max}$= 0.003

- **The maximum depth of the compression zone ($C_{max)}$**

C_{max} =$\frac{\varepsilon c,max}{\varepsilon s,min+\varepsilon c,max}$ *d

= $\frac{0.003}{0.003+0.005}$ *503 =188.62 mm

- **The maximum allowable depth of the rectangular compression block (a_{max})**

β_1 =0.85-0.05*$\frac{fc'-28}{7}$

= 0.85-0.05*$\frac{44-28}{7}$ =0.74

a_{max}= $\beta_1 C_{max}$

=0.74*188.62 =139.58 mm

a <a_{max}

- **The area of tensile steel reinforcement (As)**

As =$\frac{Mu}{\emptyset * fy * [d - \frac{a}{2}]}$ = $\frac{273.6 * 10^6}{0.9 * 870 * [503 - \frac{57.11}{2}]}$ = 736.49 mm^2

Use steel bar # 6

3#6 Bars (As provided= 856 mm^2)

- **Shear Design**

The design Shear force (V_U) =P_u =456 kN

$V_C = 0.83\sqrt{fc}\, b.d$

= $0.83\sqrt{44} * 503 * 300$=830794.61 N **(830.79 kN)**

φ V_n =φ V_C =0.75*623.096 =623.096 kN

V_u<φ V_n (O.K)But h >450mm , N12 >0.5φ V_C

- **Percentage of vertical reinforcement**

Minimum shear reinforcement requirements

Space(S) =200 mm

$A_{v,min} = \rho * b * S$

$A_{v,min}$= 300*200*0.0025 =112.5 mm^2

Use steel bar # 3; A_{bar} =77.37mm^2

Use No #3 ties with two legs at spacing of 200 mm

- **Percentage of horizontal reinforcement**

Minimum shear reinforcement requirements

Space(S) =200 mm

$A_{h,min}$ =$\rho * b * S$

$A_{h,min}$= 300*200*0.0025 =112.5 mm^2

Use steel bar # 4; A_{bar}=126.7mm^2

Use 2 #4 @ Space200 mm

Chapter Four

Results and Discussion

4.1 Introduction

A small prototype of beam as discussed in previous chapter was studied for the suitable modeling technique. In this chapter the results of small modeling were compared to that of experimental findings available in literature. Different modeling techniques, shell thick/area and truss (STM) analysis in **SAP2000**. Different parameters e.g. the cracks pattern and stress and are compared from each modeling technique and on the basis of the results obtained, best modeling technique is recommended to give better design.

4.2Analysis Results of Flexural and Shear SAP2000 Models

4.2.1Truss Element (STM)

From analysis of truss element in SAP2000 we use the tension force in tie element (Tie1-1) to flexural design (tension) in the bottom of beam is 543.97kN .and for design shear the ultimate shear force is the compression force in element (Strut1-1) multiple by 456 sin50.03 .

4.2.2Shell Element (thick)

From Shell (thick) analysis the design membrane force using for (reinforcement layer) area of steel for maximum tension stress in the bottom of beam Maximum force in X-direction (Average force in area element No 350 at bottom fiber of beam)is (710.996 kN) tension force. And for design shear the maximum shear force (force in area element at diagonal of maximum shear rang) V_u is 355146 N/mm (355.15 kN).Total load capacity predicate using strut and tie method was

456kN for ACI318-05 code predicate shear failure, however flexural failure accorded at P_{max} is 2012kN.

4.3 Results of Nonlinear Shell Layered Modeling Technique

4.3.1 Load-deflection of specimens

The maximum deflection at mid-point is determined for all beams using nonlinear shell layered model for maximum loading on the specimens P_{max} show that in Table4.1 for all specimens.

Table 4. 1: deflection at mid span at maximum load for specimens

maximum load for specimens

Beam	Maximum load (kN)	Deflection (mm)
MS1-3	2747	7.16
MS2-3	2055	9.75
MS3-2	1154	24.63
MW1-2	1568	7.63
MW3-2	411	7.01

4.3.2Crack development of specimens

The load of cracks patterns and percentage of maximum load corresponding to the first flexural crack, first diagonal strut cracks at shear span of the nonlinear shell layered showed in table 4.2.

Table 4. 2: Load and %P_{max} at different crack stages of specimens

crack stages of specimens

Beam	P_{max} kN	First flexural crack		First Diagonal strut crack	
		P (kN)	% of P_{max}	P(kN)	% of P_{max}
MS1-3	2727	213.93	7.84	653.6	24.97
MS2-3	2055	161.15	7.84	551	26.8
MS3-2	1154	71.5	6.20	283.1	24.53
MW1-2	1568	141.35	9.01	427.5	27.26
MW3-2	411	54.45	13.25	268.85	65.41

4.3.3Stress and Strains in Steel Layers

The results of stresses and strains in main tension reinforcement for three layered at mid span is determined for all beams using nonlinear shell layered model for maximum loading on the specimens P_{max} show that in Table4.3 for all specimens.

Table 4. 3: Stress and Strains in Steel Layers at mid span at maximum load Layers at mid span at maximum load for specimens

for specimens

Beam	First Layer		Second Layer		Third Layer	
	Stress MPa	Strain mm/mm	Stress MPa	Strain mm/mm	Stress MPa	Strain mm/mm
MS1-3	616.92	0.0033	541	0.0028	471.77	0.0024
MS2-3	713.52	0.0042	623.8	0.0033	452.2	0.0028
MS3-2	1241.43	0.018	1099.19	0.013	893.2	0.0073
MW1-2	736.37	0.0044	632.62	0.0034	-	-
MW3-2	368.37	0.0019	318.62	0.0016	-	-

4.4 Discussion of Results

For analysis in this chapter, specimens were classified as specimens that contained vertical web reinforcement and specimens without vertical web reinforcement. The influence of the design parameters of a/d and ρ on the behavior of the specimens were established for each classification. In SAP2000, the maximum principal stresses are denoted by **SMax**. If the value of the maximum principal stress is more concrete tensile strength then the cracking in the cover concrete must be developed in the RCC member.

4.4.1The First Cracks Pattern of Non-Linear Shell Layered

At model **MS1-3**and model **MS2-3**the crack is observed at the bottom of the beam at 55% of experimental first flexural crack load is 213.93 kN, the maximum principal stress (**SMax)** is almost 10.56% more than 4.49MPa (concrete tensile strength) for **MS1-3** and 161.15 kN, the maximum principal stress is almost 20.2%

more than 4.49MPa for**MS2-3.**which confirms the initiation of crack as shown in Figure A.4 and Figure A.5**.**

At model **MS3-2**the crack is observed at the bottom of the beam at 55% of experimental first flexural crack load is 71.5 kN, the maximum principal stress (**SMax)** is almost 20.19% more than 4.49MPa.At model **MW1-2** the crack is observed at the bottom of the beam at 55% of experimental first flexural crack load is 141.35 kN, the maximum principal stress (**SMax)** is almost 25.3% more than 4.49MPa.

4.4.2The Diagonal Cracks Pattern of Non-Linear Shell Layered

At model **MS1-3** the diagonal crack is observed at the beam at 95% of experimental first diagonal crack load is 653.6 kN, the maximum principal stress (**SMax)** is almost 20.19% more than 4.49MPa. At model **MS2-3** the diagonal crack is observed at the beam at 95% of experimental first diagonal crack load is 551kN, the maximum principal stress (**SMax)** is almost 20.19% more than 4.49MPa.At model **MS3-2** the diagonal crack is observed at the beam at 95% of experimental first diagonal crack load is 283.1 KN, the maximum principal stress (**SMax)** is almost 20.19% more than 4.49MPa.

At model **MW1-2** the diagonal crack is observed at the beam at 95% of experimental first diagonal crack load is 427.5kN, the maximum principal stress (**SMax)** is almost 20.19% more than 4.49MPa.At model **MW3-2** the diagonal crack is observed at the beam at 95% of experimental first diagonal crack load is 268.85 kN, the maximum principal stress (**SMax)** is almost 20.19% more than 4.49MPa**.**

4.4.3 Yielding of Main Reinforcement

At model **MS1-3** no yielding in main tension reinforcement, at P_{max} the maximum stress at mid span is at firs layer of the main tension reinforcement is 616.92 MPa this is only 70% of the effective stress of main reinforcement 880MPa,corresponding to strain 0.0033 mm/mm , this strains is only 52.38%the effective yield strain (ε_y=0.0063). Also this beam was yielded in vertical web reinforcement the stress is (increased from 405MPa).At model **MS2-3** no yielding in main tension reinforcement, at P_{max} the maximum stress at mid span is at first layered of the main tension reinforcement is 713.52MPa this is only 81.1% of the effective stress of main reinforcement 880MPa, corresponding to strain 0.0042mm/mm, this strains is only 66.67%the effective yield strain (ε_y=0.0063). Also this beam was yielded in vertical web reinforcement the stress is (increased from 405MPa). At model **MS3-2** at P_{max} the maximum stress at mid span is at first layers of the main tension reinforcement is1241.43MPa this stress is almost 142.70% more than 870MPa, corresponding to strain 0.018mm/mm this strains is almost 285.71%more than effective yield strain 0.0063. Also this beam was yielded in vertical web reinforcement the stress is (increased from 405MPa). At model **MW1-2** no yielding in main tension reinforcement, at P_{max} the maximum stress at mid span is at firs layer of the main tension reinforcement is 736.37 MPa this is only 84.64% of the effective stress of main reinforcement 870Mpa,corresponding to strain 0.0044mm/mm , this strains is only 69.84% of the effective yield strain (ε_y=0.0063). At model **MW3-2** no yielding in main tension reinforcement, at P_{max} the maximum stress at mid span is at firs layer of the main tension reinforcement is 368.73 MPa this is only 42.34% of the effective stress of main reinforcement 870Mpa,corresponding to strain 0.0019 mm/mm , this strains is only 30.16%of the effective yield strain (ε_y=0.0063

4.5 Failure Mode

4.5.1Flexural Failure

For specimen **MS3-2** the failure mode was flexural failure; the effective yielding stress was reached in the three layers of main tension reinforcement.

4.5.2Flexural –Splitting strut

MS2-3 the failure mode was flexural-splitting strut,

4.5.3Splitng Strut

For specimen MS1-3 the failure mode was splitting strut failure, For **MW1-2** the failure mode was splitting strut failure at a total applied load of **1568kN**. No yielding of the main tension reinforcement and For **MW3-2** the failure mode was splitting of the diagonal strut at a load of **411kN**. No yielding in the main tension reinforcement.

4.6 Compression of Results

4.6.1 Compression of flexural Design deep beam by shell thick and STM

The results of flexural design deep beam for specimen **MS1-2** from shell thick model and results of flexural design by truss model (**STM**) were compared with the results available in literature. Table 4.4 shows the compression of flexural design of deep beam (**MS1-2**) by software program SAP2000 (shell thick) and strut and tie method (**STM).**

Table 4. 4 Compression of flexural Design of deep beam between (shell/thick) Design of deep beam between (shell/thick) and truss (STM) technique for (shell/thick) and truss (STM) technique for beamMS1-2

technique for beamMS1-2

Flexural design	(shell thick)	Truss(STM)	Literature
As of main reinforcing steel mm^2	1000.96	893.16	1710.12
As provided l mm^2	1141	1141	1710.12
Number of bar	4#6	4#6	6#6

Area of top reinforcing steel	254	381	506.7
Number of Bar	2#4	3#4	2#4

4.6.2Compression of Behavior Nonlinear Shell Layered with Experimental

The results of nonlinear shell layered model were compared with the experimental results available in literature.

Table 4.5 Present the compression of nonlinear shell layered model SAP2000 results and experimental for deflection at mid span when the specimens at P_{max} for all specimens.

Table 4. 5: SAP2000 and Experimental Compression of Deflection at Mid Experimental Compression of Deflection at Mid Span

Deflection at Mid Span

Beam	**Pmax (kN) Nonlinear Shell**	**Deflection at mid span (mm)**		**Deference %**
		SAP2000	Experimental	
MS1-3	2747	7.16	7.86	9.25
MS2-3	2055	9.75	12.50	22
MS3-2	1154	24.63	35.06	29.75
MW1-2	1568	7.63	7.50	1.73
MW3-2	411	7.01	9.08	22.80

Table 4.6 and Table 4.7 presents compression of nonlinear shell layered modelsSAP2000 and Experimental results for the load of the first flexural crack and first diagonal strut cracks for all specimens.

Table 4. 6 :Compression of Load at first Flexural crack for all specimens

first Flexural crack for all specimens

Beam	**Load of First flexural crack kN**		**Deference %**
	SAP2000	Experimental	
MS1-3	213.93	389	45
MS2-3	161.15	293	45
MS3-2	71.5	130	45

MW1-2	141.35	257	45
MW3-2	54.45	99	45

Table 4. 7: Compression of Load at first diagonal crack for all specimens

first diagonal crack for all specimens

Beam	**Load of First Diagonal cracks kN**		**Deference%**
	SAP2000	Experimental	
MS1-3	653.6	688	5
MS2-3	551	580	5
MS3-2	283.1	298	5
MW1-2	427.5	450	5
MW3-2	268.85	283	5

Table 4.9 present compressions of nonlinear shell layered model SAP2000 and experimental results for the load t of yielding for vertical web reinforcement.

Table 4. 8: Compression of Loads yielding of Vertical web reinforcement for yielding of Vertical web reinforcement for all specimens

reinforcement for all specimens

Beam	**Load of Vertical web reinforcement kN**		**Deference %**
	SAP2000	Experimental	
MS1-3	1672.87	1707	2
MS2-3	956.5	969	1.3
MS3-2	685	704	2.3
MW1-2	-	-	-
MW3-2	-	-	-

Table 4.10, Table4.11 and Table4.12 presents compression of nonlinear shell layered model SAP200 and Experimental results for strains for the first (lowest), second and third layer at maid span at maximum load P_{max} for all specimens.

Table 4. 9:SAP2000 and experimental Compression strains for the first Compression strains for the first (lowest) layer for all specimens

(lowest) layer for all specimens

Beam	Strain at mid span mm/mm		Deference %
	SAP2000	Experimental	
MS1-3	0.0033	0.0035	5.7
MS2-3	0.0042	0.0042	0
MS3-2	0.018	0.010	80
MW1-2	0.0044	0.0042	4.7
MW3-2	0.0019	0.0019	0

Table 4. 10: Compression strain for the second layer for all specimens

the second layer for all specimens

Beam	Strain at mid span mm/mm		Deference%
	SAP2000	Experimental	
MS1-3	0.0028	0.0031	9.67
MS2-3	0.0033	0.0033	0
MS3-2	0.013	0.010	30
MW1-2	0.0034	0.0036	5.55
MW3-2	0.0016	0.0016	0

Table 4. 11: Compression strain for the third layer for all specimens

the third layer for all specimens

Beam	Strain at mid span mm/mm		Deference %
	SAP2000	Experimental	
MS1-3	0.0024	0.0027	12.5
MS2-3	0.0028	0.0029	3.44
MS3-2	0.0073	0.010	27
MW3-2	0.0011	0.0012	8.3

4.6.3 Influence of a/d Ratio in Nonlinear Shell Layered

- Figure 4.1, Figure 4.2 and Figure 4.3, presents deference's of effect of a/d on nonlinear shell layered model with Experimental results for strains of the first (lowest), second and third layers at maid span at maximum load P_{max} for specimens with web reinforcement.

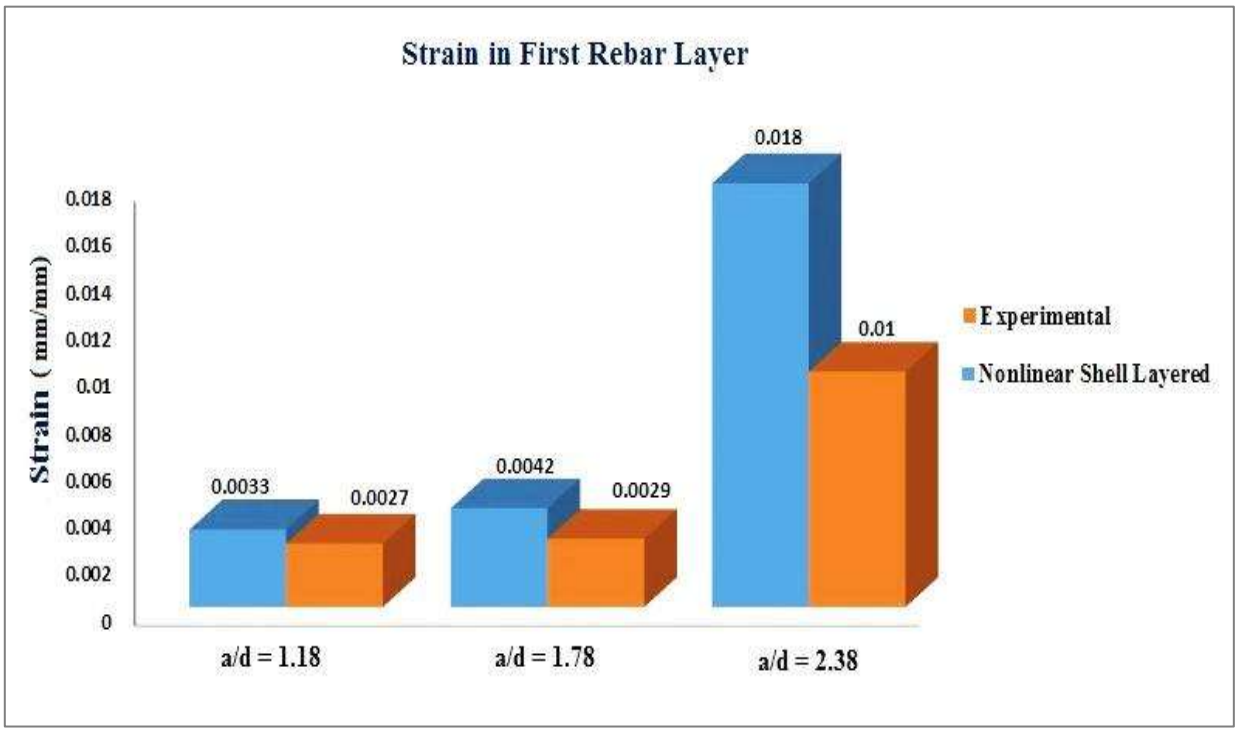

FIGURE 4. 1: Influence of a/d Ratio on Strain of First Rebar Layer

on Strain of First Rebar Layer

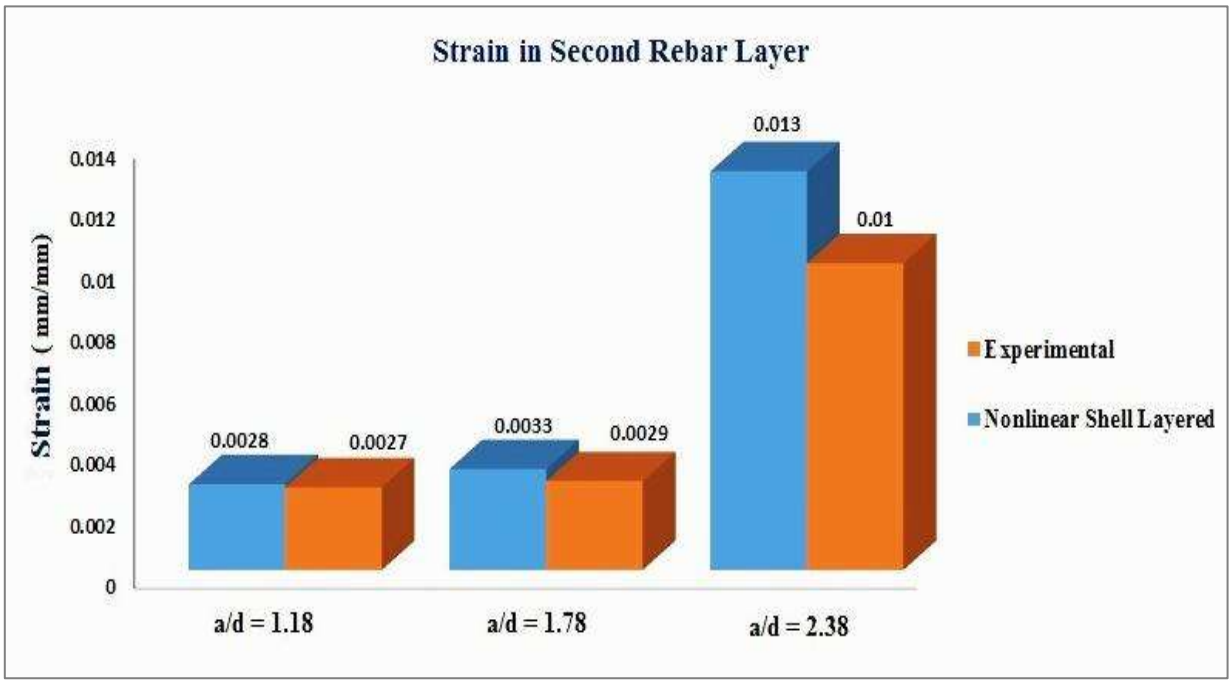

FIGURE 4. 2: Influence of a/d Ratio on Strain of Second Rebar Layer

on Strain of Second Rebar Layer

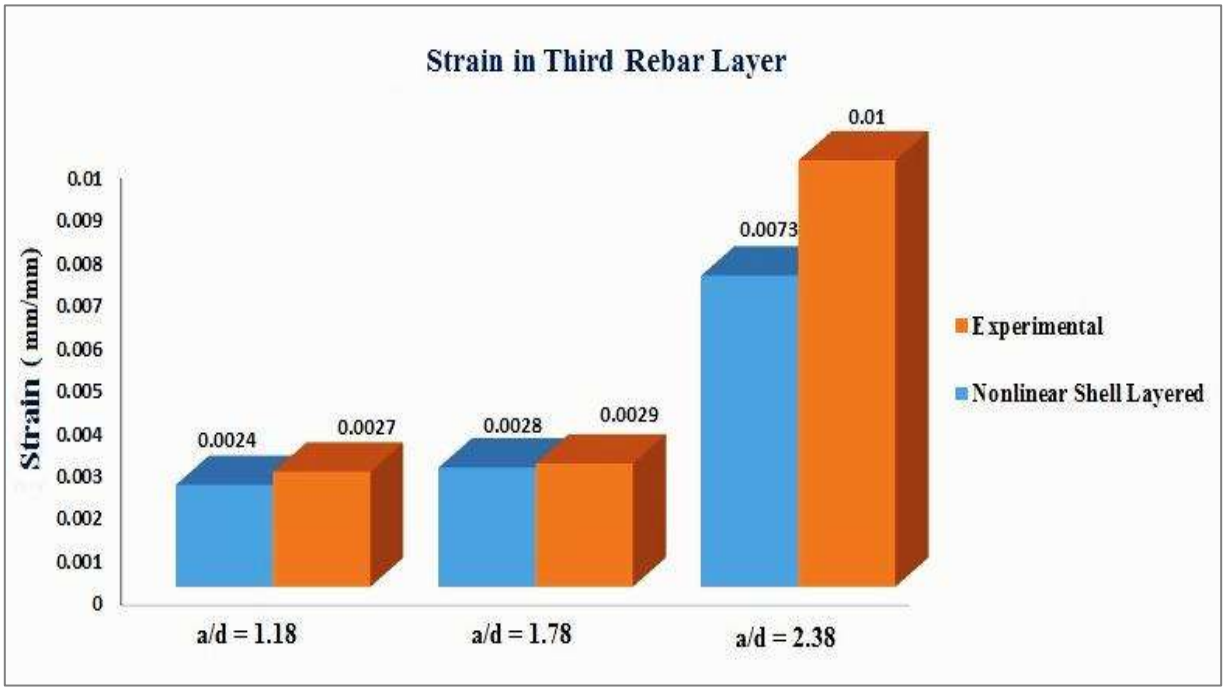

FIGURE 4. 3: Influence of a/d Ratio on Strain of Third Rebar Layer

on Strain of Third Rebar Layer

- Figure 4.4, Figure 4.5 presents deference's of effect of a/d on nonlinear shell layered model with Experimental results for strains of the first (lowest), second layers at maid span at maximum load P_{max} for specimens without web reinforcement.

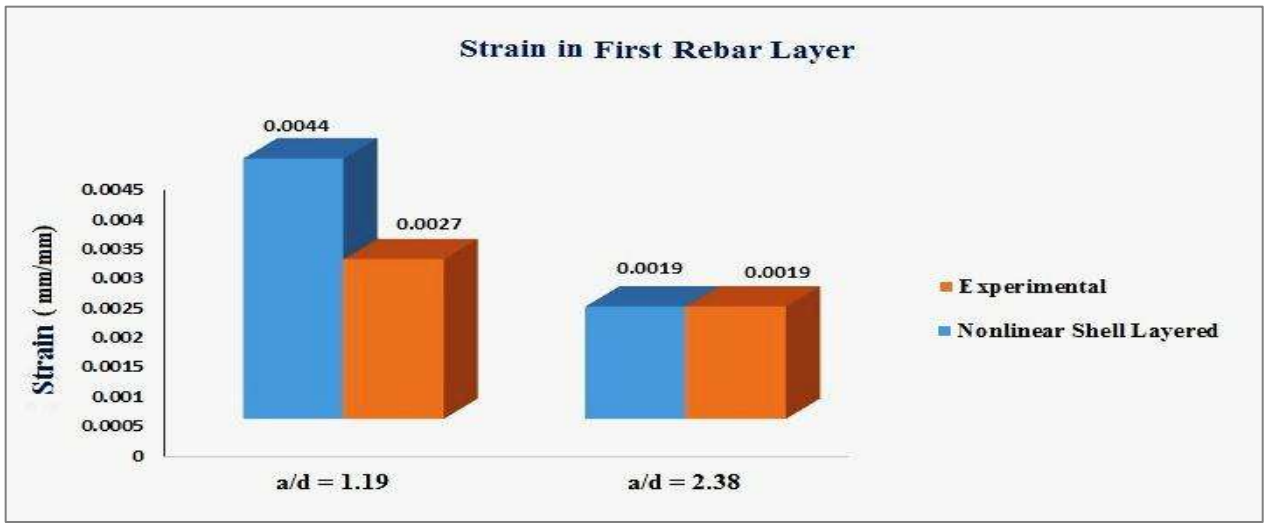

FIGURE 4. 4: Influence of a/d on Strain of First Rebar Layer (Beam without web Reinforcement)

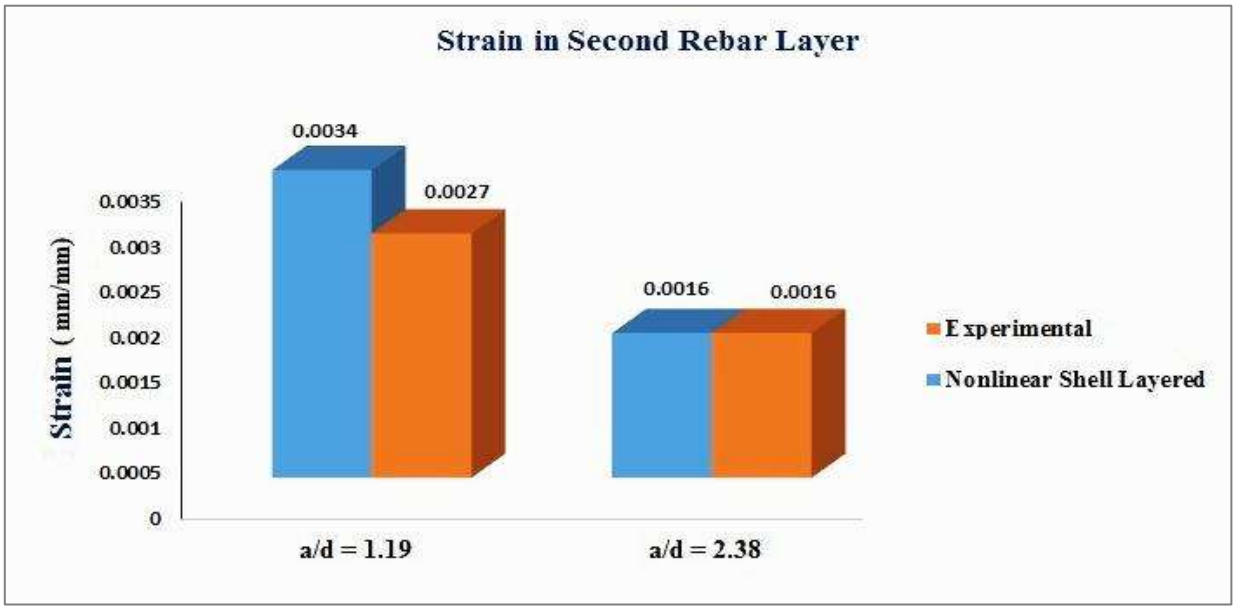

FIGURE 4. 5: Influence of a/d on Strain of Second Rebar Layer (Beam Strain of Second Rebar Layer (Beam without web Reinforcement)

without web Reinforcement)

Chapter Five

Conclusion and Recommendations

5.1 Summary of Thesis

The main aim of this work was to develop better understanding of the behavior and capacity of RC Deep beams by numerical analysis (FEM). The results were used to develop a unified strut-and-tie model and propose an accurate and reliable effectiveness factor for designing RC deep beams. This chapter gives a brief summary of the work carried out in this study and reports the main conclusions.

In this study, three different modeling techniques for concrete deep beams are applied and implemented in SAP2000software. In the first modeling are used shell (thick) and 2D truss element (STM) for analysis and design the beam , The third modeling are used nonlinear shell layered modeling technique to study behavior of reinforced concrete simply supported beam subjected increasing load. Also, model in SAP2000 software with the adopted assumption of plane stress.

5.2Conclusion

The finite element models show slightly high stiffness than the test data the nonlinear ranges, contributing to the higher stiffness of the finite element models. The following conclusions can be drawn based on the experimental data and the finite element analysis made.

- The predicted ultimate final deflection, and mode of failure by the FE model, show good agreement with the experimental data.
- The (Experimental/Predicted) failure load for all the tested beams were within (98%), while the FEM beams seem stiffer than the experimental beams during

the loading, this fact due to the absent of micro cracks in the FE model and the perfect bond assumption between the concrete and reinforcement bar.

- First (shear and flexural) cracking load predicted by FE model for all the tested beams was lower than those from experimental works tests by (153% for shear and 173% for flexural), the experimental first cracking load is the load where the first visible crack (shear or flexural) appear, while the theoretical cracking load is the load step where one of the principal stress in concrete element reach the maximum limit.
- The predicted ultimate shear stresses were higher than those from experimental work by approximately 20% for all tested beams.
- The failure mechanism of the experimentally tested reinforced concrete beams is well modeled using finite element model and the failure loads were well predicted.
- The behavior of SAP2000 models is accurate with the experimental results for beam with (a/d) less than 1.5.

5.3 Recommendations

Several finite element modeling packages have been used by various researchers to model the behavior of structural components of which deep beams is of no exception. The behavior of deep beams investigated using finite element methods has proven to be very accurate in predicting the behavior of deep beams. After work of this thesis researcher recommends the following suggestions for the future study are reported.

- Comparison of results obtained from SAP2000 software with other finite element software to ascertain the results.
- For future study use nonlinear geometric analysis to analyze deep beams to variety results of nonlinear material.

- Beams studied in this research is limited to simply supported deep beams using ACI code design .it can modified to study beams for hollow concrete deep beams and continuous deep beams and
- Beams studied in this research were under symmetrical two point loads, I recommended to take beams under uniformly distributed load may be studied in future.

References:

ACI(American Concrete Institute) 2008/ACI 318-11.Building Code Requirements for Reinforced Concrete, 2011, American Concrete Institute, Farming Hills, USA.

ACI (American Concrete Institute) Task committee., (1973). American Concrete Institute, Farmington Hills, MI, USA.

American Concrete Institute, 2002, "Examples for the design of Structural Concrete with Strut and Tie Models", January, American Concrete Institute.242 pp.

Aguilar, G., Matamoros, A. B., Parra-Montesinos, G. J., Ramírez, J. A. and Wight, J. K. , 2002, "Experimental evaluation of design procedures for shear strength of deep reinforced concrete beams" ACI Structural Journal, v 99, n 4, July-August, pp. 539-548.

Ansley, H. M., "Investigation into the structural performance of MMFX reinforcing", MMFX Steel Corporation: Technical Resources, August 13, 2002. 12 pp.

Besser, B., Macgregor, J.G "Review of concrete beams failing in shear", ASCE journal proceedings, Vol. 93, Feb 1967.

Choi, K. K., Park H. G. and Wight J.K., 2007, "Unified Shear Strength Model for Reinforced Concrete Beams—Part I: Development" ACI Structural Journal, v 104, n 2, March-April, pp. 142-152.

Choi, K. K. and Park H. G., 2007, "Unified Shear Strength Model for Reinforced Concrete Beams—Part II: Verification and simplified method" ACI Structural Journal, v 104, n 2, March-April, pp. 153-161.

Canadian Standards Association, 2004, "CAN/CSA A23.3-04 Design of Concrete Structures," CSA, Rexdale, Ontario, Canada.

Chow, L, Conway, H.D and Winter, G, "Stresses in deep beams", ASCE Journal proceedings, structural division, vol 78 May 1952.

Collins, M.P.andMitchell,D., 1991, “Prestressed Concrete Structures”, Prentice Hall, 766 pp.

Coull,A."Stress analysis of deep beams and walls". The engineer, Vol,221 Feb 1966.

Darwin D.,Browning J., Van Nguyen T. and Locke Jr C., 2002, “Mechanical and corrosion properties of high strength, high chrominium reinforcing steel for concrete”. Final Report, South Dakota, Department of transportation, March, 142 pp.

Eurocode 2, 1992, “—Design of Concrete Structures—Part 1-1: General Rules and Rules for Buildings,” EN 1992-1-1, 100 pp.

Hassoun, M. N., & Al-Manaseer, A. (2008).Shear and Diagonal Tension.In Reinforced Concrete, Mechanics and Design 4th Edition, New Jersey, John Wiley & Sons.

Juan de DoisGaray Moran and Adam S.LubellJanuaty, 2008"Behaviour of Concrete Deep Beams with High Strength Reinforcement".

Kani, M.W., Huggins, M.W.,andWittkopp, R. R., 1979, “Kani on Shear in Reinforced Concrete”, University of Toronto Press, 225 pp.

Kong, F.K., 1990"Reinfoced Concrete Deep Beams" New York, Van NostrandReinhold.

Malhas, A.F., 2002, “Preliminary experimental Investigation of the Flexural behavior of reinforced concrete Beams using MMFX Steel”, MMFX Steel Corporation: Technical Resources, July, 55 pp.

Nielsen, M.P., 1998, “Limit analysis and Concrete Plasticity”, 2nd Edition, CRC Press, Boca Raton, Fla., 908 pp.

Quintero-Febres, C. G., Parra-Montesinos, G. and Wight, J. K., 2006, “Strength of struts in deep concrete members designed using strut-and-tie method”, ACI Structural Journal, v 103, n 4, July-August, pp. 577-586.

Rogowsky, D. M., MacGregor, J. G., Ong, S. Y., 1986, “Tests of reinforced concrete deep beams”, Journal of The American Concrete Institute, v 83, n 4, July-August, pp. 614-623.

Schlaich, J., Schäfer, K., and Jennewein, M., 1987, “Towards a Consistent Design of Structural Concrete,” PCI Journal, v 32, n 3, pp. 74-150.

Seliem H. M., Lucier G., Rizkalla S. H., and Zia P., 2008, “Behavior of Concrete Bridge Decks Reinforced with High-Performance Steel” ACI Structural Journal, V. 105, No. 1, January-February, pp 78-86.

Selvam, V. K. Manicka and Thomas, Kuruvilla, 1987, “shear strength of concrete deep beams” Indian Concrete Journal, v 61, n 8, August, pp. 219-222.

Smith, K.N., and Vantsiots, A.S "deep beam test results compared with precast building code models " ACI Journal proceedings, Vol.79, No.3 July-August 1982.

Tan, K.H. and Lu, H.Y., 1999, “Shear behavior of large reinforced concrete deep beams and code comparisons” ACI Structural Journal, v 96, n 5, September/October, pp. 836-845.

Tan, KH, Teng, s., "High strength concrete deep beams with effective span and shear span variations", ACI structural journal, vol.92, No.4, July-Aug. 1995,.

Vijay, P.V.; Gangarao, V. S. and Prachasaree, W., 2002, “Bending Behavior of Concrete Beams Reinforced with MMFX Steel bars”, MMFX Steel Corporation: Technical Resources, July, 33 pp.

Yoo, T. M., Doh, J. H., Guan, H., &Fragomeni, S. (2007). Experimental work on reinforced and prestressed concrete deep beams with various web openings.

Yotakhong, P., 2003, “Flexural performance of MMFX reinforcing rebar's in concrete structures”. Thesis, November, 162 pp.

Zsutty, T. C., 1968, “Beam Shear Strength Prediction by Analysis of Existing Data,” ACI Journal, Proceedings, v 65, n 11, November, pp. 943-951.

Appendix A:

SAP2000 Output and Results

The Appendix A are used for show result of **SAP2000** software. This appendix contains printed output of Design and behavior of the cases Study as represent in chapter 3.

A.1 Results SAP2000 of Truss (STM) and Shell (Thick) Models

For truss model of beam (MS1-2) results of forces show in **Figure.A.1**.Design tension force (N_{11}) in in X-Direction bottom of shell show in **Figure.A.2** and **Figure. A.3** displayed Shear force (N_{12}) in XZ plan.

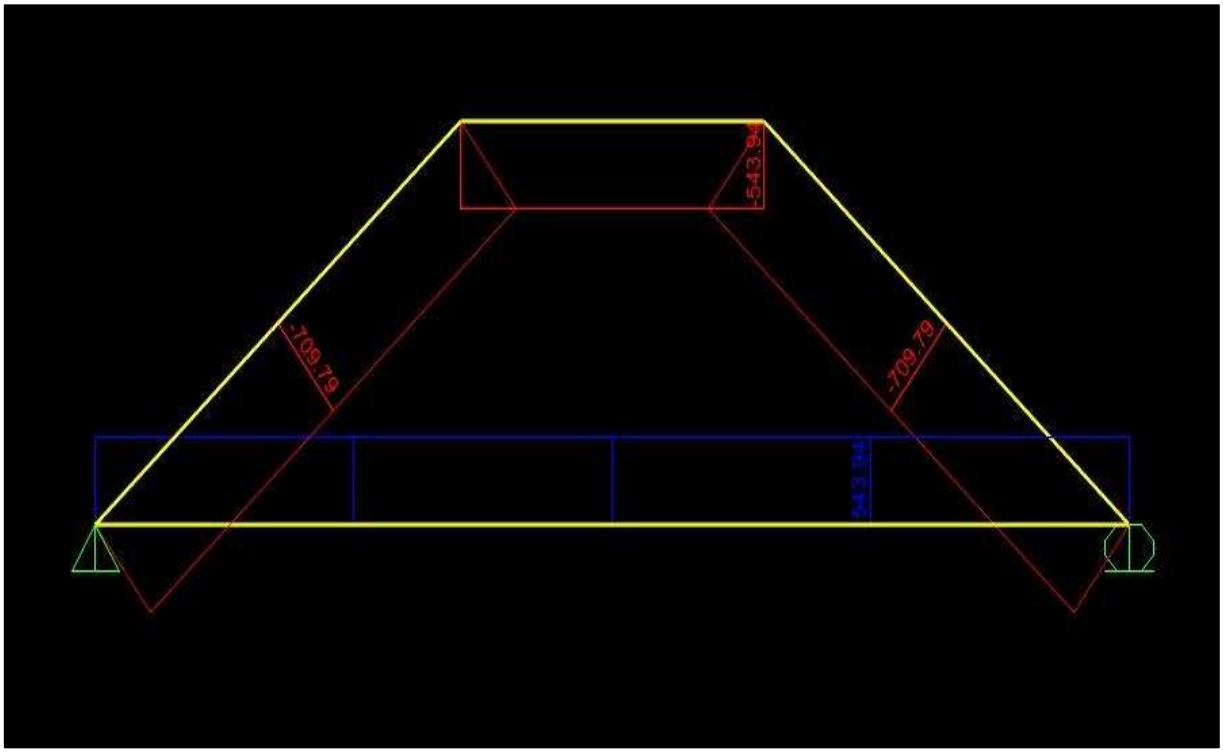

Figure A. 1: Axial Force of Truss Model (STM)

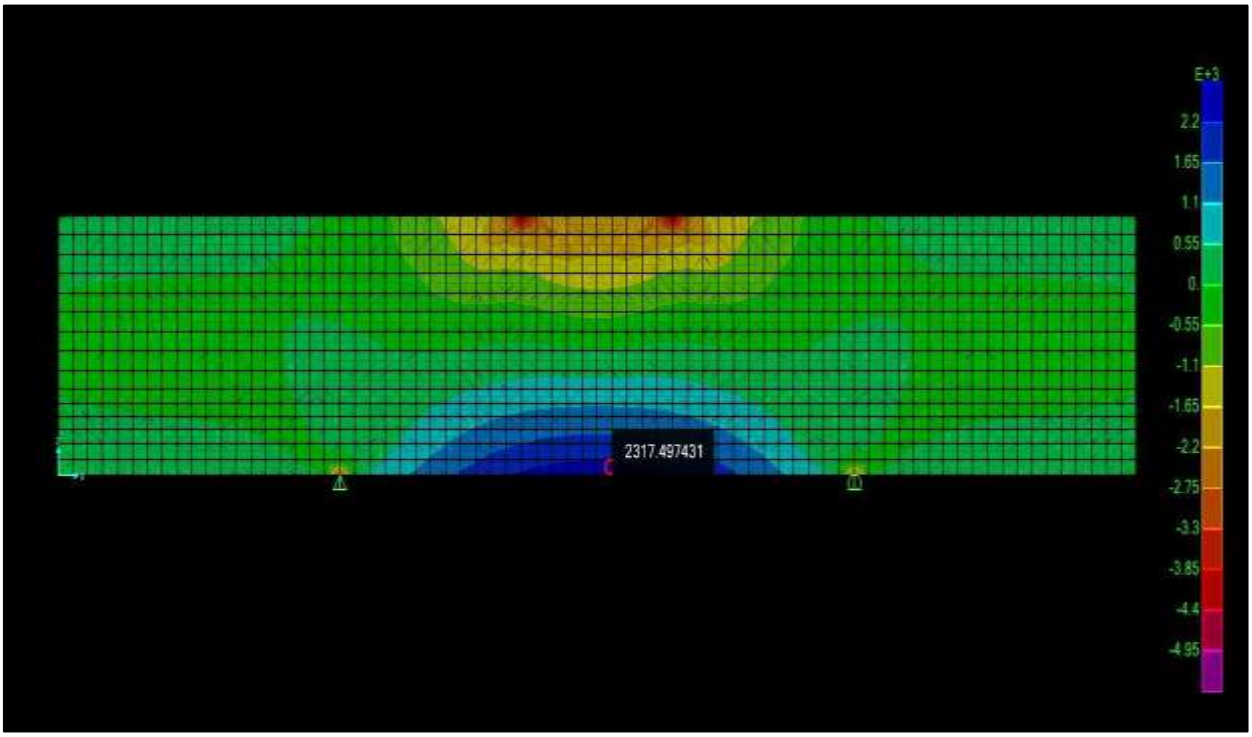

Figure A. 2: Design Tension force (N11) X-Direction

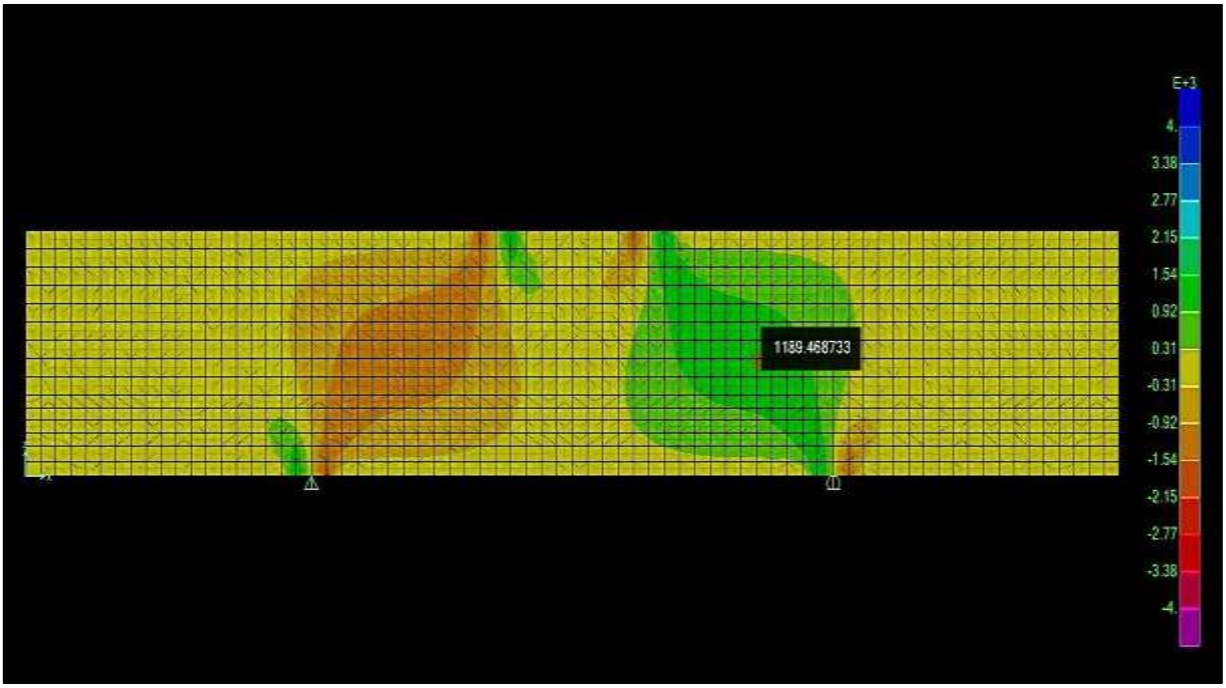

Figure A. 3: Displayed Shear Force (N12) in XZ Plan

A.2 Results of SAP2000 Crack Pattern (Flexure and Shear) for Nonlinear Shell Layered Technique

This is show first flexural and diagonal shear crack (above maximum tensile strength of concrete) ,**Figure.A.4** displayed first flexural crack of model (MS1-3) and **Figure.A**.5 displayed first diagonal shear crack of model (MS1-3) , and for model (MS2-3) first flexural crack , show that in **Figure. A.6**., diagonal shear crack of model (MS2-3) show that in **Figure. A.7**. and for model (MS3-2) first flexural crack, show that in **Figure. A.8**., first diagonal shear crack of model (MS3-2) show that in **Figure. A.9**. , for model (MW1-2) first flexural crack, show that in **Figure. A.10**. first diagonal shear crack of model (MW1-2) show that in **Figure. A.11**.and for model (MW3-2) first flexural crack, show that in **Figure. A.12**. first diagonal shear crack of model (MW3-2) show that in **Figure. A.13.**

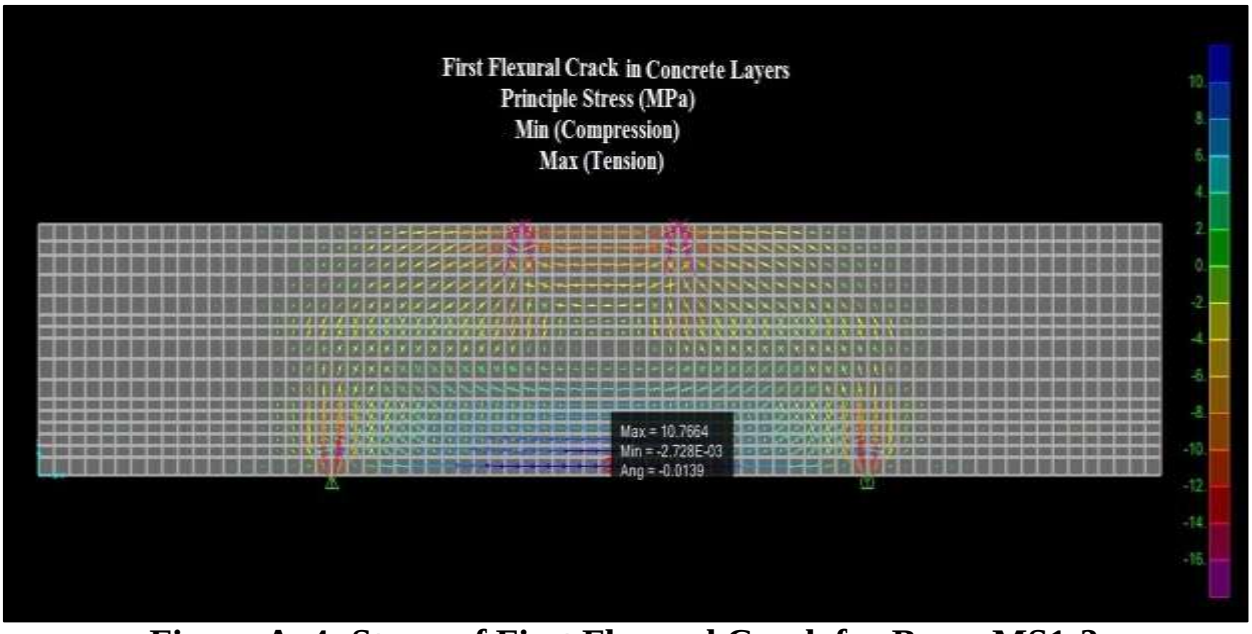

Figure A. 4: Stress of First Flexural Crack for Beam MS1-3

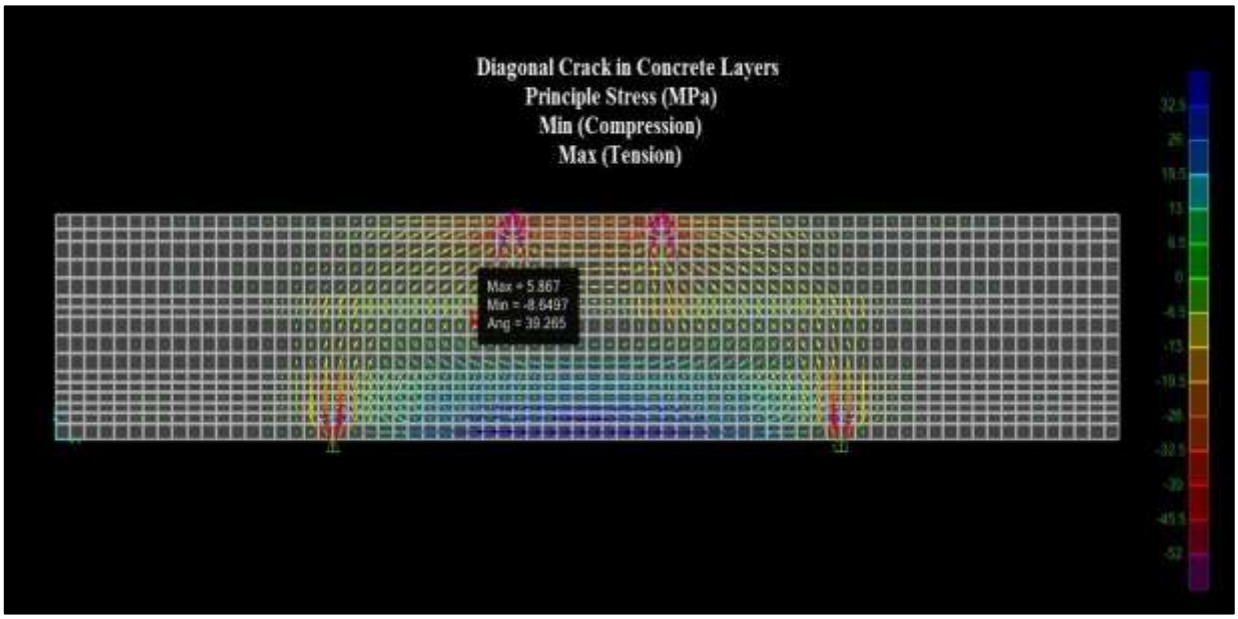

Figure A. 5: Stress of First Diagonal Crack for Beam MS1-3

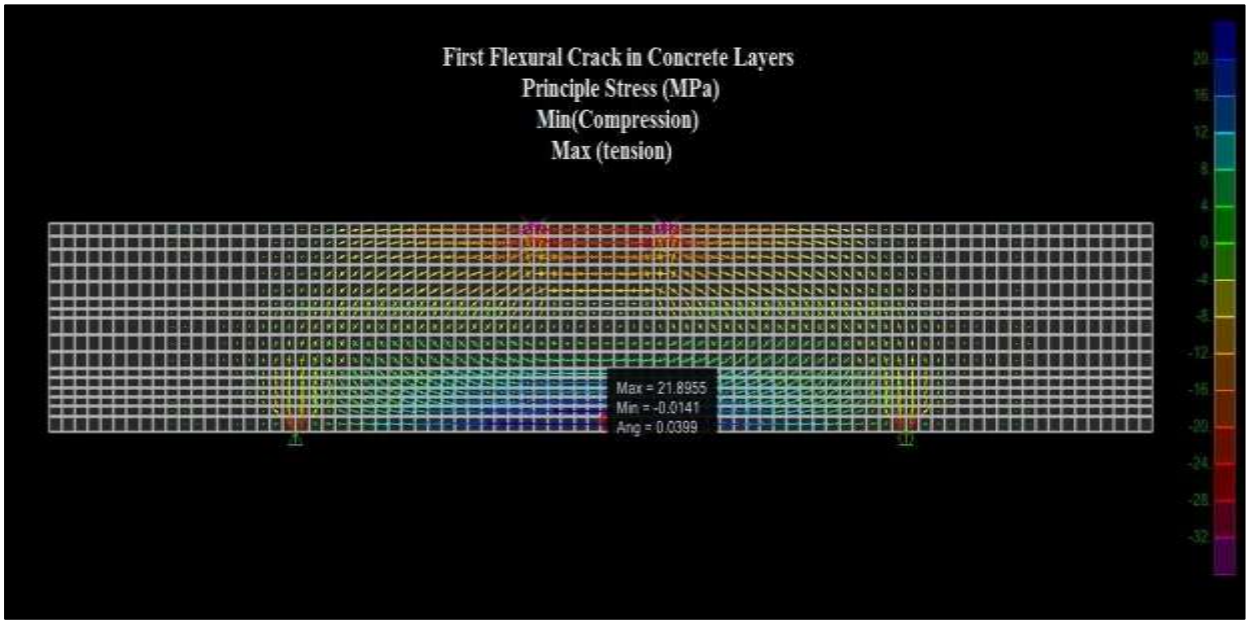

Figure A. 6: Stress of First Flexural Crack for Beam MS2-3

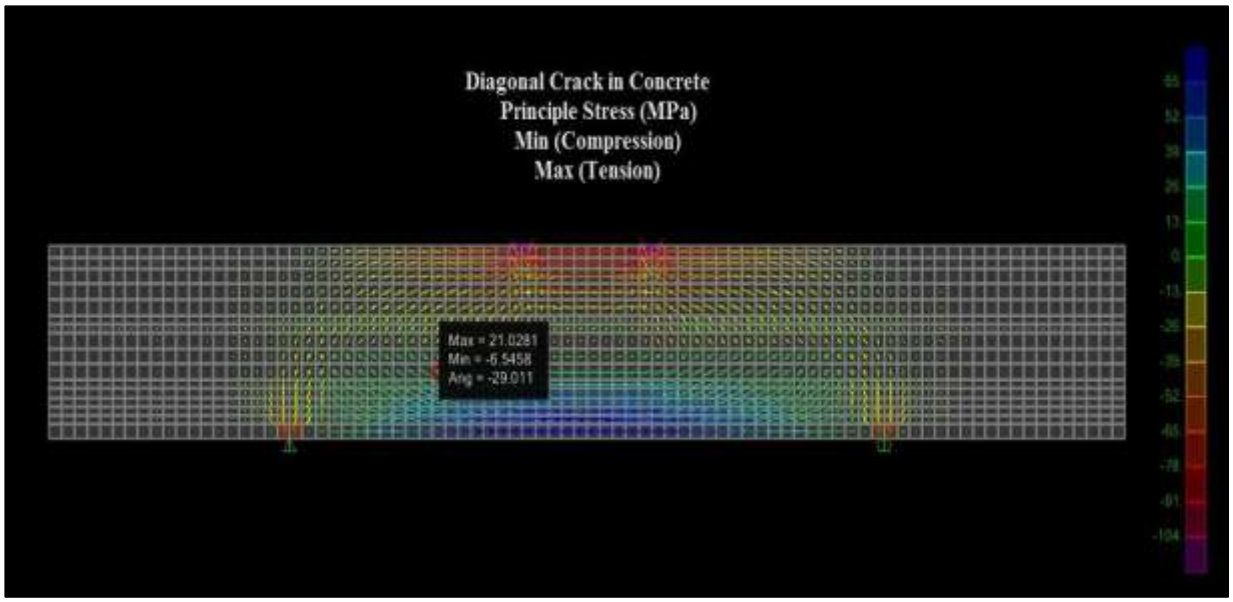

Figure A. 7: Stress of Diagonal Crack for Beam MS2-3

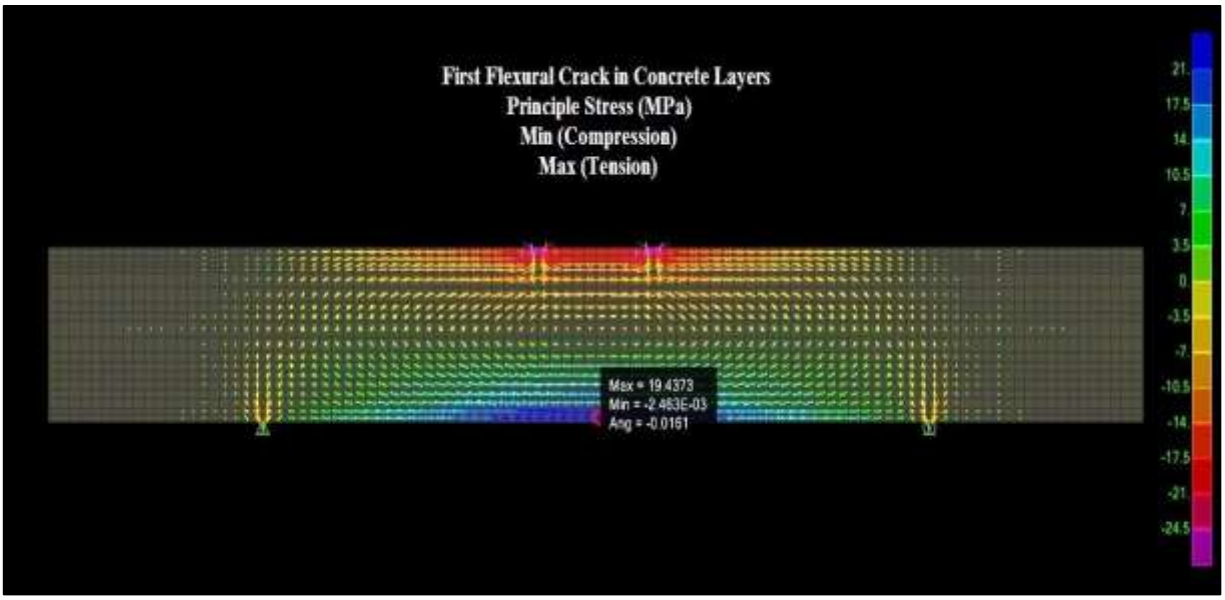

Figure A. 8: Stress of First Flexural Crack for Beam MS3-2

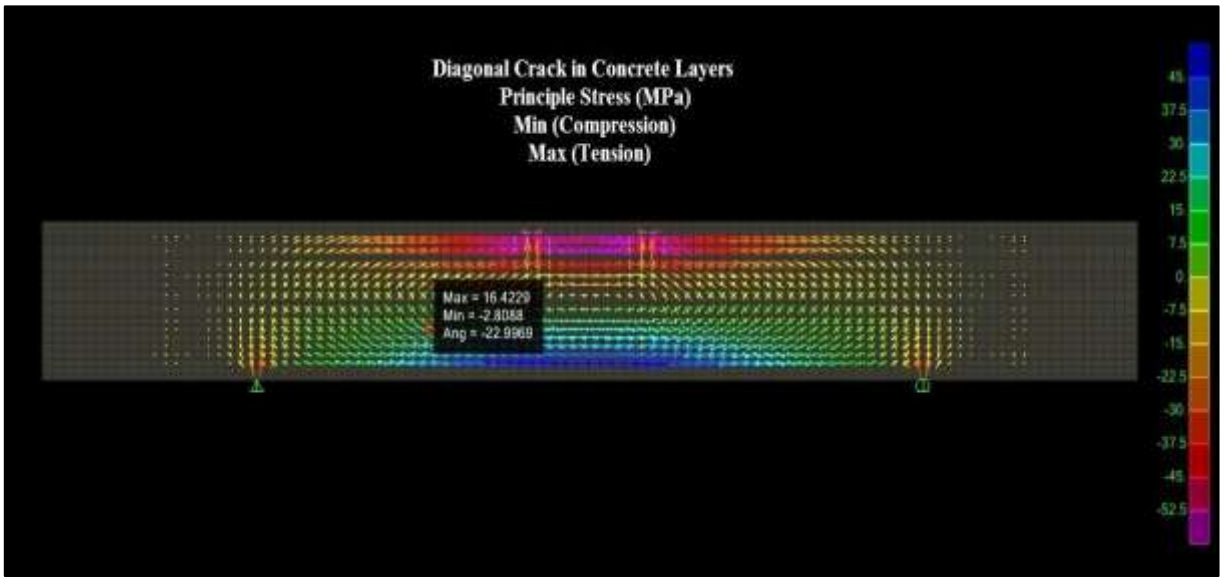

Figure A. 9: Stress of Diagonal Crack for Beam MS3-2

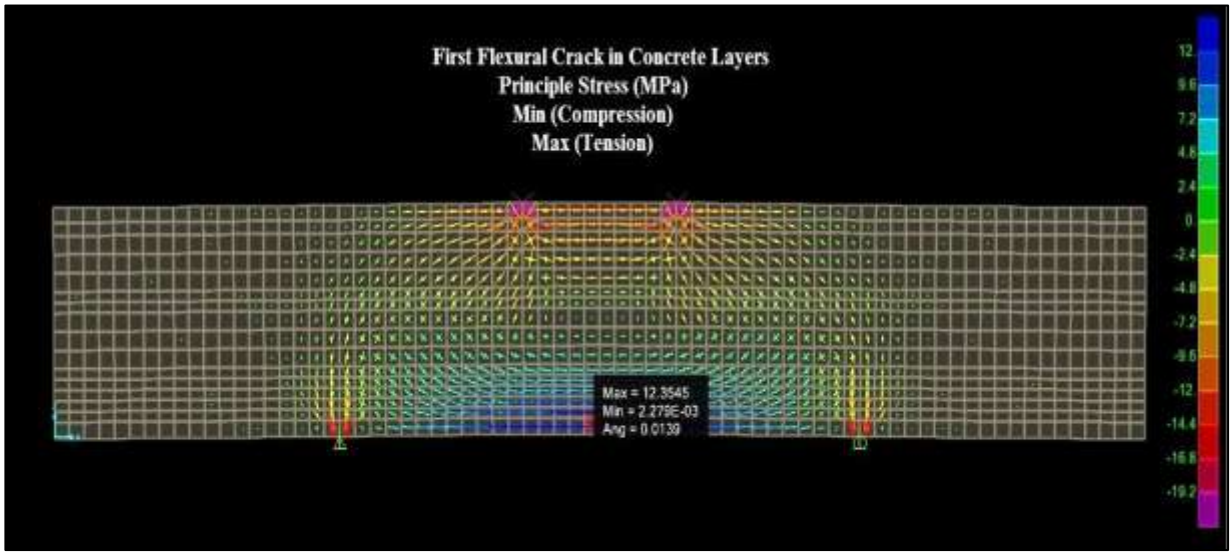

Figure A. 10: Stress of First Flexural Crack for Beam MW1-2

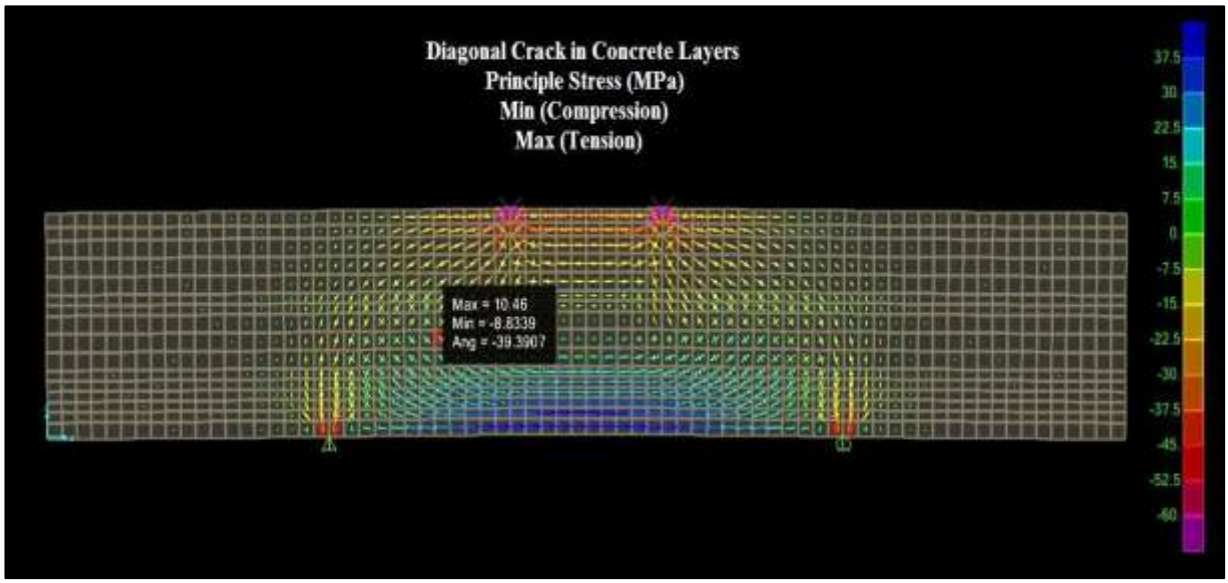

Figure A. 11: Stress of Diagonal Crack for Beam MW1-2

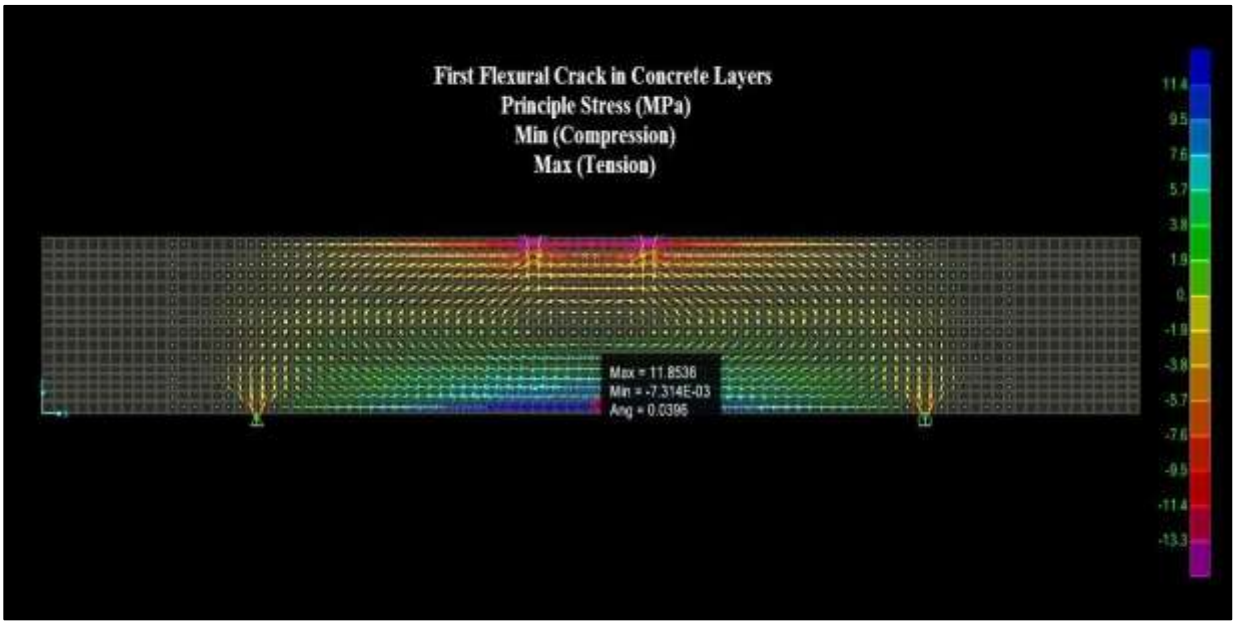

Figure A. 12: Stress of First Flexural Crack for Beam MW3-2

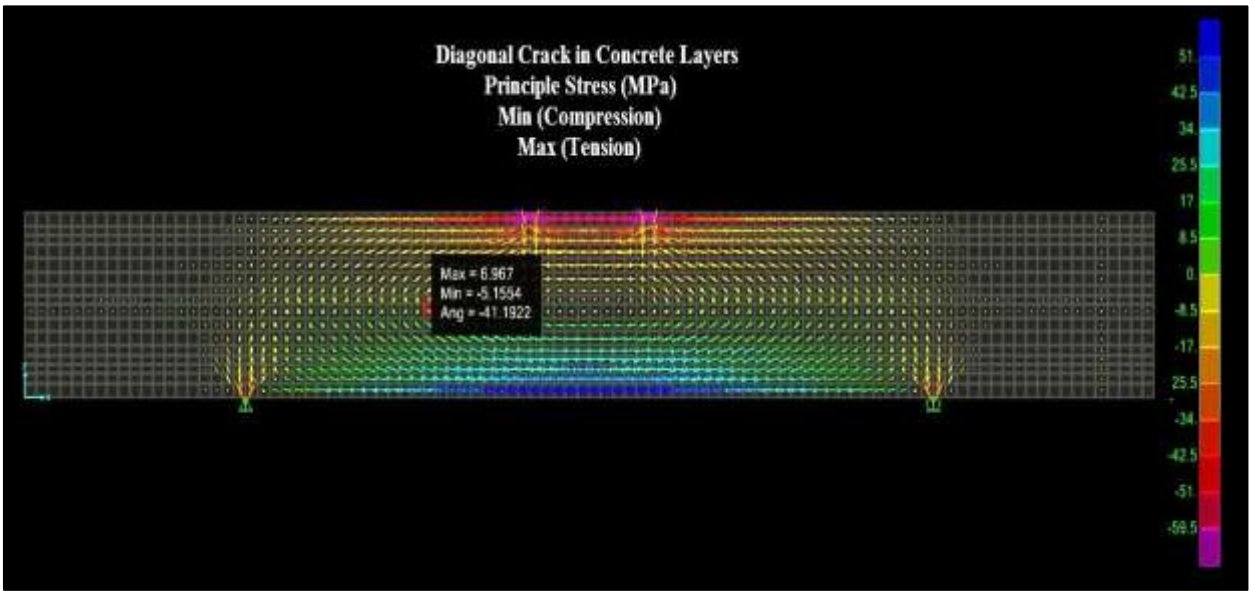

Figure A. 13: Stress of Diagonal Crack for Beam MW3-2

A.3 Results of SAP2000 Yielding of Main Reinforcement Steel Layers

- **Results of SAP2000 Yielding of Flexure (Main Reinforcement) for First Layer**

This is show the stress of main reinforcement for first layer, **Figure.A.14** displayed stress in first layer of main tension reinforcement of model (MS1-3), **FigureA.15** displayed stress in first layer of main tension reinforcement for model MS2-3, **Figure.A.16** displayed stress in first layer of main tension reinforcement for model MS3-2, **Figure.A.17** displayed stress in first layer of main tension reinforcement for model MW1-2 and **Figure.A.18** displayed stress in first layer of main tension Reinforcement for model MW3-2.

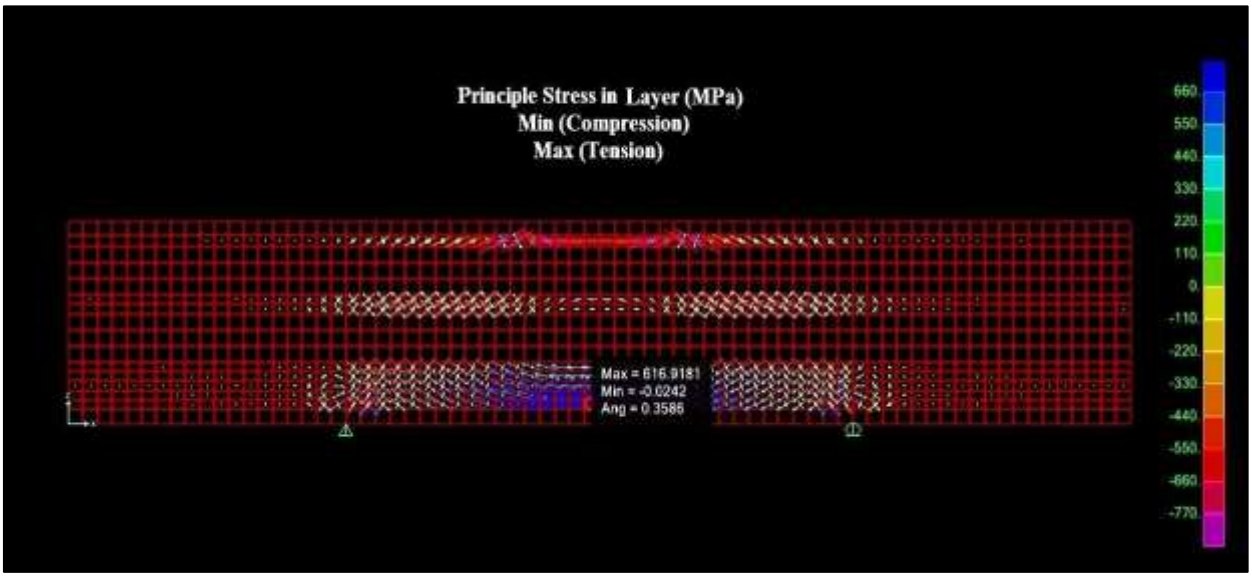

Figure A. 14: Stress in First Layer of Main Tension Reinforcement for Beam MS1-3

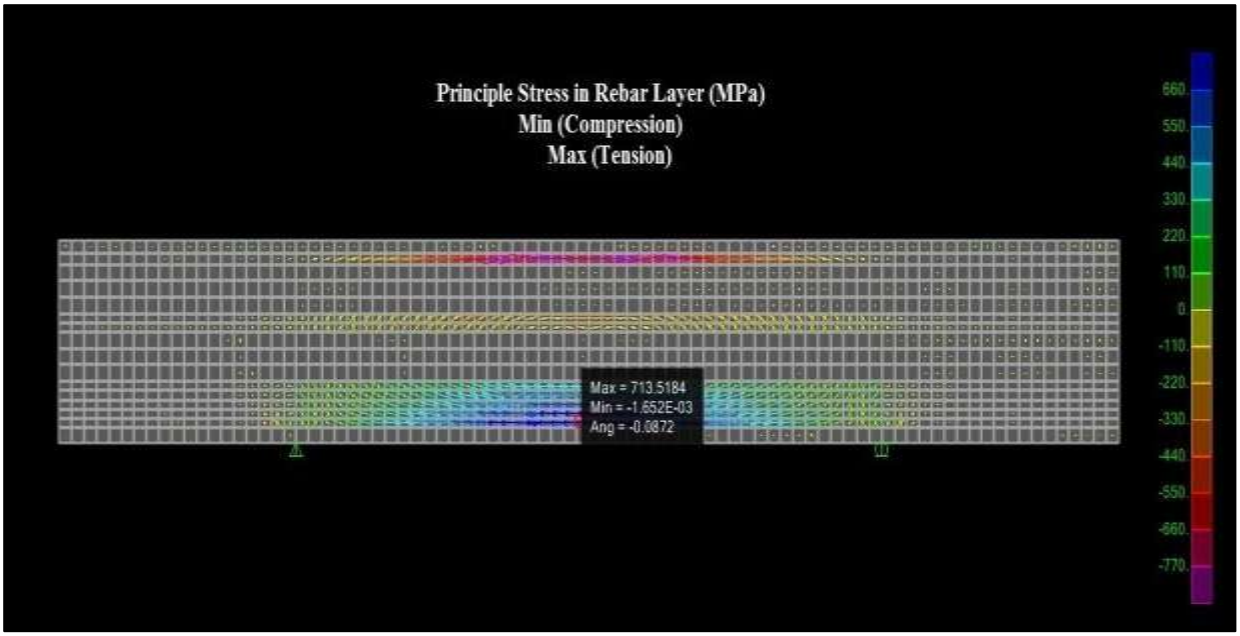

Figure A. 15: Stress in First Layer of Main Tension Reinforcement for Beam MS2-3

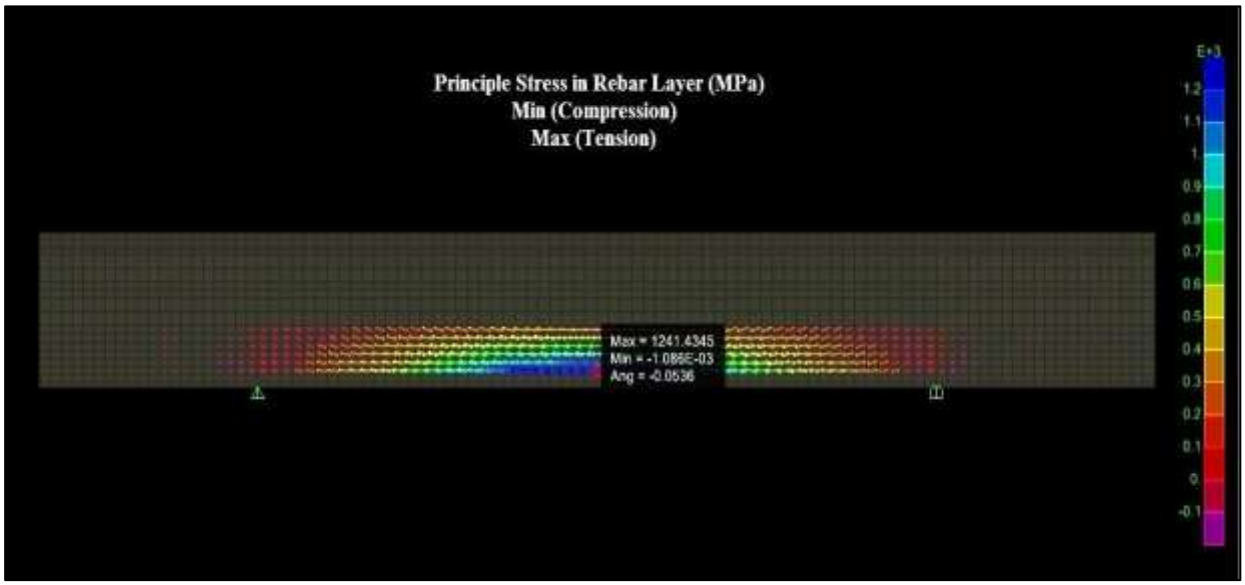

Figure A. 16: Stress in First Layer of Main Tension Reinforcement for Beam MS3-2

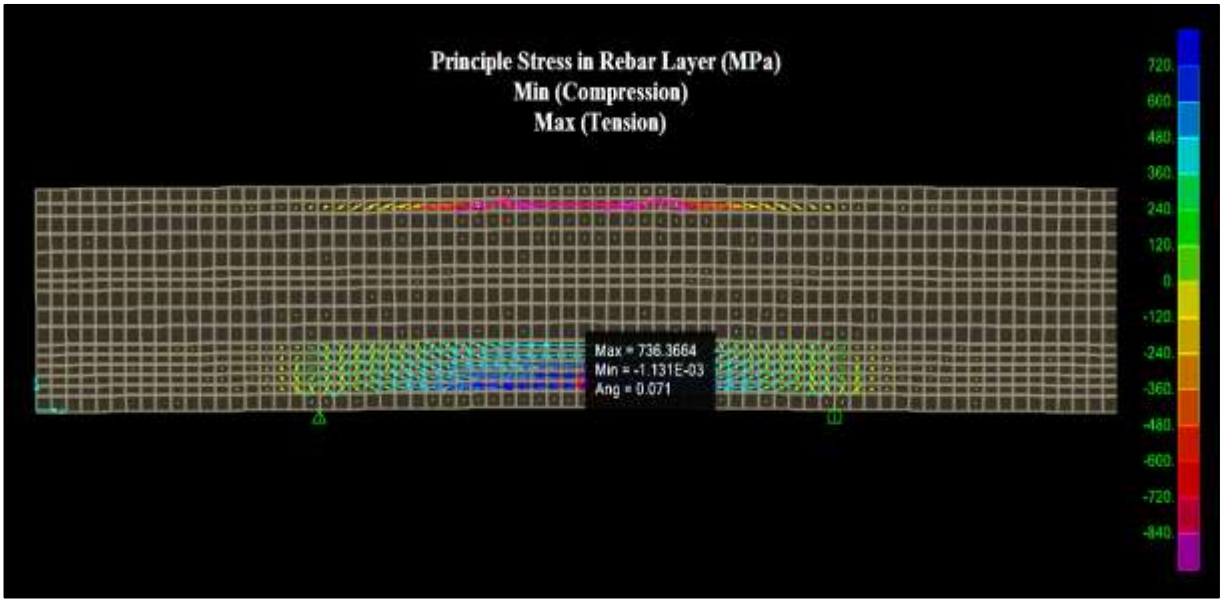

Figure A. 17: Stress in First Layer of Main Tension Reinforcement for Beam MW1-2

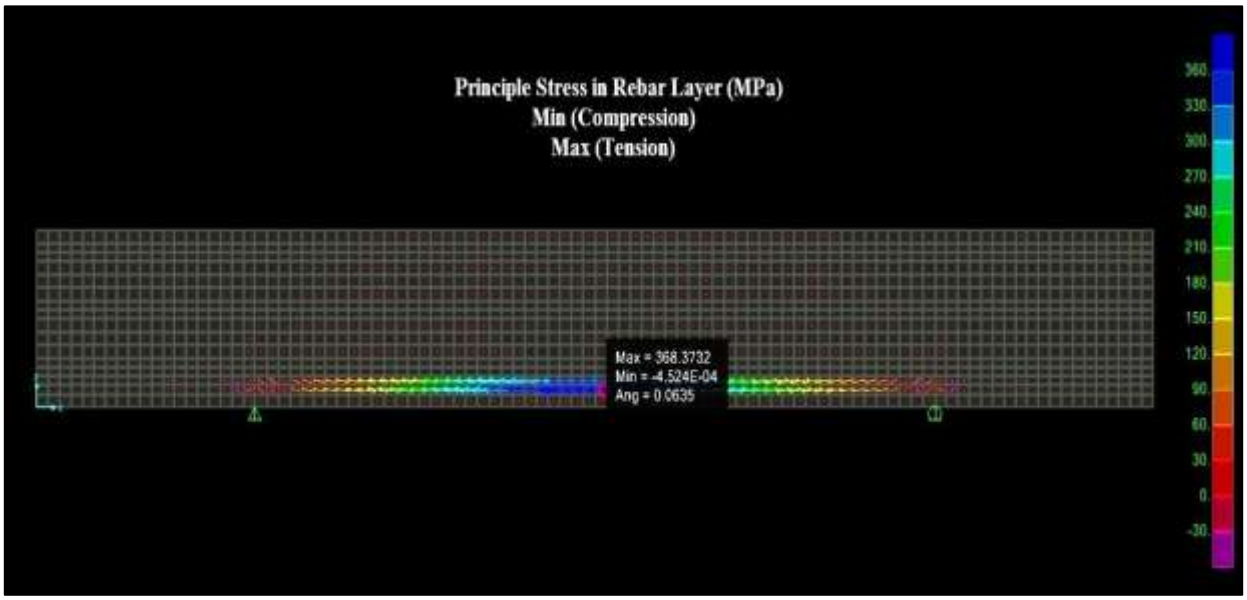

Figure A. 18: **Stress in First Layer of Main Tension Reinforcement for Beam MW3-2**

- **Results of SAP2000 Yielding of Main Reinforcement for Second Layer**

This is show the stress of main reinforcement for second layer, **Figure.A.19** displayed stress in second layer of main tension reinforcement of model (MS1-3), **FigureA.20** displayed stress in second layer of main tension reinforcement for model MS2-3, **Figure.A.21** displayed stress in second layer of main tension reinforcement for model MS3-2, **Figure.A.22** displayed stress in second layer of main tension reinforcement for model MW1-2 and **Figure.A.23** displayed stress in second layer of main tension reinforcement for model MW3-2.

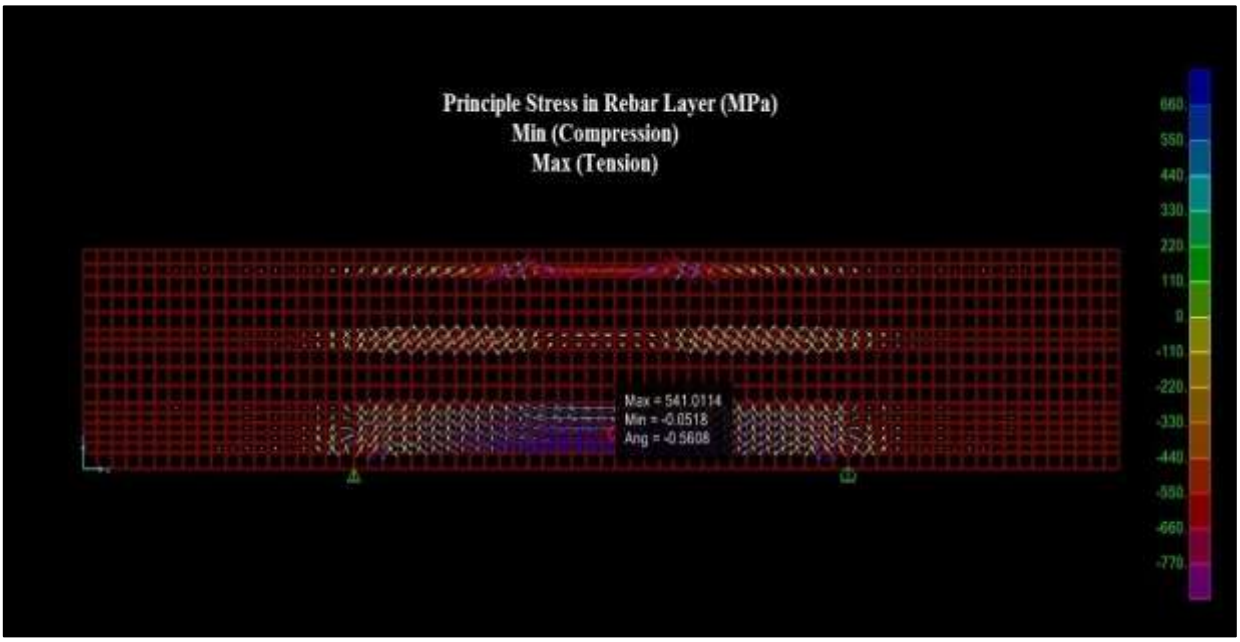

Figure A. 19: **Stress in Second Layer of Main Tension Reinforcement for Beam MS1-3**

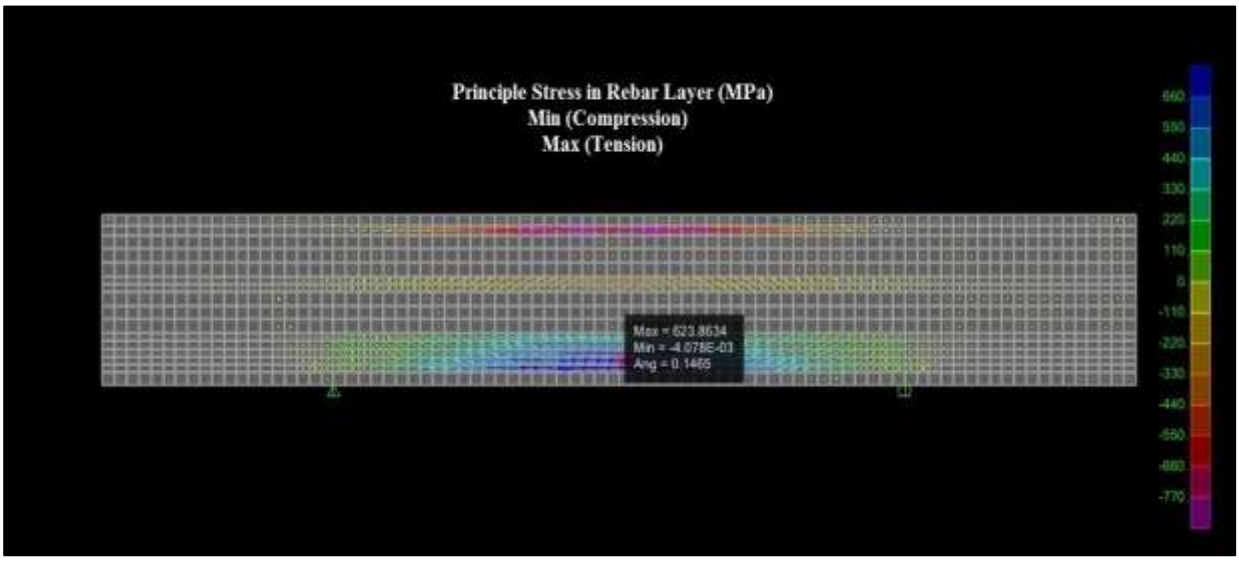

Figure A. 20: **Stress in Second Layer of Main Tension Reinforcement for Beam MS2-3**

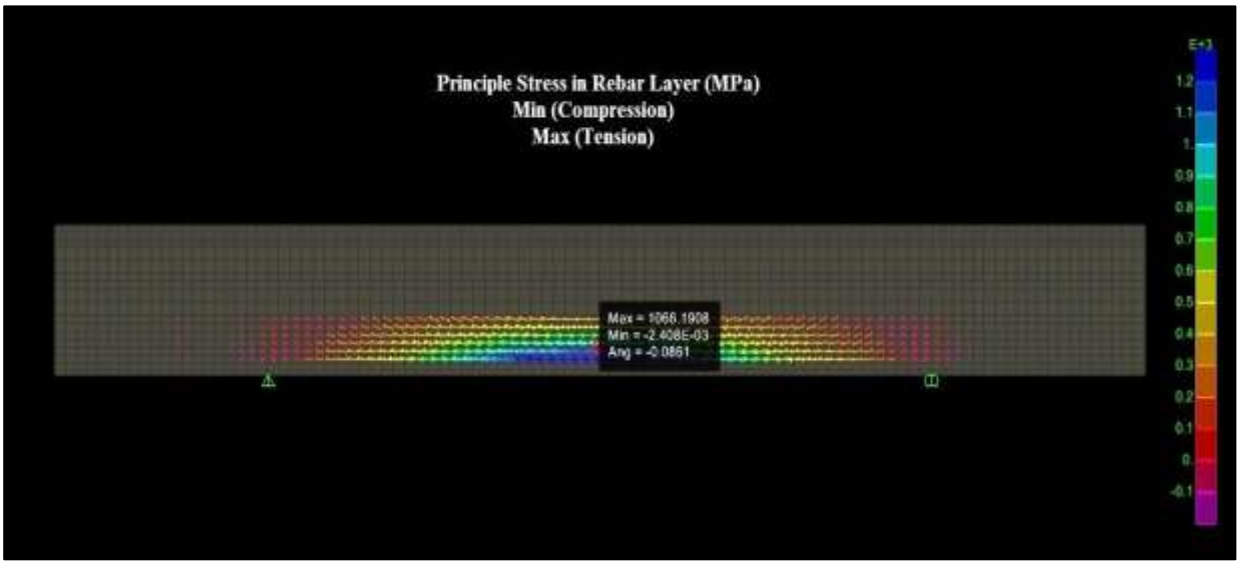

Figure A. 21: Stress in Second Layer of Main Tension Reinforcement for Beam MS3-2

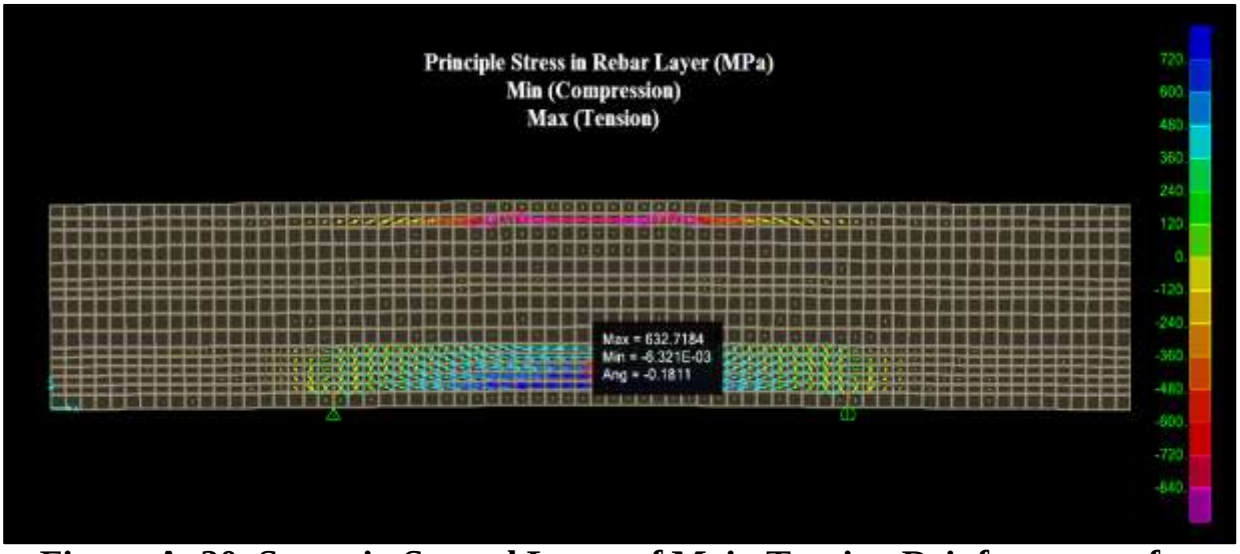

Figure A. 20: Stress in Second Layer of Main Tension Reinforcement for Beam MW1-2

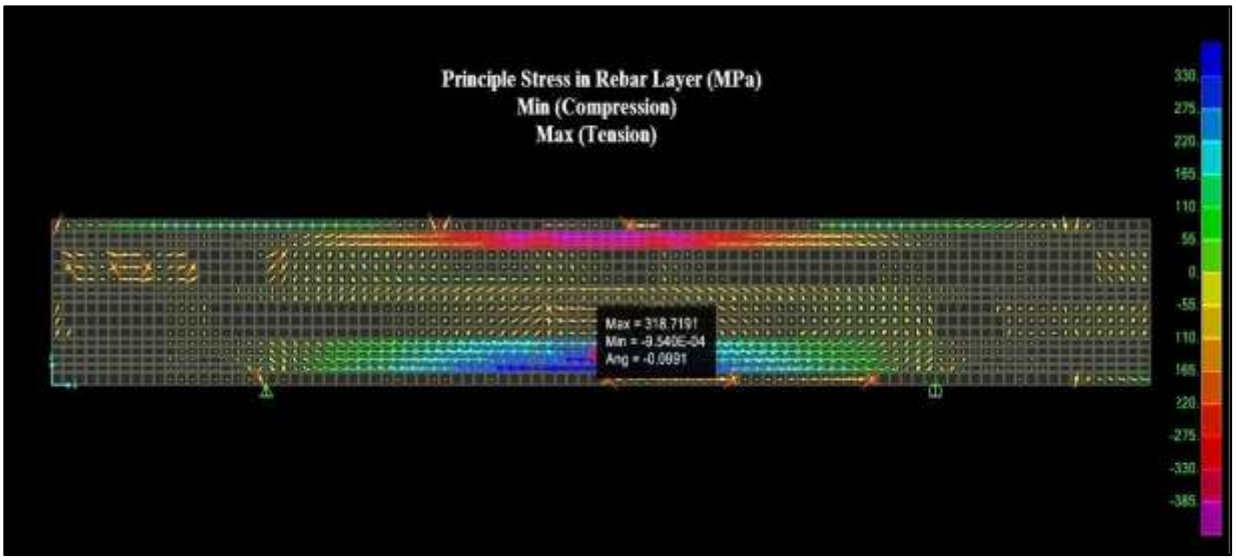

Figure A. 21: **Stress in Second Layer of Main Tension Reinforcement for Beam MW3-2**

- **Results of SAP2000 Yielding of Main Reinforcement for Third Layer**

This is show the stress of main reinforcement for third layer, **Figure.A.24** displayed stress in third layer of main tension reinforcement of model (MS1-3), **FigureA.25** displayed stress in third layer of main tension reinforcement for model MS2-3, **Figure.A.26** displayed stress in third layer of main tension for model MS3-2 and **Figure.A.27** displayed stress in third layer of main tension for model (MW3-2).

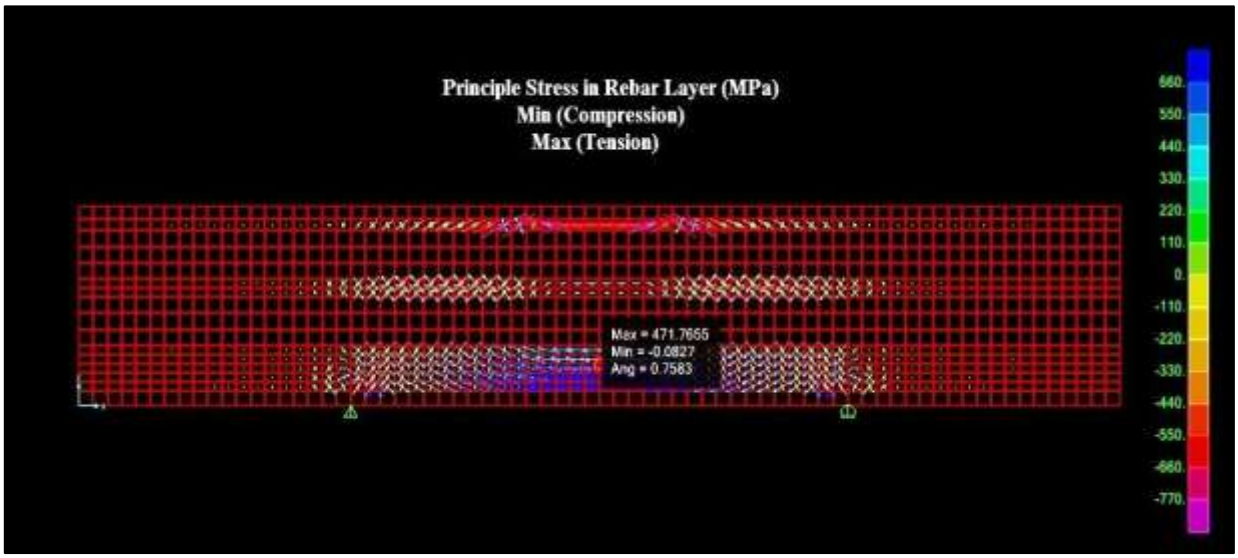

Figure A. 22: Stress in Third Layer of Main Tension Reinforcement for Beam MS1-3

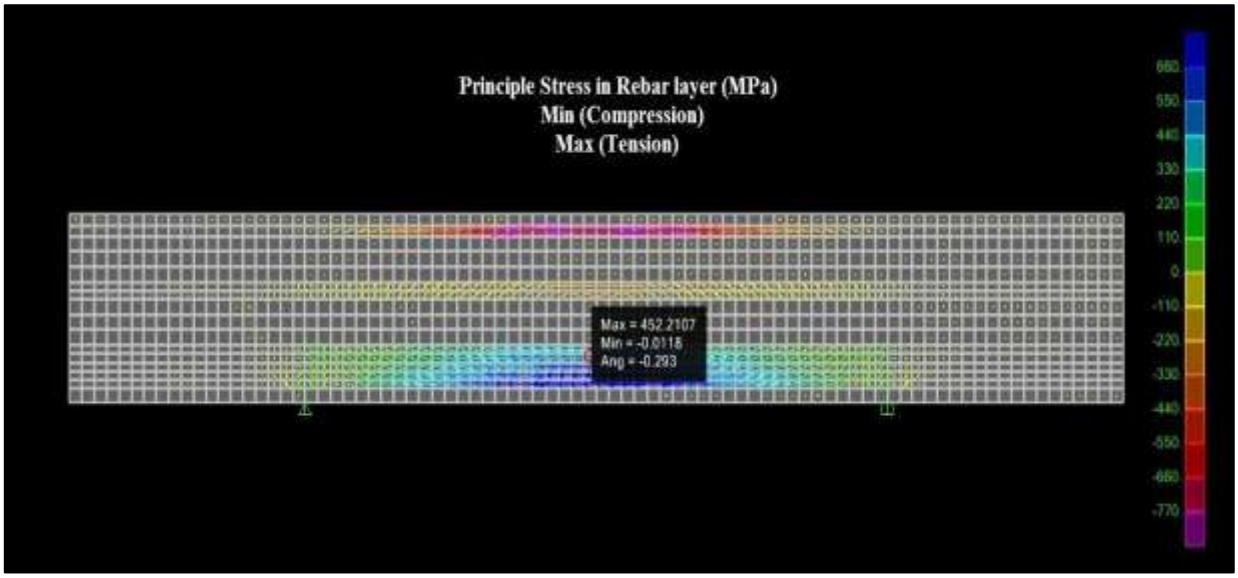

Figure A. 23: Stress in Third Layer of Main Tension Reinforcement for Beam MS2-3

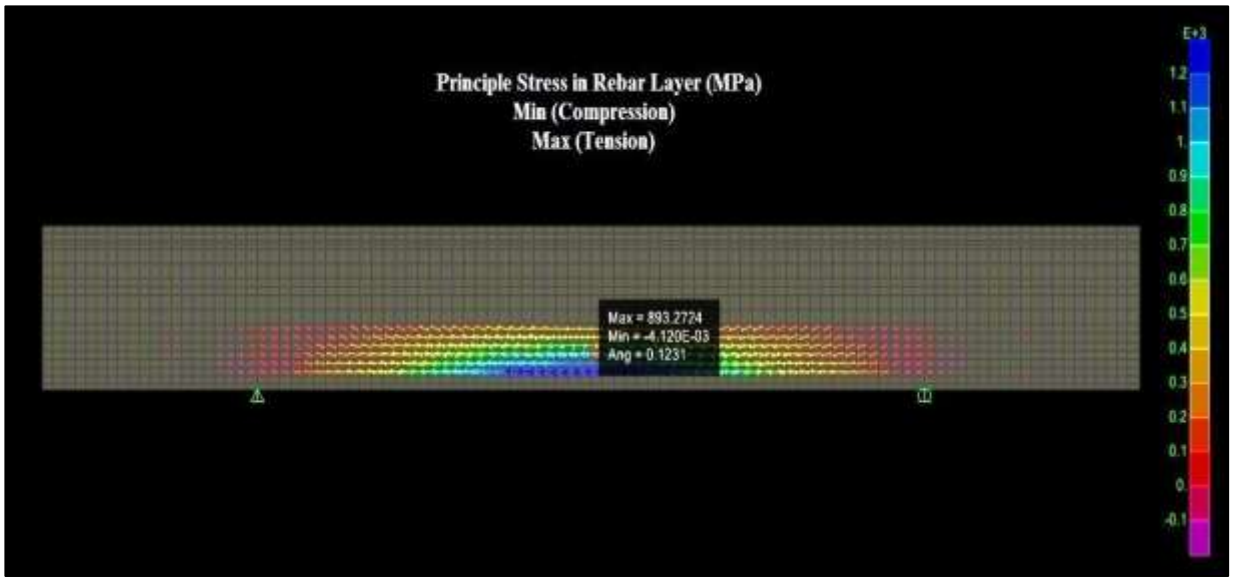

Figure A. 24: Stress in Third Layer of Main Tension Reinforcement for Beam MS3-2

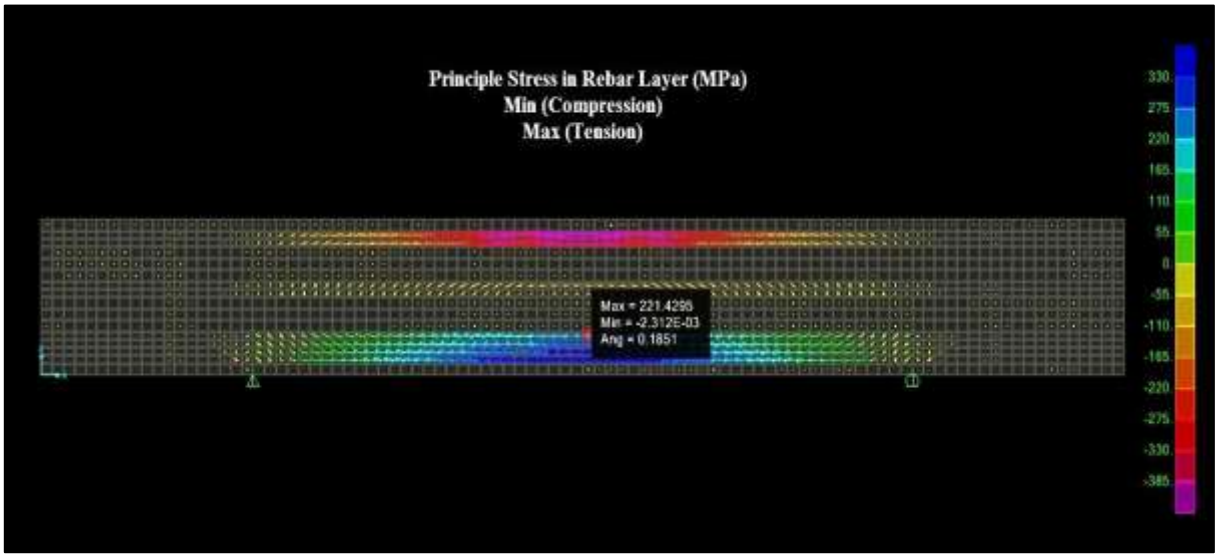

Figure A. 25: Stress in Third Layer of Main Tension Reinforcement for Beam MW3-2

A.4Results of SAP2000 Yielding Stress of Vertical Web Reinforcement

This is show the stress of vertical web reinforcement (above maximum stress of the effective yield stress of vertical web reinforcement), **Figure.A.28** displayed stress of vertical web reinforcement for model MS1-3, stress of vertical web reinforcement for model MS2-3 show that in **FigureA.29** and **Figure.A.30** displayed stress of vertical web reinforcement for model MS3-2.

2).

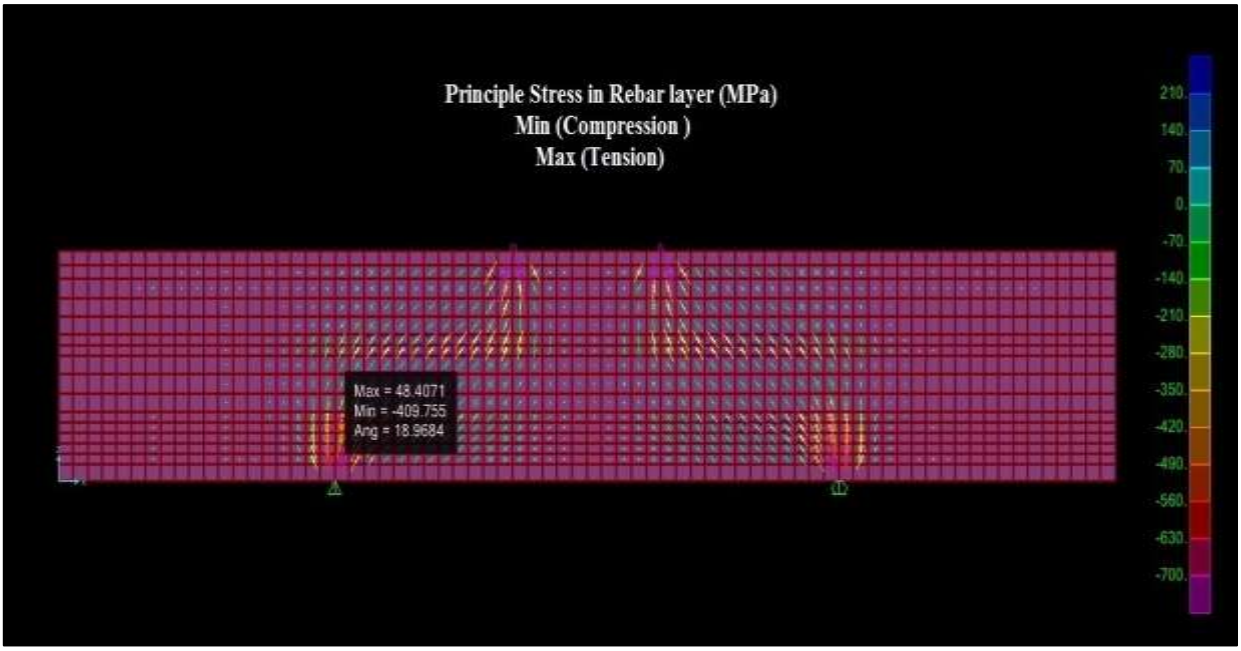

Figure A. 26: Stress in Vertical Web Reinforcement for Beam MS1-3

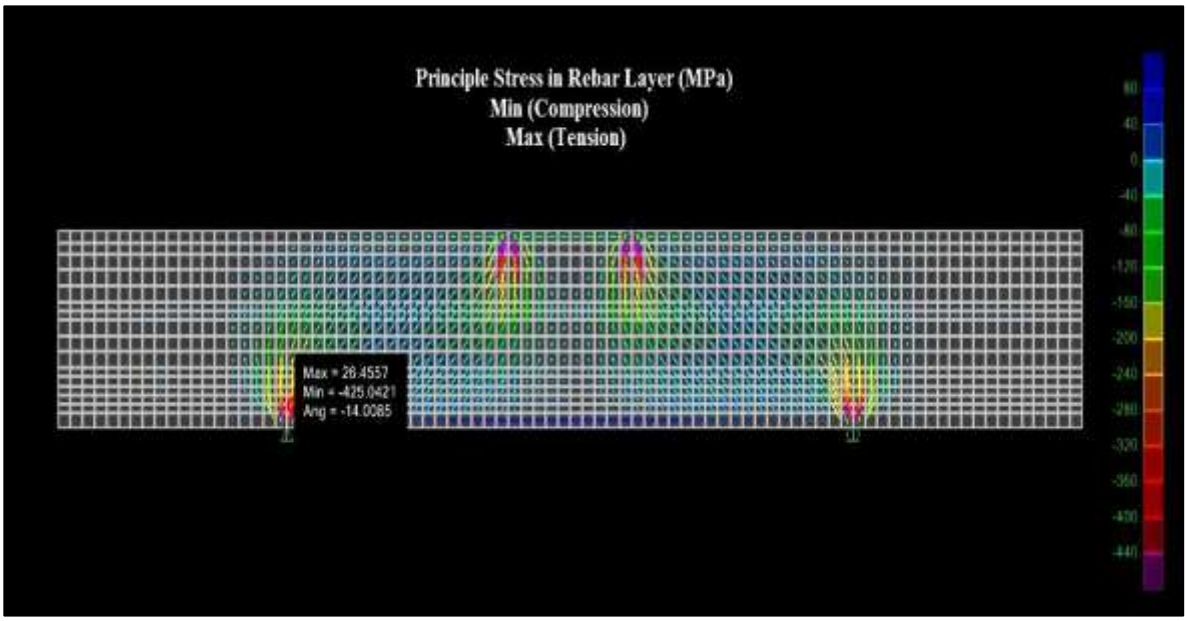

Figure A. 27: **Stress in Vertical Web Reinforcement for Beam MS2-3**

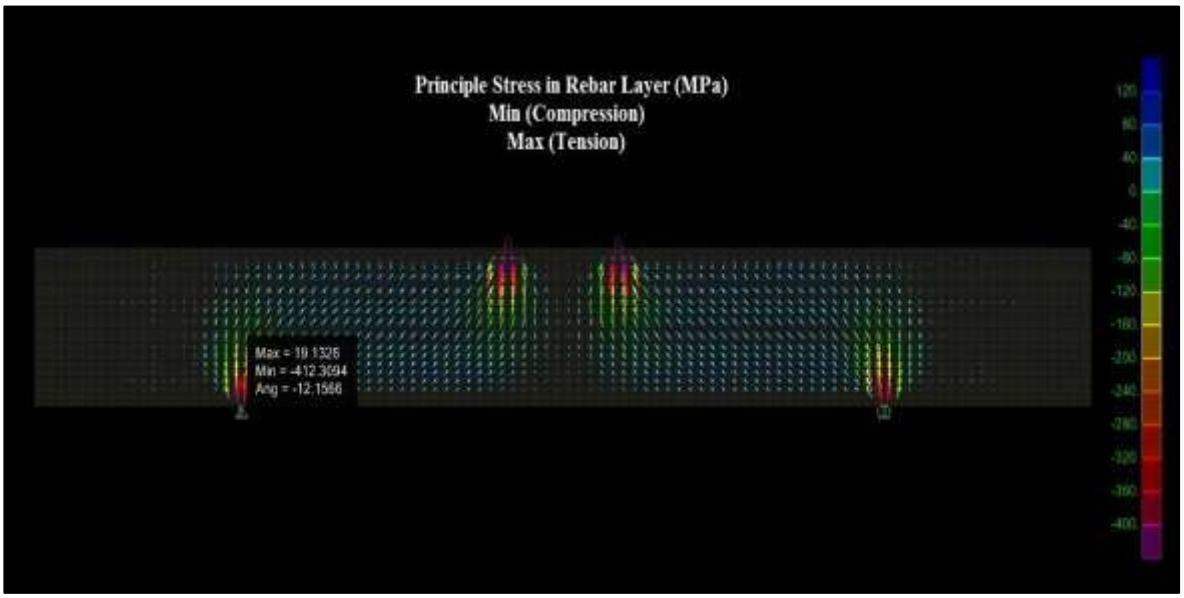

Figure A. 28: Stress in Vertical Web Reinforcement for Beam MS3-2

A.5 Results of SAP2000 Shear Stress Failure in concrete for Nonlinear Shell Layered Technique

This is show shear stress failure in concrete (above maximum shear stress of concrete) ,**Figure.A31** displayed shear stress in concrete for model MS1-3 ,**Figure.A.32** displayed shear stress in concrete for model (MS2-3) , shear stress in concrete for model (MS3-2) show in **Figure. A.33**, shear stress in concrete for model (MW1-2) show in **Figure. A.34** and **Figure.A.35** displayed shear stress in concrete for model (Mw3-2).

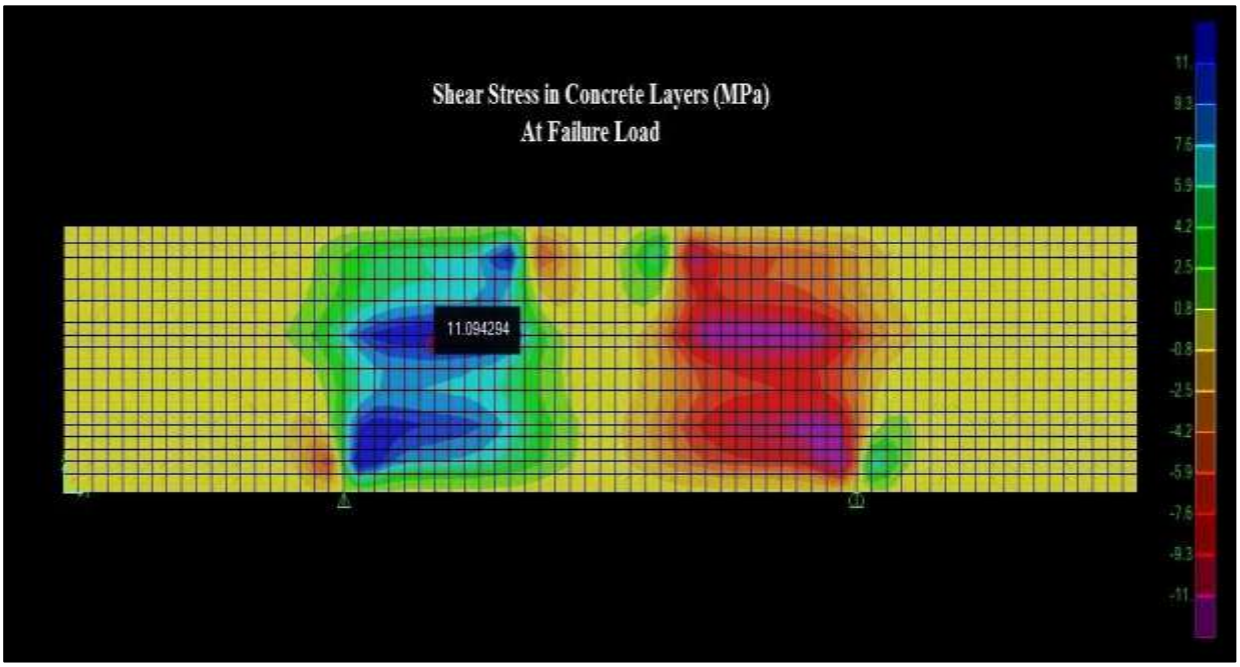

Figure A. 29: **Shear Stress at Failure in Concrete for Beam MS1-3**

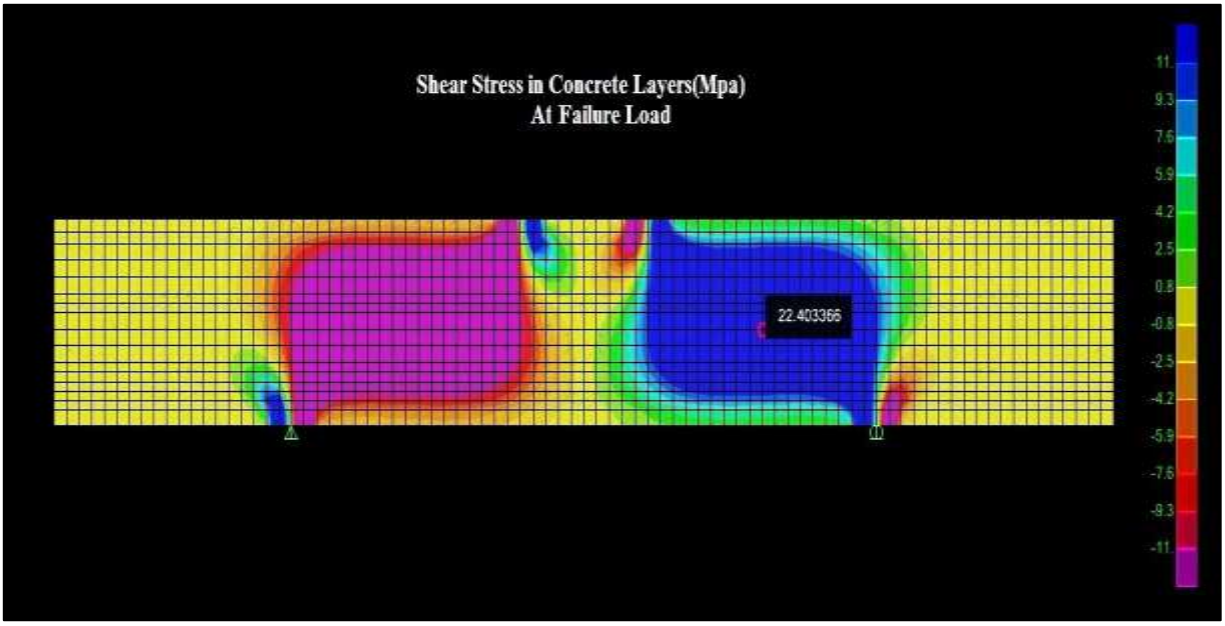

Figure A. 37: **Shear Stress at Failure in Concrete for Beam MS2-3**

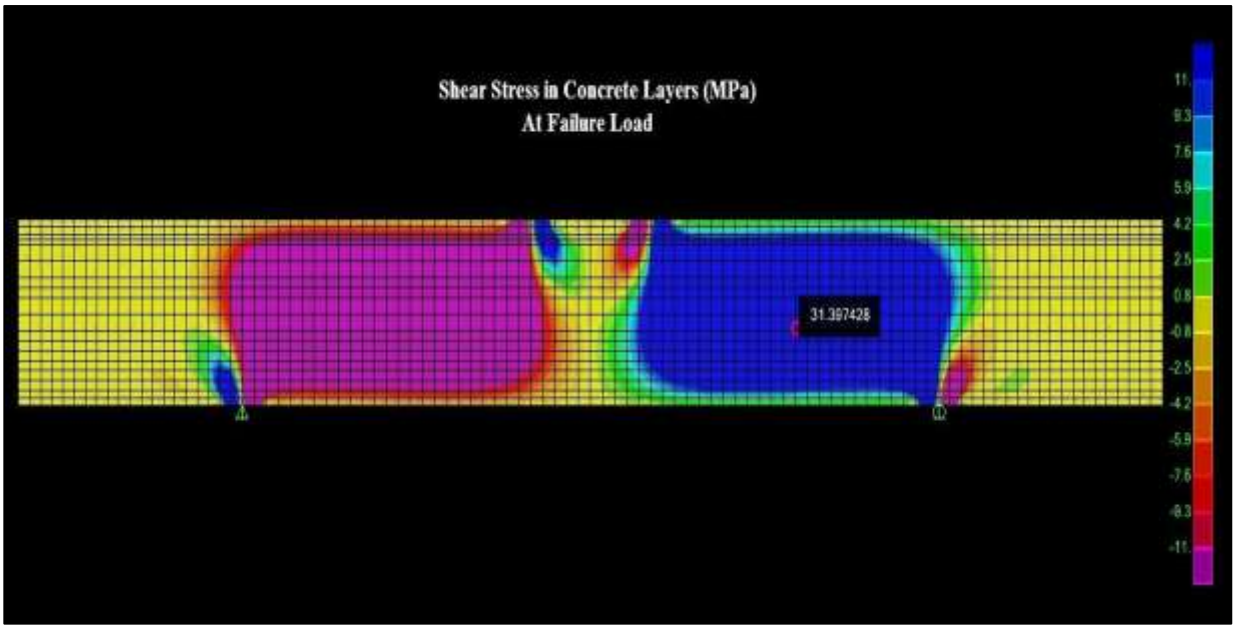

Figure A. 38: **Shear Stress at Failure in Concrete for Beam MS3-2**

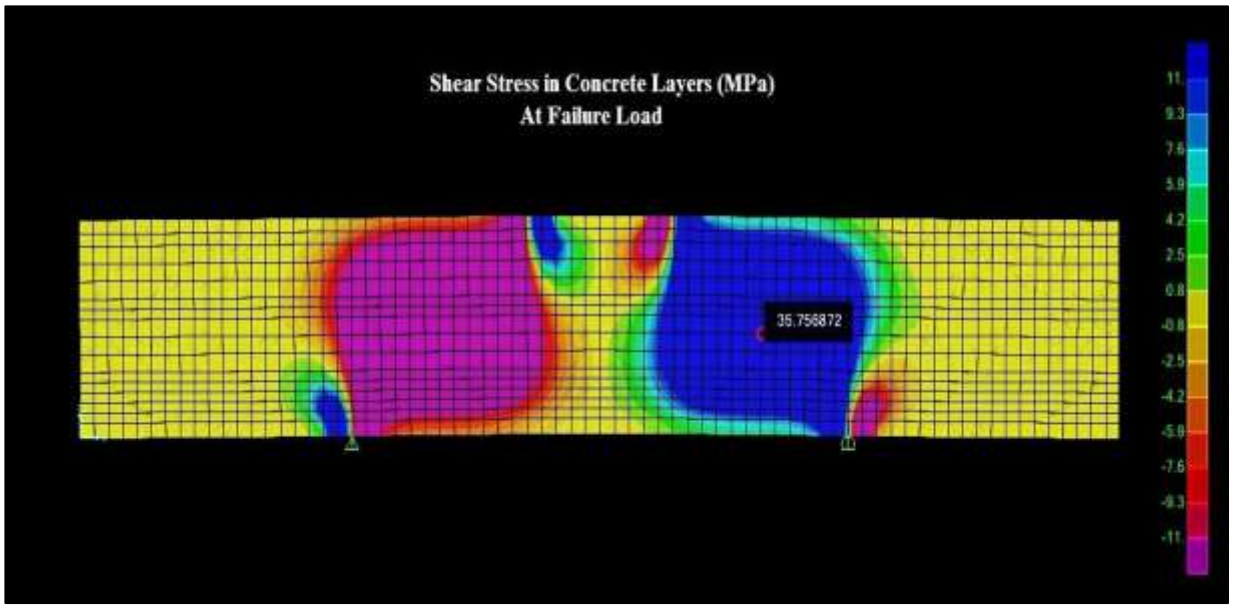

Figure A. 30: **Shear Stress at Failure in Concrete for Beam MW1-2**

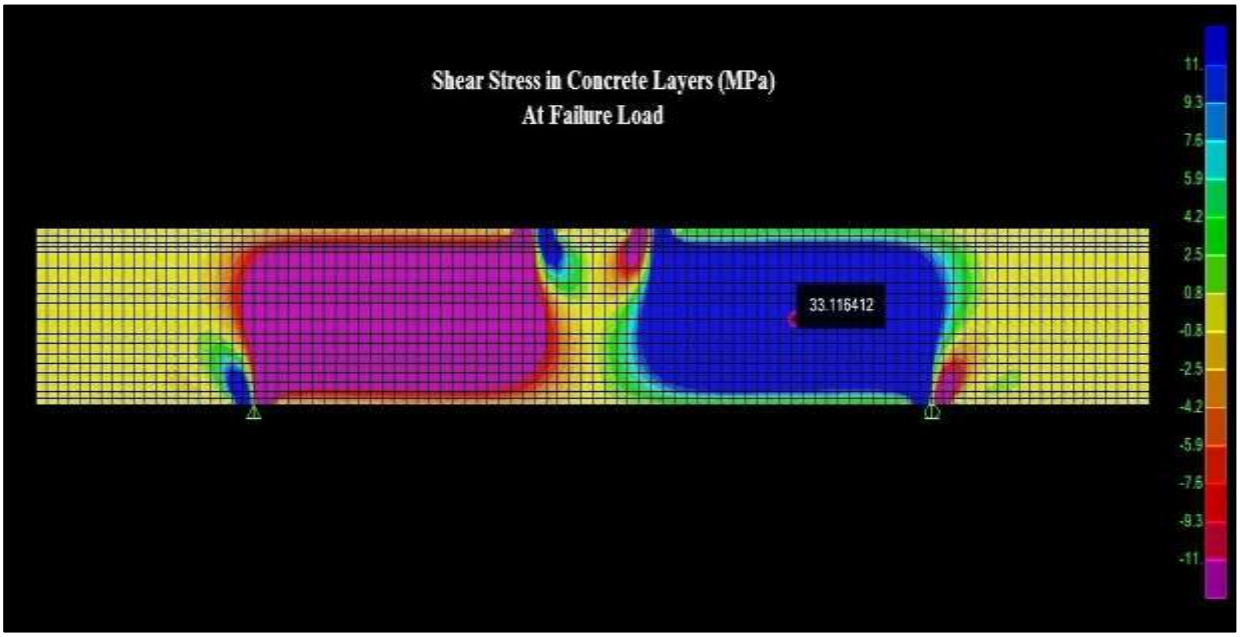

Figure A. 31: **Shear Stress at Failure in Concrete for Beam MW3-2**

A.6 Results of SAP2000 Maximum Deflections at Mid Span for Nonlinear Shell Layered Technique

This is show the maximum deflection at mid span, **Figure.A41** displayed deflection at mid span for model MS1-3, and **Figure.A.42** displayed deflection at mid span for model (MS2-3), deflection at mid span for model (MS3-2) show in **Figure. A.43**, deflection at mid span for model (MW1-2) show in **Figure. A.44** and **Figure.A.45** displayed deflection at mid span for model (MW3-2).

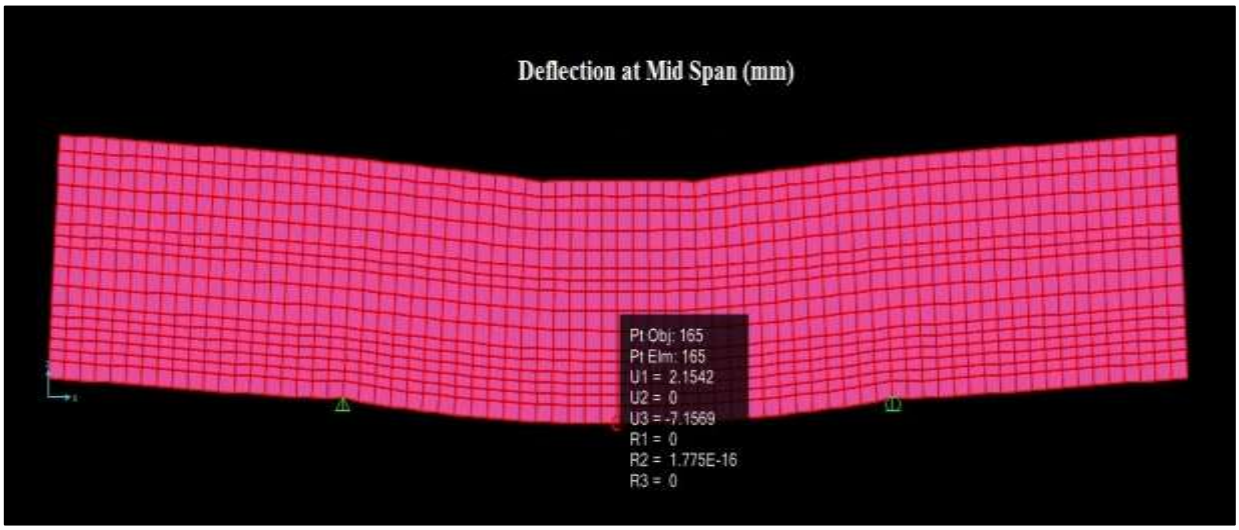

Figure A. 32: **Deflection at Mid Span for Beam MS1-3**

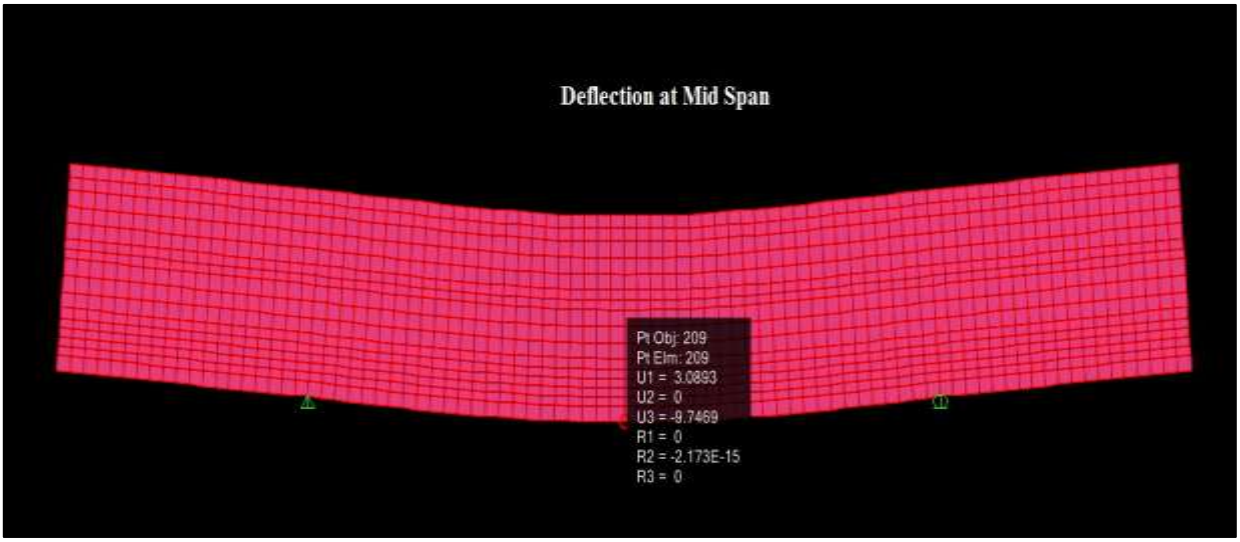

Figure A. 42: **Deflection at Mid Span for Beam MS2-3**

Figure A. 43: **Deflection at Mid Span for Beam MS3-2**

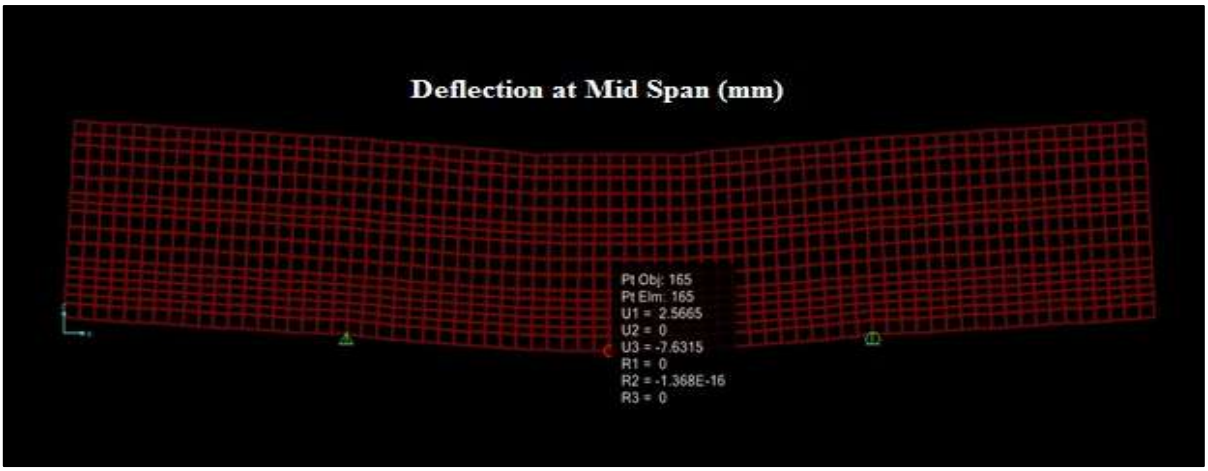

Figure A. 44: **Deflection at Mid Span for Beam MW1-2**

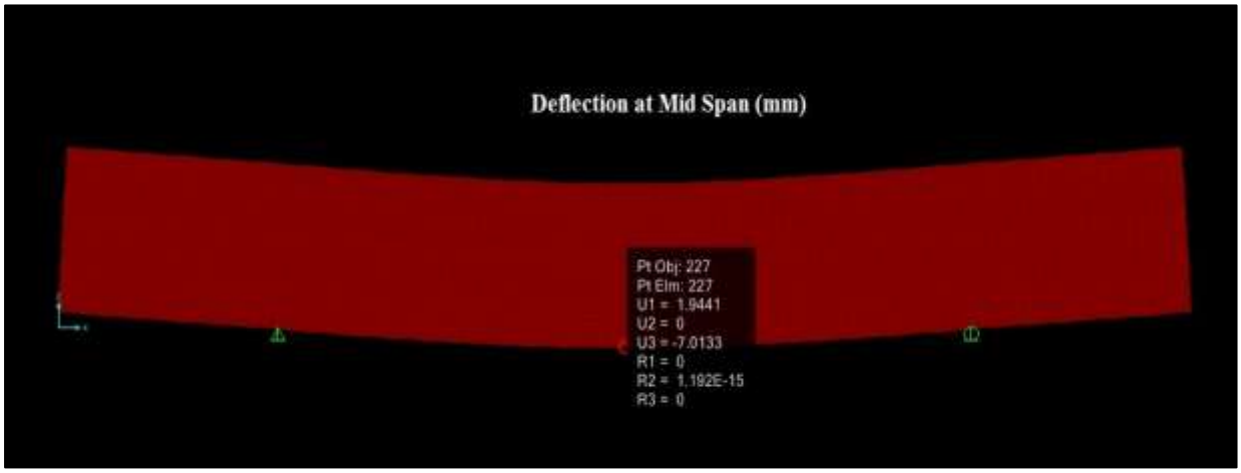

Figure A. 33: **Deflection at Mid Span for Beam MW3-2**